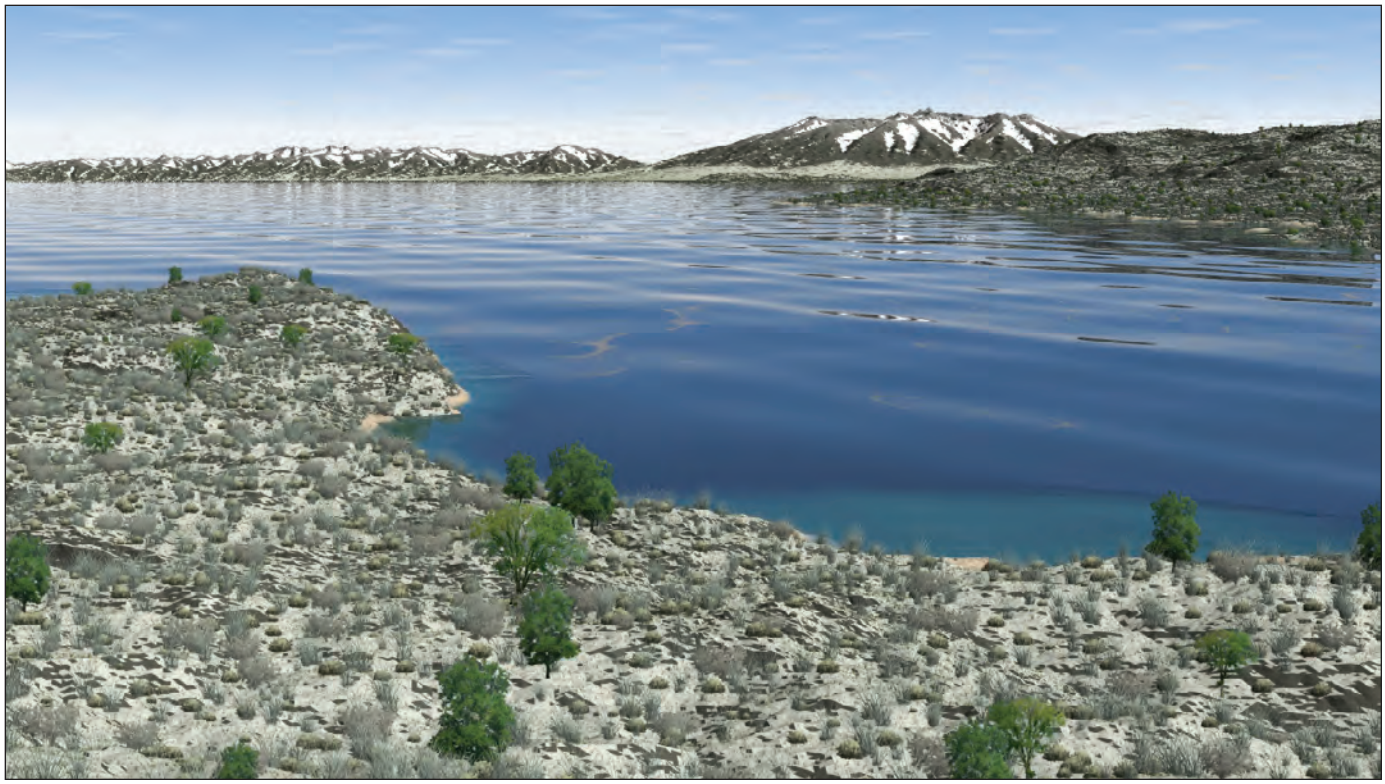

Frontispiece, Chapter B. Re-creation of Lake Alamosa. View to the northeast from the San Luis Hills (see Stop B4). Highest peak in the background is Blanca Peak at 14,345 ft asl. Visualization created in Visual Nature Studio (v. 2.7, 3D Nature Co.) by Paco Van Sistine (USGS) using 30-m DEM and a lake elevation of 7,660 ft (2,335 m).

Chapter B — Field Trip Day 2 Quaternary Geology of Lake Alamosa and the Costilla Plain, Southern Colorado

By Michael Machette, Ren Thompson, David Marchetti, and Robert Kirkham

Orientation for Day 2 — Saturday, Sept. 8, 2007

Speakers: Michael Machette and Ren Thompson
Location: Near center of Bachus pit, Road S106, about 3 mi (5 km) southwest of Alamosa, Colo. (camping location for previous day).
Alamosa West 7.5' quadrangle
GPS: NAD27, Zone 13, 418200 m E., 4144720 m N.
Elevation: 7,560 ft (2,304 m) asl at top of pit

Synopsis

On this day's field trip, we will discuss various aspects of middle Pleistocene to Pliocene Lake Alamosa, including its extent, relict geomorphic features, and age. In addition, we will see the ancient outlet of the lake and review its overflow through the Costilla Plain and into New Mexico (one subject of field-trip day 3). We will visit Mesita Cone, a 1.0-Ma basaltic vent on the Costilla Plain and stop along the base of San Pedro Mesa to discuss landslide and fault hazards along the southern Sangre de Cristo fault zone. In addition, the field-trip log contains information for optional stops B5, B6, and B7.

Introduction

Today's field-trip route is rather long (96 mi, 155 km), starting near Alamosa and ending in northern New Mexico at the Wild and Scenic Rivers Recreation Area. Most of the trip is on paved roads, but we'll be off road for about 10 mi (16 km) going to and from stop B4, which overlooks the Rio Grande. Vehicles with high ground clearance are recommended for at least this part of the trip.

Today's route is divided into three parts, only two of which we'll do on this trip. The morning portion includes stops B1–B4 and the afternoon portion includes a walking tour at stop B8 and an overview at stop B9. An optional leg that uses county gravel roads northeast of our lunch stop (B4) includes three stops (B5–B7) and is recommended for another time. After stop B9, we have a 45-minute drive (27 mi, 43.5 km) south to our campground at La Junta Point (New Mexico), which is the departure point for day 3 (chapter C).

Morning Stops

The first leg for day 2 (fig. B–1) focuses on rarely exposed sediment of Lake Alamosa (stops B1 and B3) and landforms constructed during its last and highest stand (stops B3 and B4). In addition, we'll see post-lake alluvial deposits that lie unconformably on lake sediment and show reversals of topography (stop B2). Relations at these stops are discussed in detail in chapter G, which documents the Pliocene to Pleistocene history of Lake Alamosa.

Optional Stops

An optional leg for day 2 (fig. B–2) includes three stops: (1) stop B5: barrier bar, spit, and lagoonal features that were formed during Lake Alamosa's highest stand (see also chapter G, this volume); (2) stop B6: spectacular wind-eroded rocks (ventifacts) along the southeastern margin of Lake Alamosa; and (3) B7: proposed type section for the Alamosa Formation, which is the basin-fill sediment of Lake Alamosa (stop B4). This last stop is at Hansen Bluff (see also stop A8, chapter A, this volume), a river-cut bluff that exposes early Pleistocene sediment that contains diverse faunal and floral remains, two volcanic ashes, and a well-documented magnetostratigraphic record.

Afternoon Stops

The last leg for day 2 (fig. B–3) focuses on a 1.0-Ma basalt volcano (Mesita Hill, stop B8) that is in the center of the Costilla Plain. We'll spend nearly 2 hours here reviewing the eruptive history of the

CHAPTER B

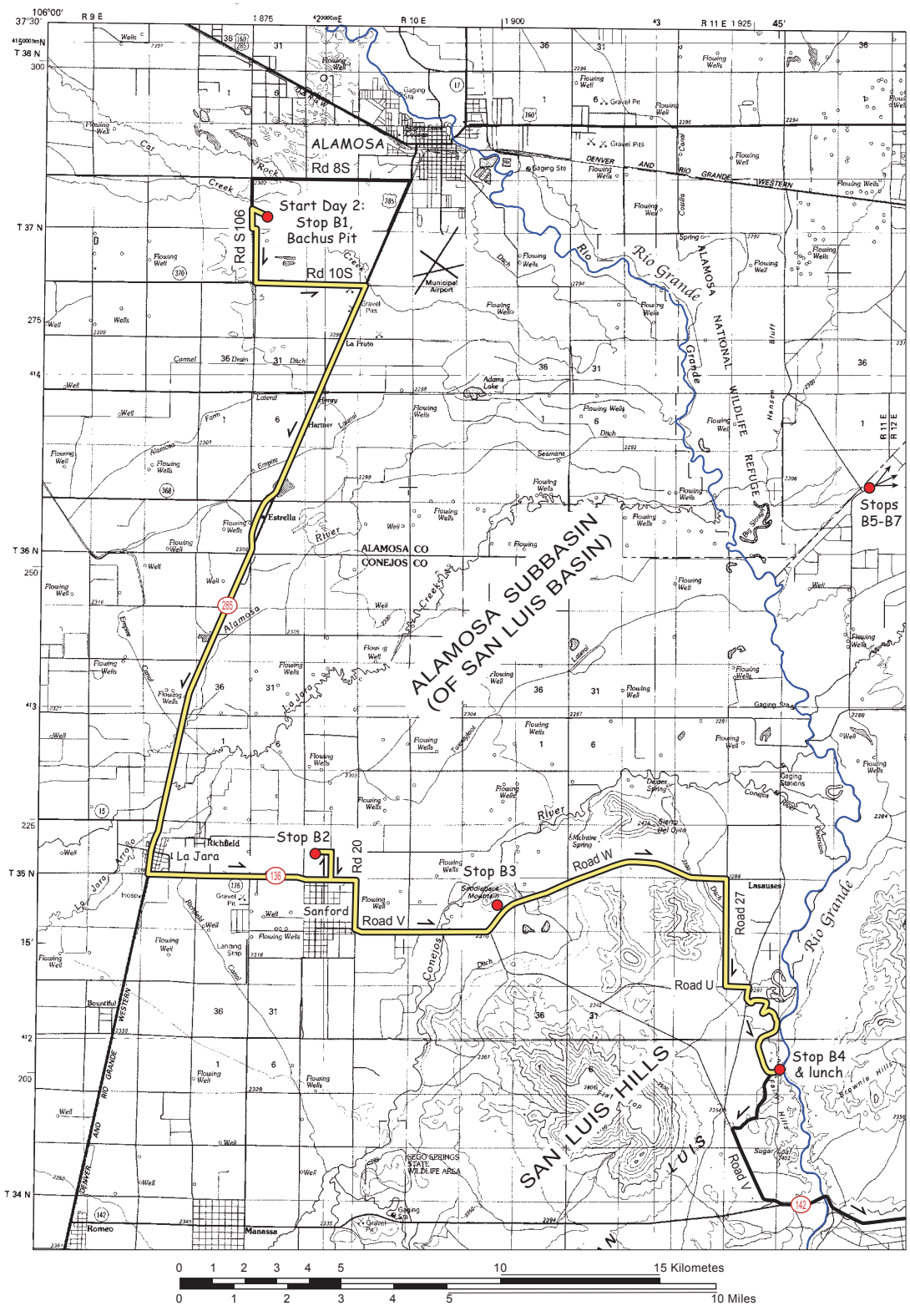

Figure B–1. Route and stops on morning of field-trip day 2. Stops B5, B6, and B7 (to the northeast of our route; shown as red dots) are optional and will not be visited.

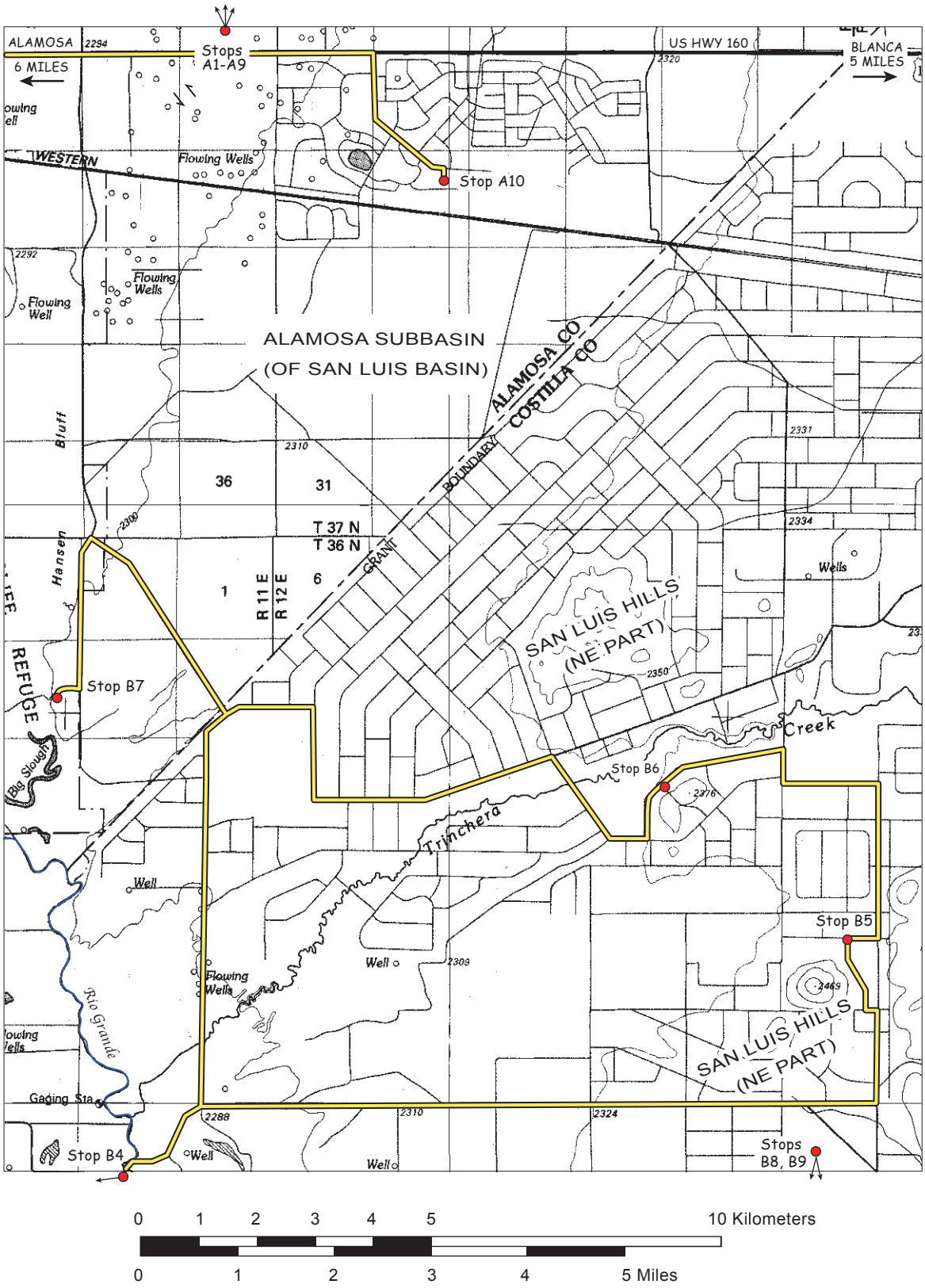

Figure B–2. Optional stops on field-trip day 2. Stops B4, B5, and B6 (to the northeast of the day 2 route; stops shown as red dots) will not be visited.

volcano, discussing the possibility that the volcano was nearly buried between 1.0 Ma and about 500 ka, and examining the western, faulted flank of the volcano. From there, we travel about 10 mi (16 km) southeast to the base of San Pedro Mesa to discuss landslide and fault hazards along the southern Sangre de Cristo fault zone, which is the southern part of the larger Sangre de Cristo fault system. This fault system has the highest documented Quaternary slip rates in the Rio Grande rift, which extends from at least Leadville, Colo. (on the north), to the Big Bend region of west Texas and to Chihuahua, Mexico (on the south).

Acknowledgments

None of the stops on this or other days of the field trip would be possible to visit without the permission of the landowners. We gratefully thank the following for allowing access to their properties during day 2 of the field trip:

Stop B1: Daniel Russell, owner, Bachus pit, Alamosa, Colo.

Stop B2: Lynn and Linda Mortensen, owners, Mortensen pit, Sanford, Colo.

Stop B3: Bureau of Land Management (public property), Monte Vista, Colo.

Stop B4: Bureau of Land Management (public property), Monte Vista, Colo.

Stop B5: Costilla County (public property), San Luis, Colo.

Stop B6: Costilla County (public property), San Luis, Colo.

Stop B7: Alamosa Wildlife Refuge, Alamosa, Colo.

Stop B8: Hecla Mining (Butte, Montana), owner, Hake and Jake Mine, Mesita, Colo.

Stop B9: Evan Melby, Melby Ranch Properties, LLC, Ventura, Calif.

In addition, we appreciate the constructive and helpful comments of James Cole (USGS) and Richard Madole (USGS-Emeritus), who reviewed a preliminary version of this manuscript. However, any errors that may remain are the responsibility of the authors.

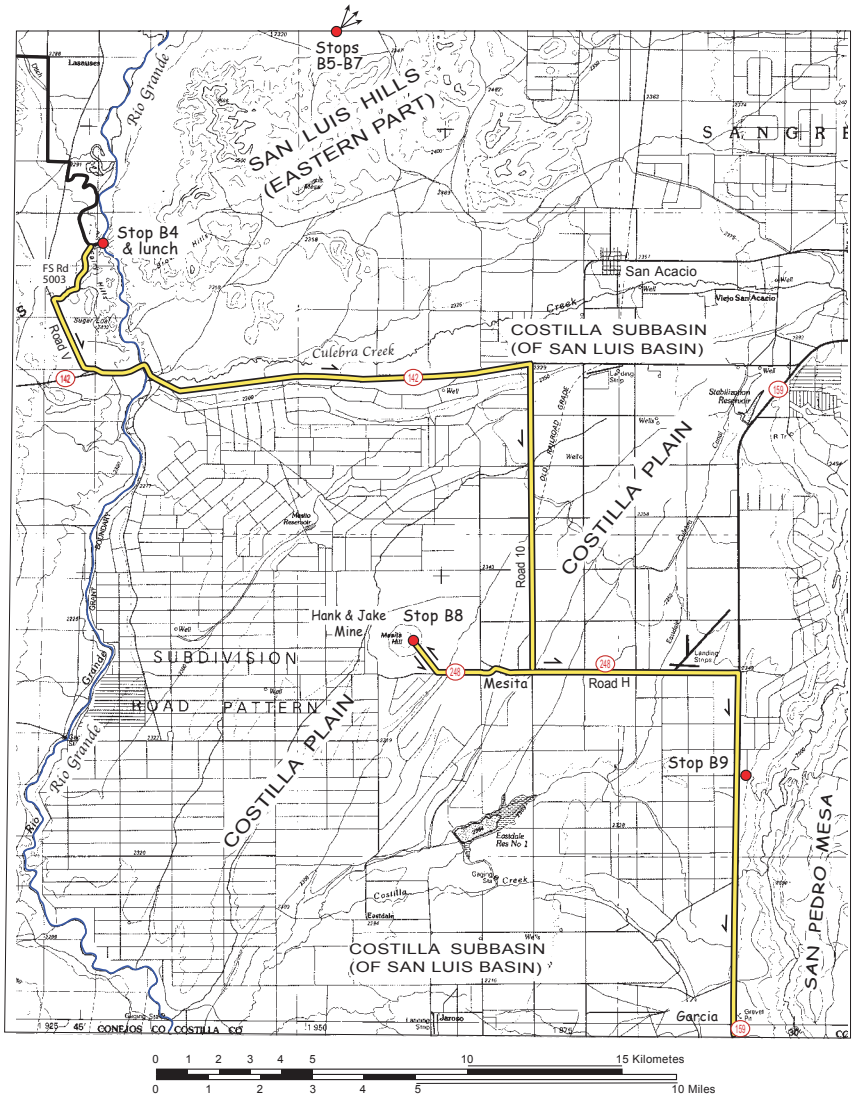

Figure B–3. Route and stops on afternoon of field-trip day 2. Stops B5, B6, and B7 (to the northeast of the day 2 route; stops shown as red dots) are optional and will not be visited on this trip.

Stop B1 — Deposits of Lake Alamosa at the Bachus Pit

Speaker: Michael Machette
Location: Various locations around perimeter of Bachus pit
Alamosa West 7.5' quadrangle
GPS: NAD27, Zone 13, 418900 m E., 4144720 m N., near center of Bachus pit
Elevation: About 7,540 ft (2,298 m) asl at base of pit; about 7,562 (2,305 m) asl at top of pit

Synopsis

Exposures within the Bachus pit show evidence of transgression and regression of Lake Alamosa, followed by incision of alluvial channels graded to post-lake base levels. The Bachus pit is one of the few places in the lake basin where lake deposits are well exposed; elsewhere, post-lake surficial deposits, high water tables, and strong efflorescence of gypsum typically obscure exposures of lacustrine sediment.

The Bachus pit extracts sand and pebble-size gravel for local use (mainly fill material). Although the pit walls change with continued mining, the base of the pit is controlled by fine-grained, water-saturated silt and clay deposited by Lake Alamosa prior to its last transgression and subsequent overflow. The walls of the pit expose well-sorted, sandy, small-pebble gravel that represents transgressive and regressive near shore and low-energy beach deposits. Between these deposits is sandy silt (deeper water phase of the lake) that is finely laminated and contorted by pressure loading from the overlying sedimentary package. The entire lacustrine section is capped, unconformably, by several meters of fine-grained alluvium that was deposited in response to falling base levels as the lake emptied through an outlet at the Fairy Hills. This alluvium is capped by loess and has relict soils, but their discontinuous Bt and Bw horizons (disturbed by animal burrows) are suggestive of middle Pleistocene age.

Sediment in the Bachus pit, together with high-energy near-shore gravel seen at stop B3 and lagoonal features seen at stop B7, are new and important stratigraphic and geomorphic evidence for the culmination and subsequent overflow of ancient Lake Alamosa.

Introduction

The Bachus pit is owned by Dan Russell of Alamosa (fig. B1–1). Dan earned a BS in Geology from Adams State College in the 1970s and currently owns and operates a land-surveying company in Alamosa. Dan's strong and enduring connection to geology is obvious from his enthusiastic support of our mapping of the Quaternary geology in this area (Machette and Thompson, 2005) and topical studies of Lake Alamosa. As a result, the Friends of the Pleistocene awarded Dan Russell its "Most Cooperative Landowner, 2007" award at its annual meeting in the Bachus pit on September 7, 2007.

Figure B1–1. Entrance to the Bachus pit, camping site for day 1 and first stop of day 2.

The Bachus pit produces well-graded sand and pebble-size gravel: the maximum gravel size is only 2–3 cm owing to its long transport distances from the eastern margin of the San Juan Mountains. Coarse gravel is so rare in the area that it is hauled from pits in coarser grained alluvial fans located about 15 km to the southwest. The Bachus pit supplies ungraded and graded sand and gravel to local contractors for use as backfill. Although the pit walls change with continued mining, the base of the pit is controlled by fine-grained, water-saturated silts and clays deposited by Lake Alamosa prior to its last transgression and subsequent overflow (see discussion in chapter G).

Local Geology

The Bachus pit is located on an east-trending topographic ridge that extends from west of our mapping area (longitude 106° W.) almost to U.S. Highway 285 (Alamosa to Antonito). Although the ridge is only about 20 ft (6 m) above the surrounding landscape, its elevated position is well above the local water table; thus, this and other similar ridges in the area are dry. They typically are the sites of churches, cemeteries, silage and sand pits, and stock ponds. This ridge is relatively planar and has a gentle east slope of less than 0.002 (that is, 2 m/km or 10 ft/mi) (fig. B1–2).

The ridge is composed of intermediate-age (middle Pleistocene) alluvium 2–3 m thick that rests unconformably on lacustrine sediment of the Alamosa Formation (see chapter G for a discussion of Lake Alamosa). Adjacent to the ridge are

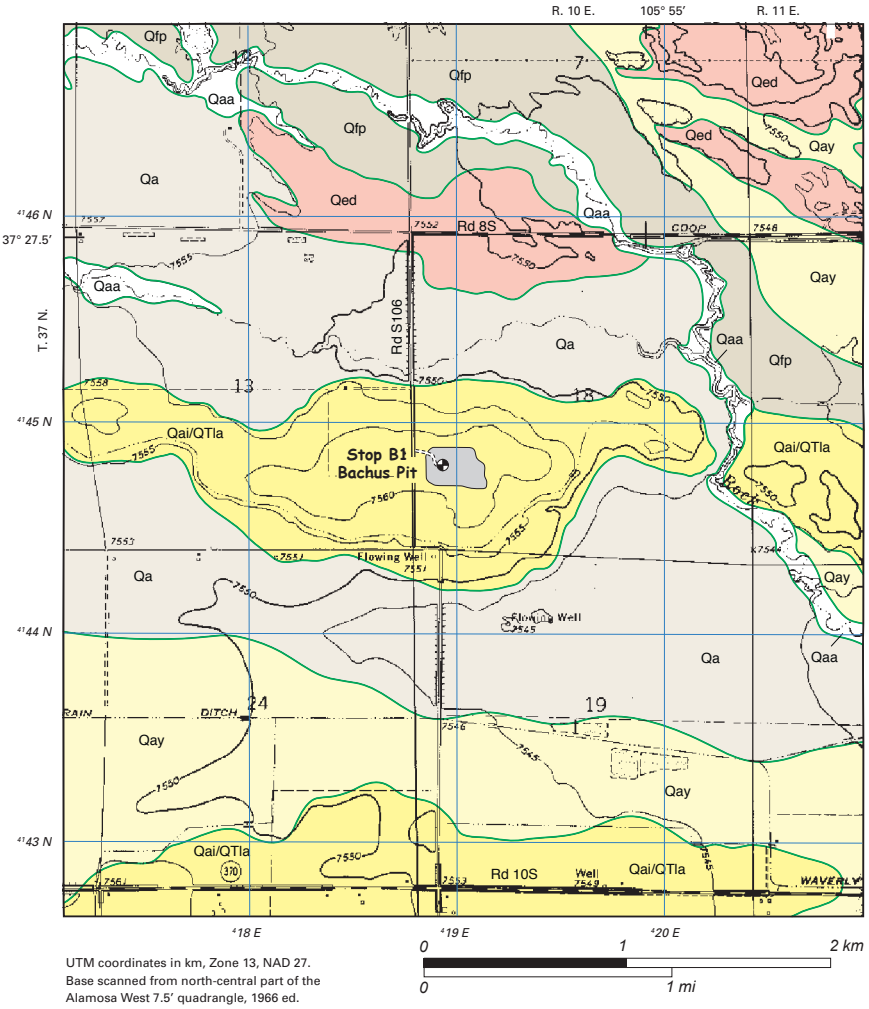

Figure B1–2. Surficial deposits and underlying near-shore lacustrine deposits of Lake Alamosa. Map units: Qe, Holocene eolian sand; Qaa, active alluvium; Qa, Holocene alluvium; Qfp, floodplain alluvium; Qay, younger (latest Pleistocene) alluvium, Qai, intermediate (middle Pleistocene) alluvium; QTla, Alamosa Formation. Geology modified from Machette and Thompson, 2005.

slightly lower valleys floored by latest Pleistocene to Holocene alluvium (fig. B1–2) and Holocene eolian sand.

Quaternary Stratigraphy

The Bachus pit has been extensively mined; the main product is sandy pebble gravel and silty sand. The pit floor is relatively flat and controlled by underlying lacustrine silt and sand (unit 5, fig. B1–3) that is commonly water-saturated at this elevation (about 7,540 ft or 2,298 m asl). Above the floor of the pit is sandy small-pebble gravel that represents transgressive near-shore, low-energy beach deposits of Lake Alamosa (unit 4, fig. B1–3). The transgressive deposits are not exposed in the west wall of the pit but were visible in 2005 on the north and east walls (exposures depend on activity in the pit and regrading of the pit walls). The near-shore sandy gravel is typically heavily stained by iron and manganese oxides, which in some locations are abundant enough to cement beds of gravel.

The transgressive deposits are overlain by sandy silt (deeper water phase of lake, unit 3 of fig. B1–3) that is finely laminated and contorted by pressure loading from the overlying sedimentary deposits (fig. B1–4). Over the silt is more sandy pebble gravel that represents regressive near-shore deposits related to drawdown of the lake (unit 2, figs. B1–3 and B1–4). We know that these are regressive deposits because they contain rip-up clasts of lake-bottom mud (derived from unit 3, fig. B1–5). Altogether, the entire cycle of lake sediment (units 2–4, fig. B1–3) is only about 3 m thick.

The Bachus pit is at an altitude of about 7,540–7,562 ft (2,298–2,305 m) asl, which is 100–120 ft (30–35 m) below the threshold (overflow) elevation of Lake Alamosa in the San Luis Hills. Thus, during the highest stand of Lake Alamosa, the Bachus pit was under about 30–35 m of water and well into the southwestern part of the lake. For example, the high-shoreline contour (7,660 ft or 2,335 m asl) is on the west side of the Monte Vista Wildlife Refuge, which is about 20 km to the west.

Above the lacustrine sediment is several meters of intermediate-age alluvial deposits (unit Qai) and loess (unit 1, fig. B1–3 and B1–4). The alluvium is relatively fine grained owing to its long transport distance from source areas in the eastern part of the San Juan Mountains. After water level in Lake Alamosa dropped, the lake floor was probably mantled by thin and discontinuous regressive near-shore deposits and deeper-water fine-grained deposits, all of which were eroded and reworked in alluvial channels that coursed across the newly exposed lake bottom. Wind erosion of the lacustrine sediment resulted in deposition of a 0.5–1 m thick layer of loess (silt and sand) that caps the alluvium. Relict soils formed on the loess and alluvium are disturbed by animal burrowing but show discontinuous Bt and Bw horizons suggestive of middle Pleistocene age (better exposures will be seen at stop B2).

Geologic History

The sediments exposed in the Bachus pit represent the last deep-water cycle of Lake Alamosa, which we believe culminated in overflow at about 440 ka (chapter G, this volume). This package may be thinner than those deposited during older

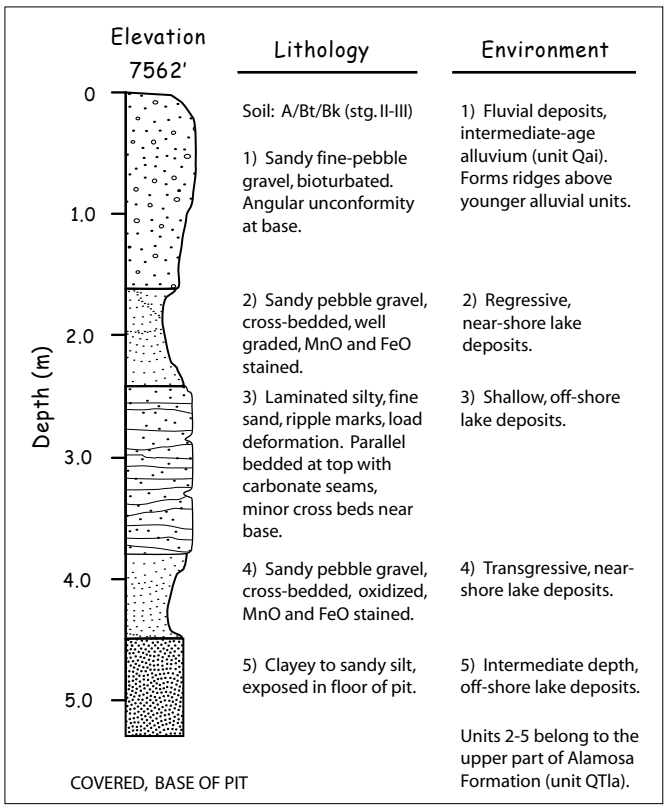

Figure B1–3. Schematic section of deposits exposed at field-trip stop B1 on west wall of the Bachus pit, as exposed in June 2004.

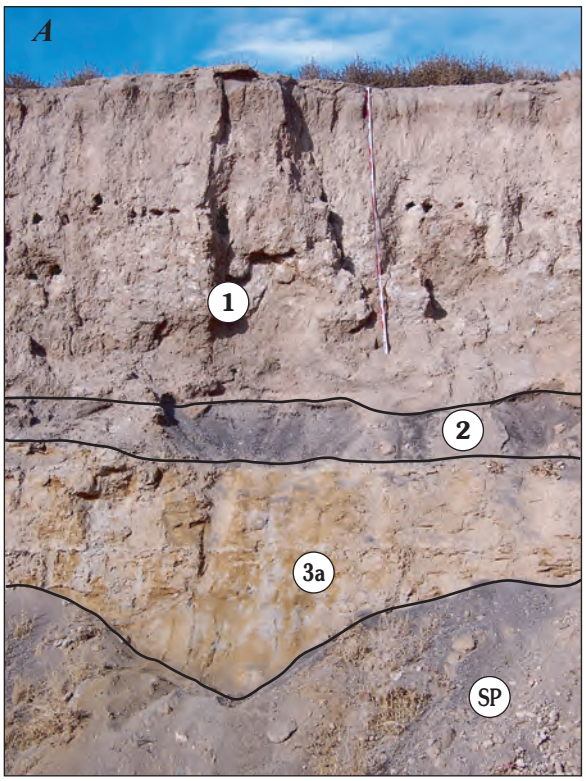

EXPLANATION

UNIT 1: Alluvium (unit Qai) and loess with soil
UNIT 2: Regressive beach deposits, sandy gravel
UNIT 3a: Deep-water lacustine sediment (silty sand)
UNIT 3b: Contorted lacustine sediment (silty sand)
UNIT SP: Spoil (shoveled away in fig. B)
UNIT 5: Deep-water lacustine sediment (below photo, forms floor of pit)

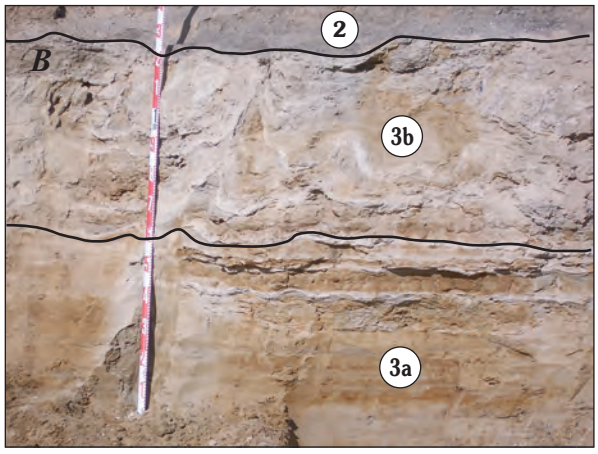

Figure B1–4. Exposures on the west wall of the Bachus pit. *A*, Alluvium (unit Qai) and loess deposits over lacustrine gravel and silty sands. Tape measure is extended 2 m. *B*, Closeup view of contorted lacustrine silty sand beds (unit 3b), which are rippled and well laminated (see unit 3a). Contortions in unit 3b are probably the result of penecontemporaneous loading by the overlying lacustrine and alluvial deposits, rather than by liquifaction (no feeder dikes were noted). Vertical exposure in this view is about 1.5 m.

cycles of the lake; the entire regressive phase of the sediment package is related to lowering of the lake as its waters flowed over and cut through the bedrock threshold in the Fairy Hills (see field-trip stop B4). If the lake had receded by evaporation, we would expect to see a thicker, coarsening-upwards section of sediment between units 3a and 2 (fig. B1–4) as the shoreline approached this site from the west and conditions changed from deep, quiet-water to shallow, near-shore conditions, rather than an abrupt unconformity between these units.

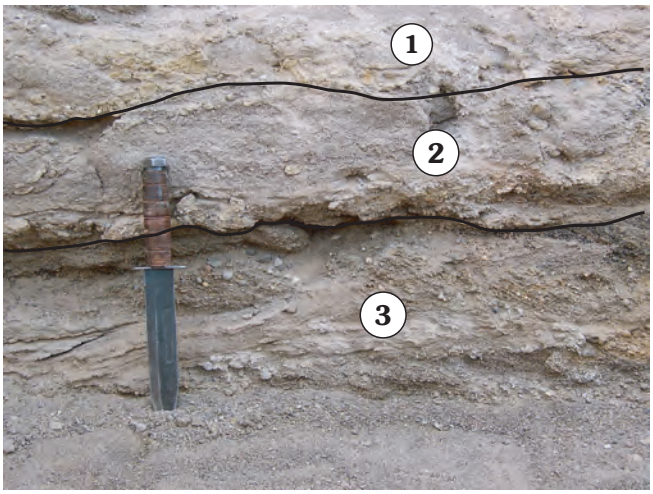

EXPLANATION

1: Layer with rip-up clasts of silty sand
2: Medium sand, crudely bedded
3: Sandy pebble gravel (1 cm max. clasts) and cross-bedded sand

Figure B1–5. Exposed lacustrine deposits on north wall of the Bachus pit. Silty oxidized clasts (1) in upper part of view are pieces of lake sediment ripped up during regression f the lake. Knife is about 20 cm long. All of these deposits are part of unit 5 in figure B1–3.

As the lake dropped, so did base level for the tributary streams emanating from the eastern part of the San Juan Mountains and streams heading on the exposed lake floor. The largest of these streams flowed northeast and east toward the Rio Grande's outlet from the Alamosa subbasin. Stream channels that cut into the exposed lake-bottom sediment became preferentially filled with alluvium (unit Qai, fig. B1–6) as the region was transformed from an exposed lake bottom to a gentle piedmont slope. However, the slightly more resistant nature of the alluvium-filled channels led to topographic reversal through time, just as basalt-filled channels become topographically reversed when less resistant bedrock is eroded preferentially.

Conclusions

The Bachus pit contains excellent exposures of sediments deposited during and after the last cycle of Pliocene to middle Pleistocene Lake Alamosa. The lacustrine sediments represent the uppermost preserved part of the Alamosa Formation (Siebenthal, 1910), which underlies almost the entire San Luis Valley north of the San Luis Hills. This uppermost part of the Alamosa Formation (about 700–440 ka) is missing from Hansen Bluff (see stop B5) owing to local erosion. Nevertheless, because this bluff is well exposed and contains abundant fossils, it is considered to be the type area of the formation as described by Siebenthal (1910). Thus, the sediments in the Bachus pit, together with high-energy, near-shore gravels seen at stop B3 and lagoonal features seen at stop B7, are new and important stratigraphic and geomorphic evidence for the culmination and subsequent overflow of Lake Alamosa.

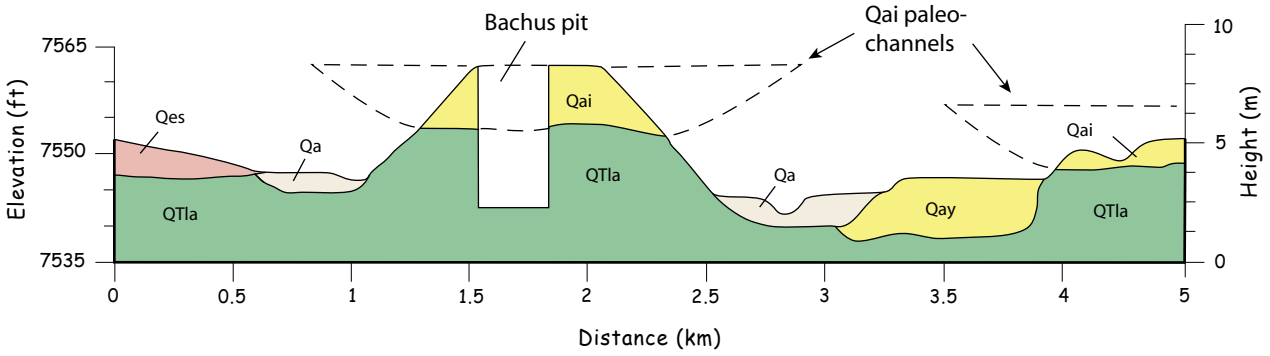

Figure B1–6. Schematic cross section through the ridge on which the Bachus pit is excavated showing position of Qai paleochannels cut into lacustrine deposits. Geologic units: Qes, Holocene eolian sand; Qa, undivided Holocene alluvium; Qay, young (latest Pleistocene) alluvium; Qai, intermediate (middle Pleistocene) alluvium; QTla, lacustrine sediment of the Alamosa Formation (Pliocene to middle Pleistocene). Geology from Machette and Thompson (2005). Vertical exaggeration is 50x.

Stop B2 — Soil on Intermediate-Age Alluvium (Post-Lake Alamosa), Sanford, Colo.

Speaker: Michael Machette
Location: Mortensen gravel pit, on low ridge about 0.6 mi (1km) north of city center of Sanford, Colo.
La Jara 7.5' quadrangle (Station LJ–MM04–19)
GPS: NAD27, Zone 13, 419880 m E., 4125652 m N.
Elevation: Top of pit is at 7,590 ft asl (2,313 m)

Synopsis

This pit exposes a thick, well-developed calcic soil formed in sandy pebble gravel that Machette and Thompson (2005) mapped as intermediate-age alluvium (unit Qai). The soil clearly represents hundreds of thousands of years of soil formation; it has a remarkable Bk horizon (stage III morphology) for this altitude (nearly 7,600 ft or 2,316 m asl). This stop is on a wide, north-trending ridge (informally named Sanford Ridge) that is only about 3–4 m above adjacent, younger alluvial surfaces. Similar to the geomorphology at stop 1, Sanford Ridge represents a reversal of topography: unit Qai gravel was deposited in a broad channel cut into lacustrine deposits (unit QTla) after Lake Alamosa had overflowed and dropped to a lower level. This relationship is common in the southwestern part of the lake basin.

Introduction

The Mortensen pit is an inactive sand and gravel pit that is owned by Lynn and Linda Mortensen of Sanford (fig. B2–1). The pit is adjacent to several reservoirs that retain irrigation water from deep wells. The pit and reservoirs are in a low, broad, north- to northeast-trending ridge of middle Pleistocene alluvium that is only about 3–4 m above surrounding surfaces formed on latest Pleistocene and Holocene alluvium (fig. B2–1). The ridge is informally named after the town of Sanford. Sanford Ridge is relatively tabular and has a gentle north slope of about 0.0016 (that is, 1.6 m/km or 8 ft/mi) as measured from the La Jara 7.5-minute topographic map. It extends about 10 km in a north-south direction (see mapping of Thompson and Machette, 1989) and is one of several in the southwestern part of the Alamosa subbasin (of the San Luis Basin) that reflect inverted topography, as discussed at stop 1. Sanford is a small Mormon farming community, whereas many of the adjacent communities (such as La Jara) are primarily Hispanic.

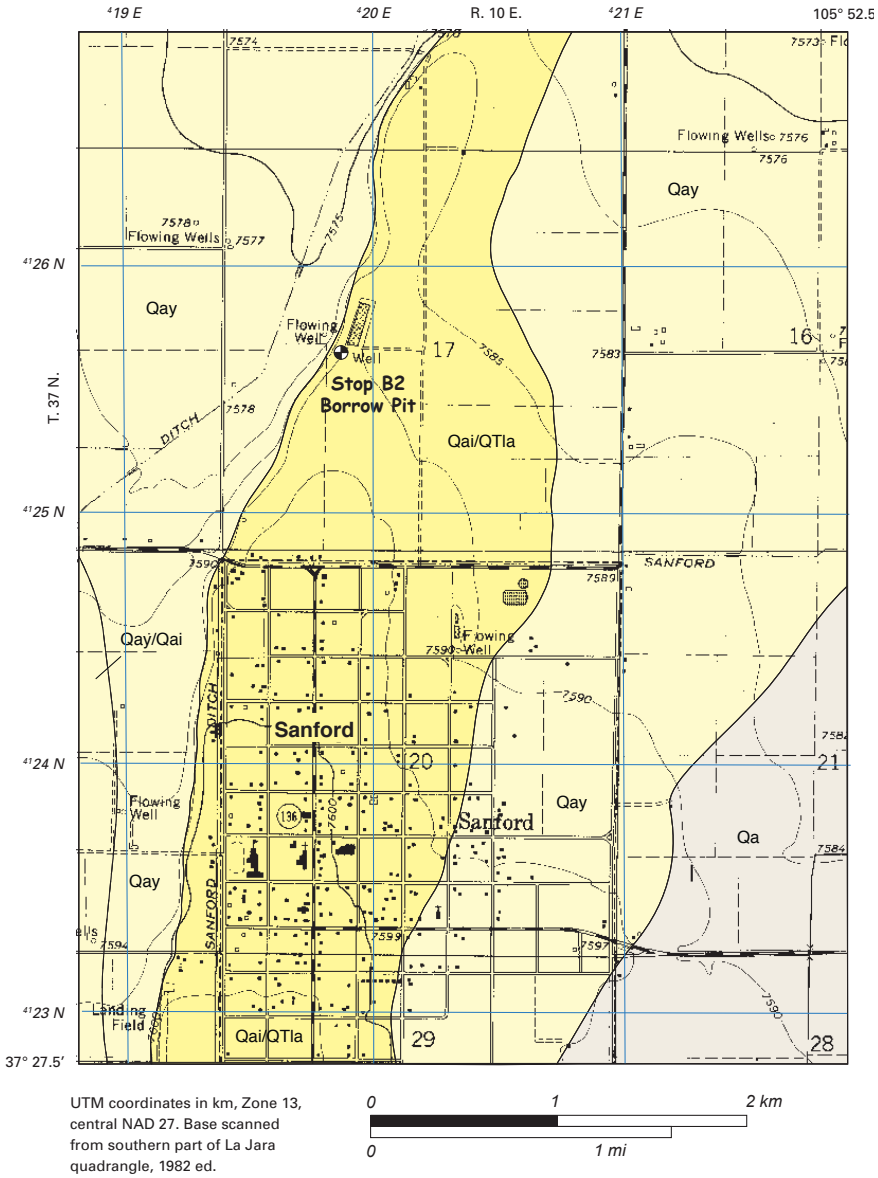

Figure B2–1. Alluvial deposits in the vicinity of the Sanford, Colo.; stop B2 is at the Mortensen sand and gravel pit. Map units: Qa, Holocene alluvium; Qay, younger (latest Pleistocene) alluvium; Qai, intermediate (middle Pleistocene) alluvium; QTla, Alamosa Formation (buried lacustrine deposits). Geology modified from Machette and Thompson, 2005.

Local Geology

The Mortensen pit is in alluvium composed of sand and pebble gravel, which has maximum clast sizes of 3–4 cm. Most clasts are derived from Tertiary volcanic rocks of the San Juan Mountains, either deposited directly from the source area or recycled from older alluvium (unit Qao) preserved above the ancient shorelines of Lake Alamosa to the southwest. At this stop and Sanford (in general), we are 20–25 m below the maximum shoreline elevation of Lake Alamosa, which is about 7,660 ft (2,335 m) asl. The material in the pit and underlying Sanford Ridge is mapped as intermediate-age alluvium (unit Qai, fig. B2–1) and may be only 2–3 m thick and, if so, rests unconformably on lacustrine sediment (unit QTla) of the Alamosa Formation (see chapter G in this volume for a discussion of Lake Alamosa). Sanford Ridge is surrounded by slightly lower surfaces formed on latest Pleistocene to Holocene alluvium (fig. B1–2). Shallow pits in these younger materials typically fill with water owing to a high water table in this part of the Alamosa subbasin. All of the alluvium in this area has been deposited by the Conejos River and adjacent tributary streams, which flow east and northeast from the eastern foothills of the San Juan Mountains.

Soils in the Mortensen Pit

As previously mentioned, exposures of alluvium at low elevations in this part of the Alamosa subbasin (of the San Luis Basin) are rare and then often water saturated. However, owing to the slightly higher elevation of Sanford Ridge with respect to adjacent surfaces, this pit is typically dry. The pit is on the western margin of the ridge, but the soils we see here have formed since the ridge was geomorphically isolated by downcutting (some unknown amount of time after deposition of alluvial unit Qai).

Soils exposed in the south wall of the pit (fig. B2–2) reflect varying degrees of development probably as a result of the site's relatively high altitude (7,590 ft or 2,313 m asl). Older soils at high elevations in the southwestern United States typically have formed in alternating climates (glacial, interglacial) that can cause losses and accumulations of carbonate both through time and space owing to vertical or lateral flow of water through the soil (see Machette, 1985). The two soils shown in figure B2–2 have differing characteristics: the soil at locality 1 has an A/Bt/Btk/Bk profile, whereas the soil at locality 2 (only 10 m to the west) has a Btk/Bk profile. The lack of A and Bt horizons at locality 2 probably reflect erosion of the soil along the margin of Sanford Ridge; conversely, its stronger and thicker Bk horizon may reflect lateral soil water flow (to the west) that has enhanced the accumulation of carbonate (that is, some of the carbonate may have precipitated from laterally flowing groundwater).

We made a quick description of the soil at locality 1 (fig. B2–3) several years ago but do not have laboratory data on its physical or chemical properties. Nevertheless, the thickness of the soil (<155 cm), presence of an argillic (Bt and Btk) horizon, and the strong carbonate morphology (stage III) suggest that this soil represents hundreds of thousands of years of formation at an altitude that is relatively high for accumulation of pedogenic carbonate.

Geologic History

The sediments exposed in the Mortensen pit reflect alluvial channel cutting and subsequent topographic reversal in response to drawdown of Lake Alamosa, which we believe occurred at about 440 ka (chapter G, this volume). As the lake dropped, so did base level for the streams emanating from the eastern part of the San Juan Mountains (such as the Rio Conejos and Rio Grande) and streams heading on the exposed lake floor, such as at stop B1. Stream channels cut into the exposed lake bottom sediment became filled with gravelly alluvium (unit Qai, fig. B2–1) as the area was transformed from a lake bottom to a piedmont slope, and the slightly more resistant alluvium in thick channels led to topographic reversal through time. This relationship is common in the southwestern part of the lake basin. Subsequent erosion (eolian and fluvial) of the lake deposits (mainly silts here) caused a topographic reversal,

Figure B2–2. South wall of the Mortensen pit (informal name). Pit is not active, and exposures are poor. However, 1–1.5 m of soil is exposed at the two labeled spots. Locality 1—Argillic B horizon over discontinuous Bk horizon. This is the locality for the soil profile shown in fig. B2–3. Locality 2—A and weak B horizons over well developed Bk horizon. View to south; town of Sanford is in background, about 1 km to south.

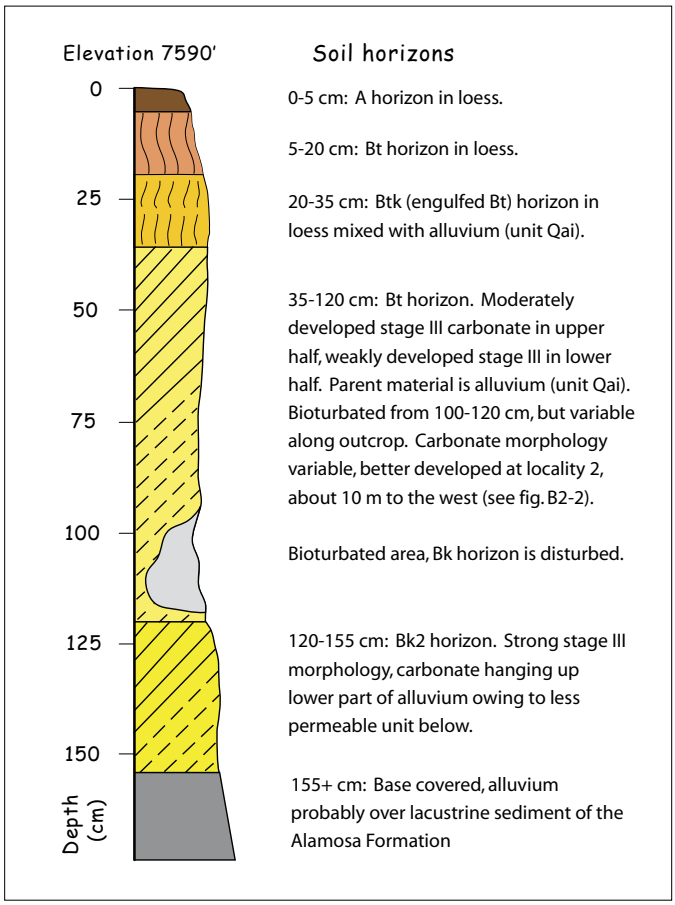

Figure B2–3. Schematic section showing soil profile at locality 1 (fig. B2–2), south wall of the Mortensen pit, as of June 2004.

such that unit Qai sits above younger alluvial deposits. In fact, just from inspecting topographic maps of the area it is obvious that most of the cemeteries are built on ridges of unit Qai alluvium for two reasons: they are high and dry.

The unit Qai ridges seen at this and the previous stop extend basinward to minimum elevations of about 7,530–7,540 ft or 2,295–2,298 m) asl, which probably reflect the base level of the Rio Grande once the gorge was cut through the San Luis Hills. The Rio Grande's channel is presently at about 7,500 ft (2,286 m) asl at the same latitude as the distal ends of the unit Qai ridges, thus there has been about 30–40 ft (9–12 m) of additional stream incision since the gorge was cut through the Fairy Hills (see stop B4).

Conclusions

The Mortensen pit contains excellent but shallow exposures of strongly developed soils on intermediate-age (unit Qai) alluvium. The alluvium fills channels of the ancient Rio Conejos, which extended its course basinward after middle Pleistocene Lake Alamosa was drained. The lacustrine sediment beneath stop B2 represents the uppermost preserved part of the Alamosa Formation, which underlies almost the entire San Luis Valley north of the San Luis Hills. Thus, the Mortensen pit is an excellent location to observe the degree of soil development on alluvium that postdates the draining of ancient Lake Alamosa. These soils represent hundreds of thousands of years of formation, but they are not as strongly developed as the soils on the highest shoreline deposits of Lake Alamosa (see stops B3 and B4), which appears to have culminated in overflow at about 440 ka (see more complete discussion of Lake Alamosa in chapter G, this volume).

Stop B3 — Soils on and Experimental Dating of Lacustrine Gravels of Lake Alamosa at Saddleback Mountain

Speakers: Michael Machette and David Marchetti
Location: Gravel spits on south face of Saddleback Mountain, about 3 mi (4.8 km) east of Sanford, Colo.; 1.5 mi northeast of bridge over Rio Costilla
Pikes Stockade 7.5' quadrangle (Stations PS–MM04–29a, PS–MM04–29b, and PS–MM05–72)
GPS: NAD27, Zone 13, 425340 m E., 4123725 m N.
Elevation: About 7,575 ft (2,309 m) asl (base of slope at turn off from paved road)

Synopsis

This stop is a key location for understanding the extent and age of Lake Alamosa. Two spits perched on the southern side of Saddleback Mountain provide unequivocal evidence for the presence of a large ancient lake (Lake Alamosa) that occupied the San Luis Basin, probably during the Pliocene and Pleistocene. Soils on these spits show strong development of calcic (Bk) horizons, which suggest a middle Pleistocene age for the spits.

The lower (stop B3.1) and upper (stop B3.2) spits were trenched in order to describe the soils formed on the lacustrine gravels and to sample for a variety of experimental cosmogenic nuclide and U/Th dating techniques. At the time this report was written, only surface-exposure dating using ^{3}He isotopes had been completed. This technique yielded an age of 439±6 ka from a single bedrock boulder (stop B3.3); thus, for the purposes of discussions of Lake Alamosa we use a time of 440 ka for its overflow and the Rio Grande's subsequent incision of the Fairy Hills.

Introduction

Saddleback Mountain, the elongate bedrock ridge north of the road, is formed by subhorizontal volcanic flows of the upper Oligocene to Miocene Hinsdale Formation (fig. B3–1). These flows are silicic alkali-olivine basalts with as much as 40 percent phenocrysts of olivine and clinopyroxene. In the San Luis Hills, these basalts have been dated at about 26 Ma (see Thompson and Machette, 1989; Dan Miggins, written commun., 2006). At Lake Alamosa's highest stand (about 7,660 ft asl), Saddleback Mountain was an island in the southern part of the lake. At this elevation, the lake extended westward to the eastern margin of the San Juan Mountains (near Monte Vista) and northward, nearly to Saguache, a distance of about 55 mi (88 km). Thus the lake had a long fetch to the northwest, and during large storms waves eroded the northern face of Saddleback Mountain and other bedrock hills to the east of this stop.

Local Geology and Climate

Young gravelly alluvium (units Qaa, Qaa, Qfp, and Qay) that surrounds the northern and western sides Saddleback Mountain was deposited by the Rio Conejos, which eroded into a preexisting platform of fine-grained lacustrine sediment of the Alamosa Formation (unit QTla, fig. B3–1). However, to the east and south of Saddleback Mountain both coarse- and fine-grained deposits of Lake Alamosa are preserved to the leeward (south) of the mountain. The fine-grained deposits are poorly exposed and highly eroded, whereas the coarse-grained deposits are preserved in gravelly spits on the south side of Saddleback Mountain and as gravel-capped, bedrock-cored saddles between hills (note: the road east from here passes through such a saddle). Younger lacustrine deposits (unit Qla, fig. B3–1), which are probably reworked from sediment of the Alamosa Formation, typically occupy playas in topographic depressions, such as the one south of Saddleback Mountain.

The bouldery spits at stop 3, rich in basaltic clasts of the Hinsdale Formation, are key to understanding the extent and age of Lake Alamosa. Two spits are present here; at most localities only one spit, shoreline or barrier bar is preserved at these elevations. However, multiple barrier bars and back-bar lagoons such as at stop B6 record a rising Lake Alamosa, prior to its overflow through the Fairy Hills (see stop B4). Here at stop 3, we have an opportunity to see constructional features of Lake Alamosa, a Pliocene to middle Pleistocene lake that occupied most of the San Luis Basin north of the San Luis Hills.

The spits at stop B3 were formed by long-shore (southwest) transport of eroded bedrock blocks and subsequent deposition of sandy cobble to boulder gravels on the leeside of Saddleback Mountain (figs. B3–2, B3–3). The tops of both spits are planar and gently east sloping, which reflects deposition into deepening water to the south and southeast of Saddleback Mountain.

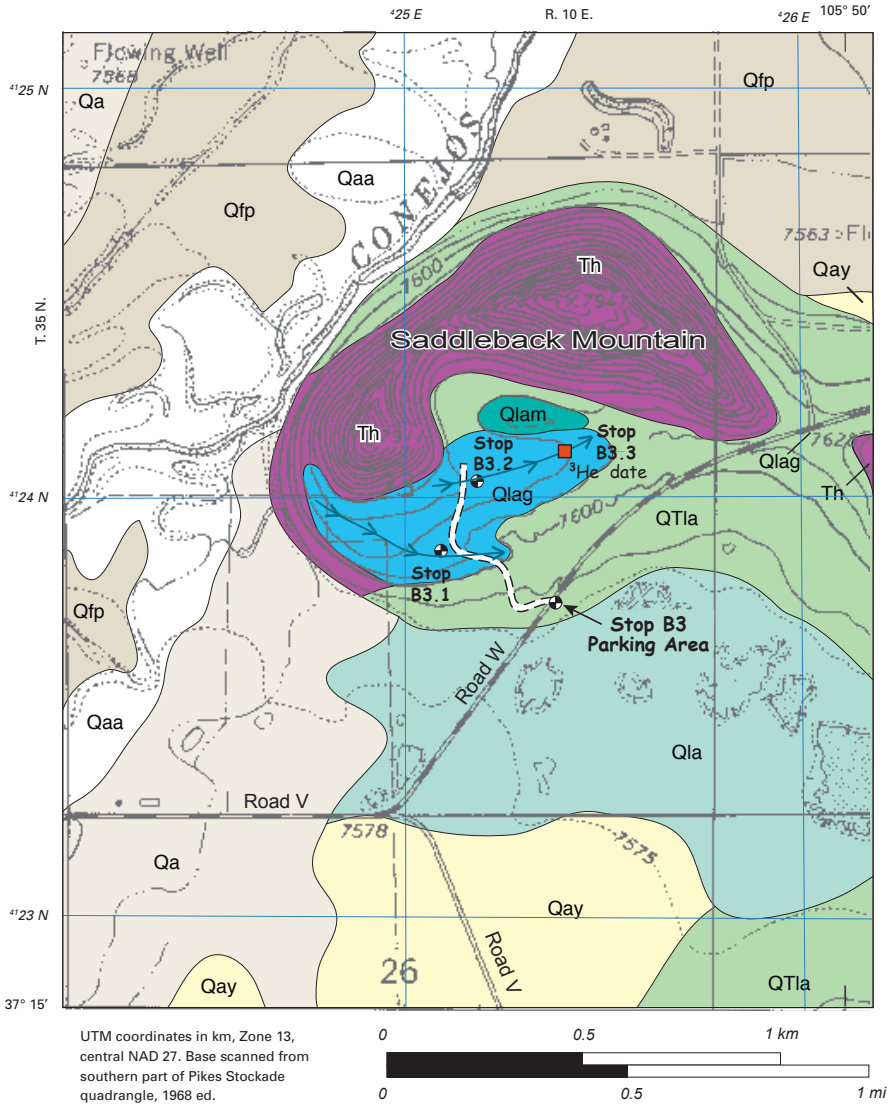

Figure B3–1. Bedrock, alluvial deposits, and lacustrine deposits of Lake Alamosa. Map units: Qaa, active alluvium; Qa, Holocene alluvium; Qfp, floodplain alluvium; Qay, younger (late Pleistocene) alluvium, Qla, lacustrine deposits (post-Lake Alamosa); Qlag (gravelly) and Qlam (lagoonal) near-shore deposits of Lake Alamosa (middle Pleistocene part of QTla); QTla, Alamosa Formation (undivided, fine grained deposits here), and Hinsdale Formation (26 Ma). Geology modified from Machette and Thompson, 2005.

The elevation in this part of the basin ranges from about 7,550 to 8,000 ft asl, so it is a little surprising (to Machette) to find abundant, thick calcic soils on the older landscapes (see also, stops B1 and B2). However, the climatic conditions are conducive to their formation now and apparently in the past also. Modern climatic conditions in Alamosa, about 15 mi (24 km) to the north of this stop, are cold (41°F or 5°C mean annual temperature (MAT)) and relatively dry (about 7 in. or 180 mm mean annual precipitation (MAP)) on average for the year (see http://www.wrcc.dri.edu). These conditions are well within the normal limits of pedocal formation (see Machette, 1985). Rainfall increases slightly across the basin as you gain distance from the San Juan Mountains, which creates a strong rain shadow in the San Luis Valley. Glacial climates must have been considerably colder and probably drier than present, thus preventing massive leaching of calcium carbonate from the soil.

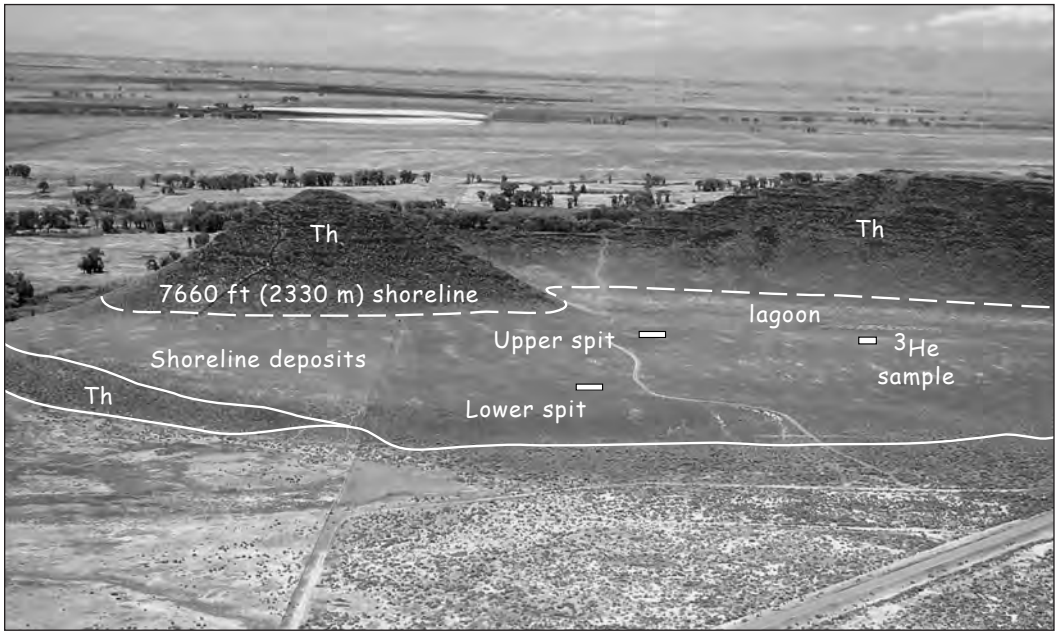

Figure B3–2. Oblique aerial photograph of the south side of Saddleback Mountain, location of stop B3. Unit Th, Hinsdale Formation (upper Oligocene andesitic basalt). View to the northeast.

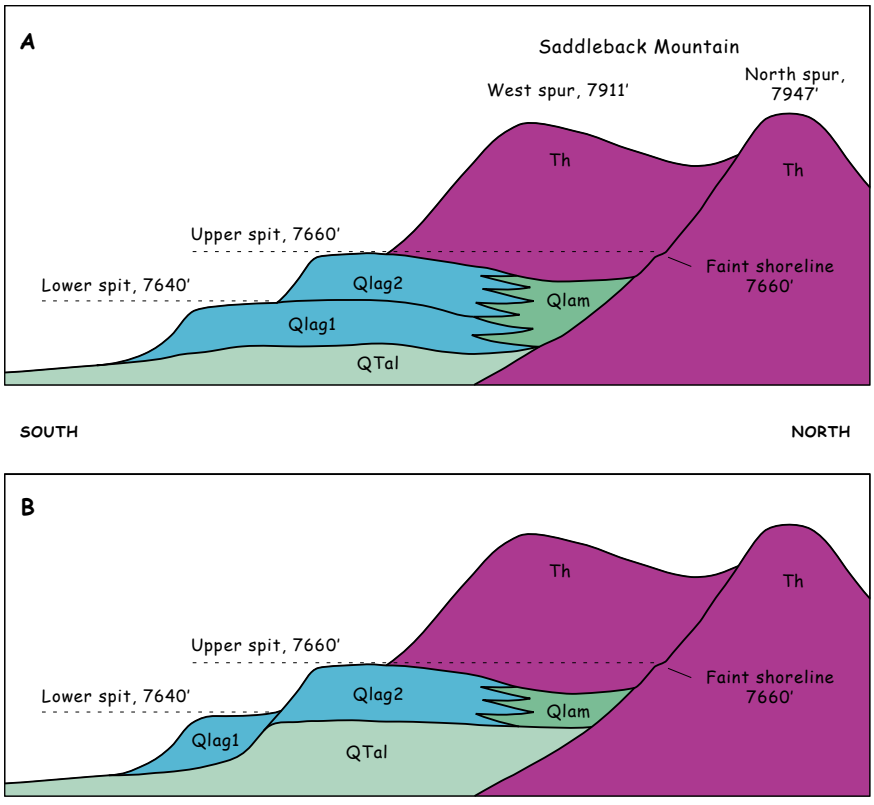

Fig. B3–3. Schematic cross section of surficial and bedrock geology at Saddleback Mountain, location of stop B3. *A*) Stacked spits (Qlag1 is older than Olag2). *B*) Superposed spits (Qlag1 is younger than Olag2). Map units: Qlam, lagoonal deposits of Lake Alamosa; Qlag, gravel (spit) deposits of Lake Alamosa (Qlag1, lower spit; Qlag2, upper spit); QTal, Alamosa Formation, undivided; Th, Hinsdale Formation (upper Oligocene andesitic basalt). View to the west. Based on geologic mapping of Machette and Thompson, 2005.

Stop B3.1 — Lower Spit, Soil Profile

Location: Lower of two spits, filled soil pit
Pikes Stockade 7.5' quadrangle (Station PS–MM04–29b)
GPS: NAD27, Zone 13, 425107 m E., 4123885 m N.
Elevation: 7,640 ft (2,329 m) asl

Overview

The lower spit has a very well developed calcic soil that is morphologically identical to the soil on the upper spit (stop B3.2), but it is not as well developed in terms of thickness and total carbonate. In New Mexico to the south, similar calcic soils are formed on middle Pleistocene deposits. Considering the site's semiarid climate and high elevation (7,640 ft or 2,329 m asl), this soil is particularly well developed in a noncalcareous sandy basalt-rich gravel.

Soil Development

The soil is formed in basaltic gravel (fig. B3.1–1) that has no easily weatherable source of Ca^{++}. The entire Bk horizon is about 95 cm thick and has a maximum stage III morphology with a maximum of 50 percent $CaCO_3$ in the <2 mm portion of the Bk2 horizon (fig. B3.1–2). Texturally, the parent material for this soil is a sandy silt, with about 25 percent <2 mm matrix in a coarse cobble to boulder gravel. Textural analyses of the soil (see data in table B3.2–1) show a dominance of sand in the profile, but the silty component (as much as 41 percent) may be lacustrine in origin or be deeply translocated dust. Chittick analyses of the lowest Bk subhorizon show 3.8 percent $CaCO_3$ in the <2 mm fraction; thus, we estimated that the parent material has only 1.0 percent $CaCO_3$ in the <2 mm fraction.

At lower elevations of about 4,500–5,500 ft (1,370–1,675 m) asl in New Mexico to the south, morphologically similar soils are middle Pleistocene in age (Machette, 1985; Machette and others, 1997). Thus, the relict calcic soil on the lower spit is particularly well developed considering it is in a semiarid climate and at a high elevation (7,640 ft or 2,329 m asl).

Although we cannot prove the stratigraphic relations between the lower and upper spits, we consider the lower one to be slightly younger and project under the upper spit (as shown schematically in fig. B3–3A). If the lower spit is younger than the upper spit (fig. B3–3B), it would be evidence for a multistage drawdown of the lake (rather than a single drop) as the Rio Grande cut a gorge through the Fairy Hills (see stop B4) in an intermittent manner.

Figure B3.1–1. Soil- and cosmogenic-sampling pit at stop B3.1 on the lower spit (unit Qlag1) at Saddleback Mountain. Pit is about 2.5 m deep in coarse sandy gravel. View to the southwest.

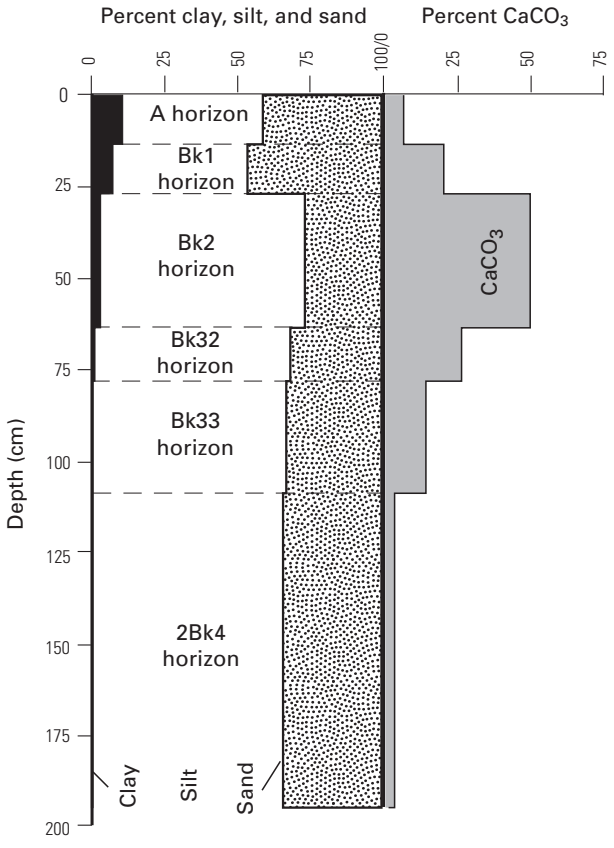

Figure B3.1–2. Profile data for soil on lower spit, stop B3.1.

Stop B3.2 — Upper Spit, Soil Profile and Experimental Dating

Location: Upper of two spits, filled soil pit.
Pikes Stockade 7.5' quadrangle (Station PS–MM04–29a)
GPS: NAD27, Zone 13, 425136 m E., 4124048 m N.
Elevation: 7,660 ft (2,335 m) asl

Overview

The upper spit has a very well developed calcic soil that is morphologically identical to the soil on the lower spit, but it contains about 30 percent more calcium carbonate (on a total profile basis). The Bk horizon (undivided) is about 40 cm thicker and has a maximum of 64 percent $CaCO_3$ in the <2 mm portion of the Bk2 horizon.

Marchetti obtained a single ^3He surface-exposure age of 439±6 ka for a large boulder on this spit (see discussion in stop B3.3 and chapter G). However, in order to date the spit further, we sampled for three other experimental techniques: U-series dating of carbonate pendants and terrestrial cosmogenic nuclide (chlorine and helium) dating of soil-depth profiles. Unfortunately, none of the results from these other techniques were available when this discussion was written in the spring of 2007.

Soil Development

Soils on the upper and lower two spits (and two other sites) were described by Alan Stuebe (fig. B3.2–1) of the National Resource Conservation Service in Alamosa. Janet Slate (USGS) and Michael Machette sampled for soil and cosmogenic-chlorine analyses at the same time. The backhoe pits in the soils were about 2.5 m deep, but they quickly filled with loose materials so we sampled from the bottom up.

Figure B3.2–1. Alan Stuebe preparing to describe the soil on the upper spit (unit Qlag2) at Saddleback Mountain, stop B3.1. Alan is with the National Resource Conservation Service (formerly SCS) in Alamosa and has mapped tens of thousands of square kilometers of soils in the San Luis Valley.

As with the lower spit, this soil is formed in basaltic gravel (fig. B3.1–1) and thus has no easily weatherable source of Ca^{++}. The entire Bk horizon is about 150 cm thick and has a maximum stage III morphology and about 64 percent $CaCO_3$ in the <2 mm portion of the Bk2 horizon (fig. B3.2–2). The parent material for this soil is very gravelly sandy silt that contains about 25 percent <2 mm matrix in a coarse cobble to boulder gravel. Textural analyses of the soil (fig. B3.2–3; see also data in table B3.2–1) shows a dominance of silt (as much as 65 percent) in the <2 mm fraction; thus, much of the silt may be lacustrine in origin or deeply translocated eolian dust. The lowest Bk subhorizon has an estimated 4 percent $CaCO_3$ in the <2 mm fraction; thus, we assumed that the parent material has only 1.0 percent $CaCO_3$ in the <2 mm fraction (these assumptions are based on the soil on the lower spit).

Carbonate Accumulation

We have calculated calcium carbonate accumulation rates at this site for comparison with rates at other sites in New Mexico, mainly as a relative dating tool. One can approximate the total amount of $CaCO_3$ in a soil profile from the following parameters for each horizon as shown in table B3.2–1: thickness (column C), percent <2 mm fraction (column H), percent $CaCO_3$ in the <2 mm fraction (column I), and bulk density of the <2 mm fraction (column J). For a more complete discussion of this method, see Machette (1978, 1985). The only fraction of pedogenic $CaCO_3$ not accounted for in the following discussion are the thick pendants (rinds) that have accumulated on the base of some clasts. We suspect that this component might add as much as 10 percent to the calculations shown in table B3.2–1.

The two soils that we analyzed have quite different amounts of pedogenic $CaCO_3$: the lower spit (stop B3.1) has about 26.6 g of $CaCO_3$ per cm^2 column through the soil, whereas the upper spit (stop B3.2) has about 35.0 g (30 percent more). Using 30±5 g as an average value and a duration of soil formation of 440 ka (see following discussion of ^3H dating, stop B3.3) yields a long-term accumulation rate of about 0.074 g/cm^2/1,000 yr. The upper spit contains the most carbonate; using its 35 g content yields a rate of about 0.080 g/cm^2/1,000 yr. By comparison, soils that Machette (1985) considered to be about 0.5 Ma in New Mexico had much higher calculated accumulation rates of 0.2–0.4 g/cm^2/1,000 yr. However, new dating control for the deposits that host these soils show that they may be as much as five times older than considered in 1985, reducing the New Mexico accumulation rates to only 0.04–0.08 g/cm^2/1,000 yr. Thus, the maximum rate of 0.080 g/cm^2/1,000 yr calculated for that this stop suggests that calcic soils in the San Luis basin may have accumulated as fast as those in Albuquerque.

The calculated total pedogenic $CaCO_3$ contents of 26.6–35 g per cm^2 of soil column from the spits reflects only the $CaCO_3$ retained in their soils. The wide variability in the amount and morphology of $CaCO_3$ seen in soils in this area suggests that former glacial or pluvial climates and vegetation (for instance, forests) may have caused leaching and

Table B3.2–1. Physical and calcium carbonate data for relict soils on spits of Lake Alamosa, Saddleback Mountain, stop B3.

Sample	Depth (thickness) (cm)	Horizon	<2 mm texture	Percent sand, 64–2000 µm	Percent silt, 2–64 µm	Percent clay, <2 µm	Percent <2 mm	$CaCO_3$ content (percent)	Bulk density (g/cm^3)	$CaCO_3$ concentration (g/cm^3)	Horizon $CaCO_3$ (g/cm^2)	Cumulative profile $CaCO_3$ (g/cm^2)
A	B	C	D	E	F	G	H	I	J	K	L	M
Stop B3.1. Soil from lower spit, Saddleback Mountain (samples PS–MM04–29b)												
–S1	0–14 (14)	A	Silty sand	60.6	29.1	10.3	95	6.1	1.55e	0.10	1.3	1.3
–S2	14–27 (13)	Bk1	Silty sand	59.9	33.4	6.7	50	20.0	1.77	0.18	2.3	3.6
–S3	27–64 (37)	Bk2	Silty sand	56.2	41.0	2.8	45	50.2	1.70e	0.38	14.2	17.8
–S4	64–79 (45)	Bk32	Sand	81.9	16.8	1.3	35	25.9	1.65e	0.15	6.7	24.5
NS	79–109 (30)	Bk33	Sand	85e	14e	1e	35e	15e	1.6e	0.08	2.5	27.0
–S5	109–195 (86)	2Bk4	Sand	91.0	8.3	0.7	25	3.8	1.6e	0.02	1.3	28.3
NS	(195)	PM	Sand	-----	-----	-----	50e	1.0	1.55e	0.008	–1.7	26.6
Stop B3.2. Soil from upper spit, Saddleback Mountain (samples PS–MM04–29a)												
–S1	2–11 (9)	A	Silty sand	42.2	44.9	12.9	95	8.7	1.54	0.127	1.1	1.1
–S2	11–38 (27)	Bk1	Silty sand	47.4	43.5	9.1	40	28.7	1.6e	0.18	5.0	6.1
–S3	38–83 (45)	Bk2	Sandy silt	26.9	64.9	8.2	35	64.3	1.7e	0.38	17.2	23.3
–S4	83–147 (64)	Bk3	Sandy silt	32.4	59.8	7.8	35	21.6	1.6e	0.12	7.7	31.0
–S5	147–160 (13)	Bk4	Sandy silt	33.9	56.1	10.0	30	26.7	1.6e	0.13	4.1	35.1
NS	160–220 (60)	2Ck	Sandy silt	35e	60e	5e	25	4.0e	1.55e	0.04	1.6	36.7
NS	(220)	PM	Sandy silt	-----	-----	-----	50e	1.0	1.55e	0.008	–1.7	35.0

Abbreviations: e, estimated value; NS, not sampled (or analyzed); PM, parent material.

Notes on calculated values:

Column C—PM, parent material. Values assumed based on typical noncalcareous, sandy beach (spit) gravels. These are used to calculate primary carbonate (see Machette, 1978 and 1985; Machette and others, 1997).

Column K—Concentration of $CaCO_3$ (g/cm^3) in each horizon calculated as column H (percent)/100 x column I (percent)/100 x column J (g/cm^3).

Column L—Total $CaCO_3$ (g/cm^2) in each horizon calculated as column B (cm) x column K (g/cm^3).

Column M—Cumulative $CaCO_3$ (g/cm^2) in each profile is calculated as sum of values in column L, from the surface though the entire Bk horizon.

Figure B3.2–2. Upper 1.2 m of calcic soil formed on the upper spit (unit Qlag2) at Saddleback Mountain, stop B3.2. Backhoe excavating arm for scale.

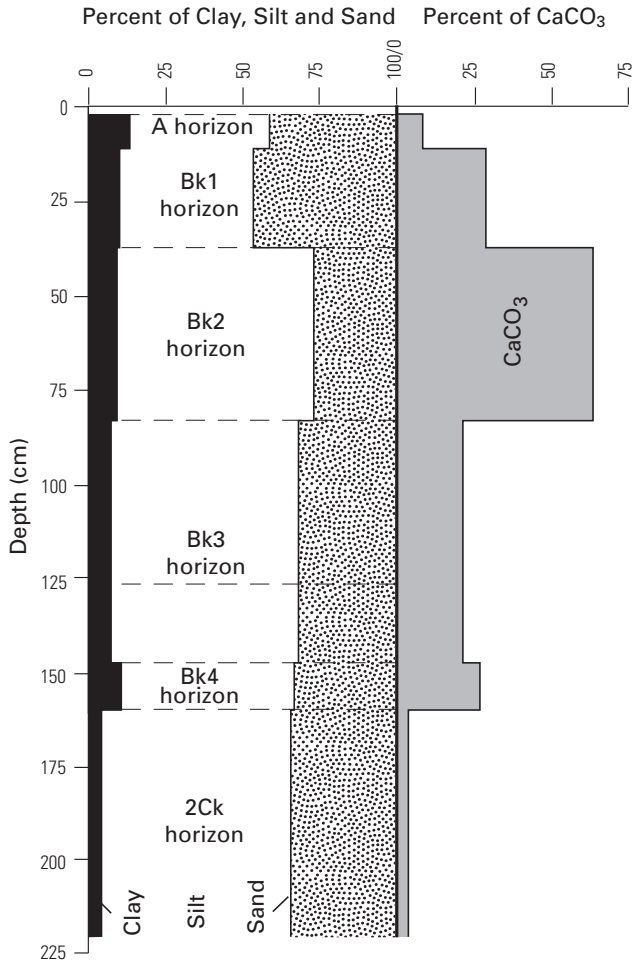

Figure B3.2–3. Profile data for soil on the upper spit, stop B3.2.

losses of previously accumulated $CaCO_3$. As one moves upslope to higher, forested elevations, $CaCO_3$ accumulations in soils become discontinuous and spotty, even at the outcrop level. Thus, as one approaches the pedocal-pedalfer boundary at high elevation or moist sites, studies of total pedogenic $CaCO_3$ contents make it more difficult to assume steady-state processes for soil formation in this region (Machette, 1985; Birkeland, 1999).

Experimental Age Dating

In an effort to date the highest (and youngest) shorelines of Lake Alamosa, we have focused on these spits. In addition to the relative degree of soil development and the calculations of total $CaCO_3$ accumulation, we are attempting to use a variety of isotopic techniques to date the time of deposition of the spits. These spits have been trenched several times to sample for specific dating techniques:

1. Surface-exposure dating (basalt boulders) using ^3He isotopes. These analyses were done in 2006 at the University of Utah's Noble Gas Laboratory (Salt Lake City) by David Marchetti (see Machette and Marchetti, 2006). This technique can date the exposure of eroded boulders that have been at the surface as long as 1.0 million years if they have the appropriate mineralogy (olivine or pyroxene).

2. Terrestrial cosmogenic nuclide profile dating using ^3He isotopes. David Marchetti is performing these analyses at the University of Utah's Noble Gas Laboratory (Salt Lake City). This technique uses small gravel clasts collected through a vertical profile at least 2–3 m deep and can date deposits as old as 1 Ma if they have the appropriate mineralogy (olivine or pyroxene).

3. Terrestrial cosmogenic nuclide profile dating using ^{36}Cl isotopes. These analyses are being performed by the PRIME Lab at Purdue University (Lafayette, Indiana) and the modeling work is being done in cooperation with Fred Phillips of New Mexico Institute of Mining and Technology (Socorro). This technique (see Gosse and Phillips, 2001) uses small gravel clasts collected through a vertical profile at least 2–3 m deep, and it can date deposits as old as 300 ka.

4. Experimental U/Th dating using a laser-ablation mass-spectrometer techniques (see Sharp and others, 2005). These analyses are being done as part of a cooperative project with Warren Sharp at the University of California at Berkeley Geoscience Center. This technique uses calcium-carbonate rinds on the bases of large clasts. The best rinds are typically in the Bk horizon of a thick calcic soil. The technique can date deposits as old as 750 ka if they have small amounts of detrital thorium, are dense (not porous), and are a closed system (for example, no dissolution and reprecipitation).

At the time this report was written (spring 2007), only the surface-exposure dating using ^3He isotopes had been completed. This technique yielded an age of about 439±6 ka for the boulder; thus, for the purposes of discussions of Lake Alamosa we use a time of 440 ka for its overflow and lowering.

Stop B3.3 — Upper Spit, ^{3}He Surface-Exposure Dating

Location: 1-m-diameter basalt boulder on upper spit
Pikes Stockade 7.5' quadrangle (Station PS–MM05–72)
GPS: NAD27, Zone 13, 425353 m E., 4125111 m N.
Elevation: 7,650 ft (2,332 m) asl

Overview

The upper spit has a large number of basalt boulders at the surface but most of them have been eroded by sand blasting (formation of ventifacts), or may have been split or spalled by weathering processes such as freeze-thaw, fires, or thermal expansion. The largest unweathered-appearing boulder on this upper spit is located about 220 m east of the soil pit (stop B3.2). Cosmogenic surface-exposure dating of this single 1-m diameter, best-candidate boulder (sample PS–MM05–72He) yielded a ^{3}He age of 439±6 ka, which should reflect the length of time that this boulder has been exposed to cosmic radiation and thus provide a minimum time for the overflow and draining of Lake Alamosa.

Figure B3.3–1. Largest boulder on the upper spit of Saddleback Mountain. The upper 2–3 cm (left of the GPS receiver) of this 1-m-wide boulder was sampled for ^{3}He surface-exposure dating. Notebook (15 x 25 cm) for scale. Sample locality is shown on figures B3–1 and B3–2.

^{3}He Surface Exposure Dating—Results

Although the other dating results (see below) are still pending, we have been able to date the upper spit at Saddleback Mountain (stop B3.3) using ^{3}He isotopes. At this locality, the spits are composed almost entirely of reworked basalt boulders and lacustrine silty sand. The basalt boulders start out as angular blocks, but they are rounded and abraded in the surf zone as they are transported (slowly) around the west side of the Saddleback Mountain, a minimum of about 400 m to 1 km. The largest exposed basalt boulder is 1 m in diameter (fig. B3.3–1), of which 30–40 cm is exposed above the ground surface. The basalt boulders have mineralogy suitable for ^{3}He dating since they contain phenocrysts of olivine and pyroxene, two minerals that retain cosmogenic He isotopes. At least three sources of error common to surface exposure dating could be at play here:

1. Inheritance of ^{3}He isotopes from rock surfaces that were exposed to cosmic radiation—this makes reported ages too old,
2. Excessive erosion of a boulder surface (owing to various processes)—this makes reported ages too young, and
3. Shielding of a boulder surface (by snow or sand)—this makes reported ages too young.

Various strategies are employed to minimize or eliminate these potential errors, such as selecting long-transported boulders (error source 1), selecting rounded, nonpitted, or fresh-appearing boulders (error source), and selecting large (high) boulders in areas of minimum sand cover. We believe that we selected the best possible boulder for dating on these spits; however, a larger dated number of boulders (such as 6–8) would allow us to see if there is a preferred exposure age. Since so few boulders are candidates for this method, we have pursued other allied dating techniques (see following discussion).

A pyroxene separate from the surface of the large boulder (sample PS–MM05–72He) yielded a preliminary ^{3}He exposure age of 439±6 ka. This age was determined using the total ^{3}He concentration and an absolute ^{3}He production rate of 116 atoms gram^{-1} year^{-1} (Licciardi and others, 1999) that was scaled to the sample's altitude and latitude using Lal (1991) (see table B3.3–1). Pyroxenes from rocks with older (>1–2 Ma) crystallization ages can have significant noncosmogenic ^{3}He from nucleogenic reactions on ^{6}Li (^{6}Li (n, α) ^{3}H$\rightarrow^3$He). Marchetti and Cerling (2005) and Marchetti and others (2005) used samples shielded from cosmic radiation to account for noncosmogenic ^{3}He in pyroxenes from intermediate volcanic rocks exposed on the western edge of the Colorado Plateaus Province in Utah.

The volcanic rocks in those studies are remarkably similar in terms of crystallization age (~25 Ma) and petrology to the sample we dated in this study (~26 Ma; Hinsdale Formation, unit Th on fig. B3–1). Applying the ^{3}He/^{4}He shielded correction of Marchetti and others (2005) to the He data of the sample in this study changes the exposure age only slightly, from 439 to 431±6 ka (see table B3.3–2), and does not change our interpretation of the age of the spits. A more complete discussion of ^{3}He surface-exposure dating is included in chapter G, this volume.

Table B3.3–1. Sampling data for ^{3}He surface-exposure dating of basalt at stop B3.3.

Sample	Latitude (N)	Longitude (W)	Altitude (m)	Topo shielding factor	Self-shielding factor	Total shielding factor	^{3}He Production Rate (atoms g^{-1} year^{1})*
PS-MM05-72c	37.262416	105.842416	2324	0.999	0.942	0.941	598

*Determined using an absolute ^{3}He production rate of 116 atoms g^{-1} yr^{-1} (Licciardi et al., 1999) that was scaled using Lal (1991). No corrections for potential snow shielding were applied to the production rate.

Table B3.3–2. He isotope data for cosmogenic surface-exposure dating of basalt at stop B3.3.

Sample	$^{4}He_{total}$ (10^{12} atoms g^{-1})	$^{3}He_{total}$ (10^{6} atoms g^{-1})	^{3}He/^{4}He fusion	$^{3}He_{c}$ (10^{6} atoms g^{-1})	$^{3}He_{c}$ %	Exposure age (ka) ± 2σ
PS-MM05-72c	22.92±0.06	262.5±3.5	1.15 x 10^{-5}	262.5±3.5	100	**439 ± 6**
PS-MM05-72c*	22.92±0.06	262.5±3.5	1.15 x 10^{-5}	257.7±3.5	98.2	**431 ± 6**

*Sample corrected using an estimated ^{3}He/^{4}He correction. The $^{3}He_{c}$ (cosmogenic) component was determined using the following relationship: $^{3}He_{c} = {}^{3}He_{total} - ({}^{4}He_{total} \times {}^{3}He/{}^{4}He_{shielded})$. Where the $^{3}He/^{4}He_{shielded}$ is from Marchetti et al. (2005), and is 2.08×10^{-6}.

Conclusions

Using the ^{3}He surface exposure date of 439 ka, we conclude that the upper spit at Saddleback Mountain was deposited at about 440 ka, which roughly corresponds with the glaciation during marine oxygen-isotope stage 12 which, in turn, appears to have ended between 452 ka and 427 ka (see chapter G). Marine oxygen-isotope stage 12 is associated with one of coldest glacial climates and, by inference, most extensive glaciations in North America (see fig. G–5, chapter G, this volume). The age of 440 ka should reflect the time since this boulder was exposed to cosmic radiation, and thus it provides a minimum time for the overflow and draining of Lake Alamosa.

Stop B4 — Overview of the Rio Grande Outlet

Speakers: Michael Machette and Ren Thompson
Location: Overlook, east of BLM Road 5003, west side of Rio Grande, about 3.6 mi (5.8 km) south of Lasauses, Colo.; about 1.5 mi southeast of Lasauses Cemetery
Mesito Reservoir 7.5' quadrangle
GPS: NAD27, Zone 13, 433780 m E., 4118190 m N.
Elevation: 7,610 ft (2,319 m) asl (turn around point overlooking river)

Synopsis

This scenic overview of the Rio Grande is located near the overflow point of Lake Alamosa. The gap between the Fairy Hills and Brownie Hills to the south of here is the lowest point in the San Luis Hills, and thus it represented the first opportunity for a rising Lake Alamosa to overtop a hydrologic sill. Overflow of the lake through the Fairy Hills cut a deep, narrow gorge and allowed the lake waters to drain southward across the Costilla Plain and northern Taos Plateau, eventually joining the Red River and Rio Grande, west of Questa, N. Mex. In addition, stop 4 is near the point where Jacob Fowler described the first account of Lake Alamosa—in 1811–12.

On the route to our lunch stop (B4), we drove uphill and across a bedrock-cored saddle, just north of stop B4.1. This saddle is covered with small rounded pebbles of reworked volcanic rock from the adjacent slopes. These gravels represent low-energy, beach (shoreline) deposits of Lake Alamosa at its highest stand (about 7,660 ft or 2,335 m asl). A soil pit excavated about 20 m west of this gravel road exposed sandy

pebble to small cobble gravel that was deposited just offshore (west of) the highest shoreline. Further west, gullies expose fine-grained sand, silt, and marl that represent deeper water, offshore deposits (Alamosa Formation) of Lake Alamosa.

Discussion

Our lunch site on this small rounded hill of Tertiary volcanic rock provides a popular and scenic overview of the Rio Grande, opposite the Indian Cave. Here, we are located near the overflow point of Lake Alamosa and below a bedrock sill (to the west of the fork in BLM Road 5003) at about 7,650 ft (2,332 m) asl. This sill is devoid of gravel, probably having been swept clean during the overflow of the lake. About a half mile (0.8 km) north (at optional stop 4.1), abundant well-rounded pebbles attest to wave action and shoreline erosion at elevations of 7,650–7,660 ft (2,332–2,335 m) asl, which is about 185 ft (56 m) above the present river channel.

The gap between the Fairy Hills and Brownie Hills is the lowest point in the San Luis Hills, and thus it represented the first opportunity for a rising Lake Alamosa to overtop a hydrologic sill. Overflow of the lake though the Fairy Hills cut a deep, narrow gorge and allowed the lake waters to drain southward across the Costilla Plain and northern Taos Plateau, eventually joining the Red River and Rio Grande, west of Questa, N. Mex.

In 1821–22, Jacob Fowler made his way up the Rio Grande on a hunting and trapping expedition. This expedition preceded those of pioneer scientists and geographers such as Hayden and Powell by more than 50 years and settlement of the area by about 30 years. (San Luis, the oldest town in Colorado, was established in 1854.) Fowler was obviously a keen observer of topography and geography. His journals include this prescient passage that is particularly relevant to our lunch stop, probably near where he recorded the following note (from Siebenthal, 1910, p. 112–114).

> *"I Have no doubt but the River from the Head of those Rocks up for about one Hundred miles Has once been a lake of about from forty to fifty miles Wide and about two Hundred feet deep—and that the running and dashing of the Watter Has Woren a Way the Rocks So as to form the present Chanel."*

We suspect that Jacob Flower made this observation from the San Luis Hills (probably in the Fairy Hills, above the river's gorge near here), looking north into the upper San Luis Valley. Jacob accurately estimated the size, depth and overflow history of the lake—185 years ago (see chapter G for a full discussion of Lake Alamosa).

A half century later, in 1875, F.V. Hayden led a team of scientists through the San Luis Valley. In his report dated 1877, geologist F.M. Endlich (1877) reports the following about the valley (our additions are in brackets):

> *"Judging from the evident deflection of rivers, the failure of mountain-streams to carry specimens of the rock through which they pass into the valley for any distance, . . . and the cañoned outlet of the Rio Grande, I have come to the conclusion that at one time San Luis Valley was covered by two large lakes, the northern and the southern* [there is no evidence for a southern lake on the Costilla Plain]. *These I have named . . . Coronado's Lakes. Of these the former covered about 1,400 square miles [3,626 km^2]; the latter 300 square miles* [777 km^2]. *I have alluded to the cañon near station 105, cut through the trachyte* [Conejos Formation]. *It is about three miles* [5 km] *in length, and its general direction is perfectly straight. In case that narrow passage* [gorge through the Fairy-Brownie Hills], *which I assume to have been opened by seismic force, should be closed today, the result would be an accumulation of water in the northern end of the San Luis Valley, the formation of a lake. This lake would reach a certain depth of water, consequently increase in area until the slight rise southwest of Fort Garland would be overcome, and it would flow over into the southern region* [Costilla Plain] . . . . *It may seem curious that no heavy deposits of alkali or old 'shore-lines' mark the presence of these ancient lakes. If, however, the assumption that the Grande found a sudden egress through the deep fissure produced by a volcanic earthquake is true, there is no reason why the waters should not have flown off by far too rapidly to permit of the formation of either . . ." (p. 147 in Hayden's 1875 "Ninth Annual Report" dated 1877).*

Not surprisingly, many of the details reported by the Hayden team have proved wrong, such as the presence of a southern lake, eastern flow path for the Rio Grande, and lack of shoreline (related) features, but Hayden accurately suspected that fault weakened rocks led to quick and easy erosion of the canyon through the Fairy–Brownie Hills. It seems unlikely that an earthquake caused a fissure and sudden draining of the lake, but rather that the discharge was the result of a rising lake that overtopped a natural bedrock sill during pluvial conditions (see chapter G).

Local Geology

Upper Oligocene intrusive and extrusive rocks of the Conejos Formation (fig. B4–1) dominate the bedrock geology in the San Luis Hills (see also Thompson and Machette, 1989). These hills are the surface expression of a large northeast-southwest-trending horst that divides the sedimentary fill of

the San Luis Basin into subbasins. To the north of the hills, the Alamosa subbasin is primarily an east-tilted half graben, although seismic reflection and geophysical data show internal complications (such as two grabens and an intervening horst). To the southeast of the San Luis Hills, the Costilla subbasin extends into New Mexico as far south as Questa. The Costilla subbasin contains the Culebra graben on the east (Fort Garland south to Sanchez Reservoir), San Pedro Mesa (a Precambrian-cored Miocene horst) and the Costilla Plain on the west. We will traverse the Costilla Plains later today (stops B8 and B9).

The lower part of the Conejos Formation is exposed throughout the Fairy and Brownie Hills. Most of the bedrock is 29- to 30-Ma andesitic to porphyritic dacite flows, but dacite dikes with north to north-northeast trends are common (note a prominent weathered dike along BLM Road 5003 on our way south from this stop; fig. B4–2). Although unmapped by Thompson and Machette (1989), Burroughs (1972) mentioned a major north-south-trending Neogene fault (the Lasauses fault) that parallels the course of the Rio Grande. There is little stratigraphic evidence for this fault (Conejos against Conejos). However, extensive subparallel dikes and hydrothermally altered rock in this area seem to support extensive deformation and weakening of the bedrock (Conejos Formation) in the eventual outlet area for Lake Alamosa.

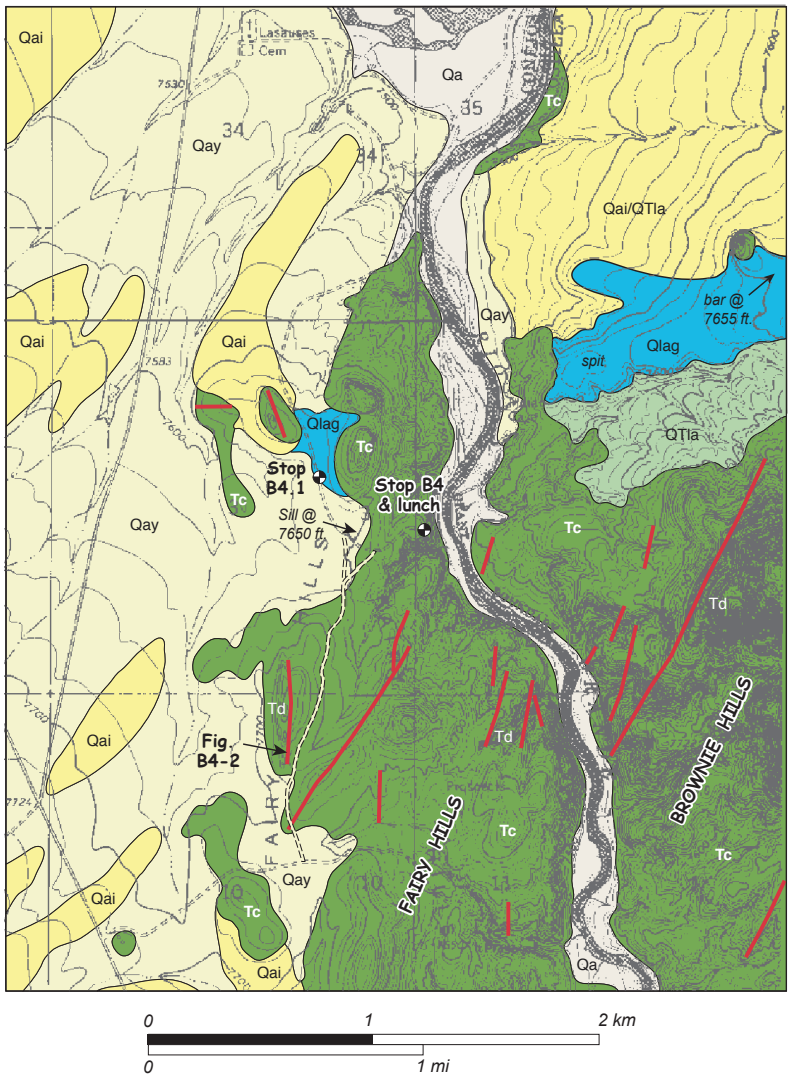

Figure B4–1. Bedrock and surficial deposits near the overflow threshold (sill) of Lake Alamosa and canyon that the Rio Grande cut through the Fairy and Brownie Hills. Map units: Qa, Holocene alluvium; Qay, younger (latest Pleistocene) alluvium; Qai, intermediate alluvium (middle Pleistocene) ; Qlag, near-shore, coarse-grained deposits of Lake Alamosa (uppermost part of unit QTla); QTla, Alamosa Formation (undivided, middle Pleistocene to Pliocene); Tc and Td (dikes) of the Conejos Formation (29–30 Ma). Bedrock geology modified from Thompson and Machette (1989), surficial geology simplified from Machette and Thompson (2005). Base from Manassa NE and Mesito Reservoir quadrangles.

Before an outlet for the lake was carved through the San Luis Hills, they were a formidable barrier to southward-flowing streams. The rocks of the San Luis horst extend from near Antonito on the southwest to about 5 mi (8 km) southwest of Blanca on the northeast. In essence, these hills blocked the entire south margin of the Alamosa subbasin. In addition, eruption of theoliitic flood basalts (for example, the Servilleta Basalt) from 4.8 to 3.7 Ma also blocked possible southward drainage (or drainages) from the San Luis Basin. These flows extended north from the Taos Plateau at least to the areas of La Jara on the west and Fort Garland on the east. Thus, by middle Pliocene time (about 3.5 Ma), drainage southward from the Alamosa subbasin was blocked across the entire width of the San Luis Valley (fig. G–6, chapter G, this volume). Although it is undated, we assume that the lacustrine sediment at the base of the Alamosa Formation is at least this old (3.5 Ma).

Sedimentation in the closed Alamosa subbasin led to aggradation of the basin floor, although Pliocene to Pleistocene movement on the Sangre de Cristo fault system probably continued to keep the eastern side of the basin somewhat lower. As with classic, one-sided grabens (such as Death Valley), fans on the passive (west) side of the San Luis Valley are very large, whereas the east-side fans tend to be more compact owing to downdropping and continued burial.

By middle Pleistocene time, Lake Alamosa had grown laterally to such an extent that it occupied most of the Alamosa subbasin. The single ^{3}He-exposure date from basalt in the upper spit at stop 3.3 suggests that the lake reached its highest (topographic) level at about 440 ka during oxygen-isotope stage (OIS) 12, which was one of the major continental glaciations in the northern hemisphere (see chapter G for more details and references). At a water level of 7,660 ft (2,335 m asl), Lake Alamosa would have surrounded many of the isolated

Figure B4–2. Weathered dacite dike (upper Oligocene Conejos Formation) in the Fairy Hills. This 5-m-high dike is on the west side of BLM Road 5003, about 1 mile south-southwest of stop B4. View to the west.

hills in this area and formed an embayment into the Fairy-Brownie Hills, as shown in figure B4–3.

From our lunch stop (B4), one would have looked northwest across the Lake Alamosa (fig. B4–4) about 30 mi (48 km) to see the Sangre de Cristo Mountains and Blanca Peak, which at 14,345 ft (4,372 m) asl, is the highest point between Pikes Peak and the San Juan Mountains. At its highest elevation of 7,660 ft (2,335 m) asl, Lake Alamosa would have occupied most of the San Luis Valley north of here. As such, the lake would have been 105 km (65 mi) from north to south and as much as 48 km (30 mi) from west to east (along the route of Highway 160; see chapter G, this volume). The 7,660 ft contour extends west to the Monte Vista Wildlife Refuge and beneath Monte Vista (town), north to a point several miles southwest of Saguache and south of Mineral Hot Springs in the north end of the valley and then south along the east margin of the valley. The contour is coincident with several natural springs that emerge from the western base of the Great Sand Dunes.

Long Spit, Across River

Due east of stop B4, waves from the lake eroded Tertiary rocks of the Brownie Hills and deposited a long and wide southwest-trending spit that extended into the southernmost bay of the lake. The spit is underlain by sandy well-rounded gravel about 5–15 m thick that rests on a platform of Tertiary volcanic rock. This spit extends west about 1.4 km from an isolated bedrock hill at 7,660 ft (2,335 m) asl to the vicinity of Indian Cave, where the top of the spit is at about 7,620 ft (2,322 m) asl (fig. B4–5). This spit is one of the longest, but not volumetrically largest, in the basin. The largest spit is probably the one on the south side of Sierra Del Ojito, which is located about 5 km east of stop B3 and north of Road W (see mapping of Machette and Thompson, 2005).

Overflow and Erosion

When Lake Alamosa rose to 7,660 ft (2,335 m) asl, water could spill south over the low divide between the Fairy Hills (on the west) and the Brownie Hills (on the east). There may

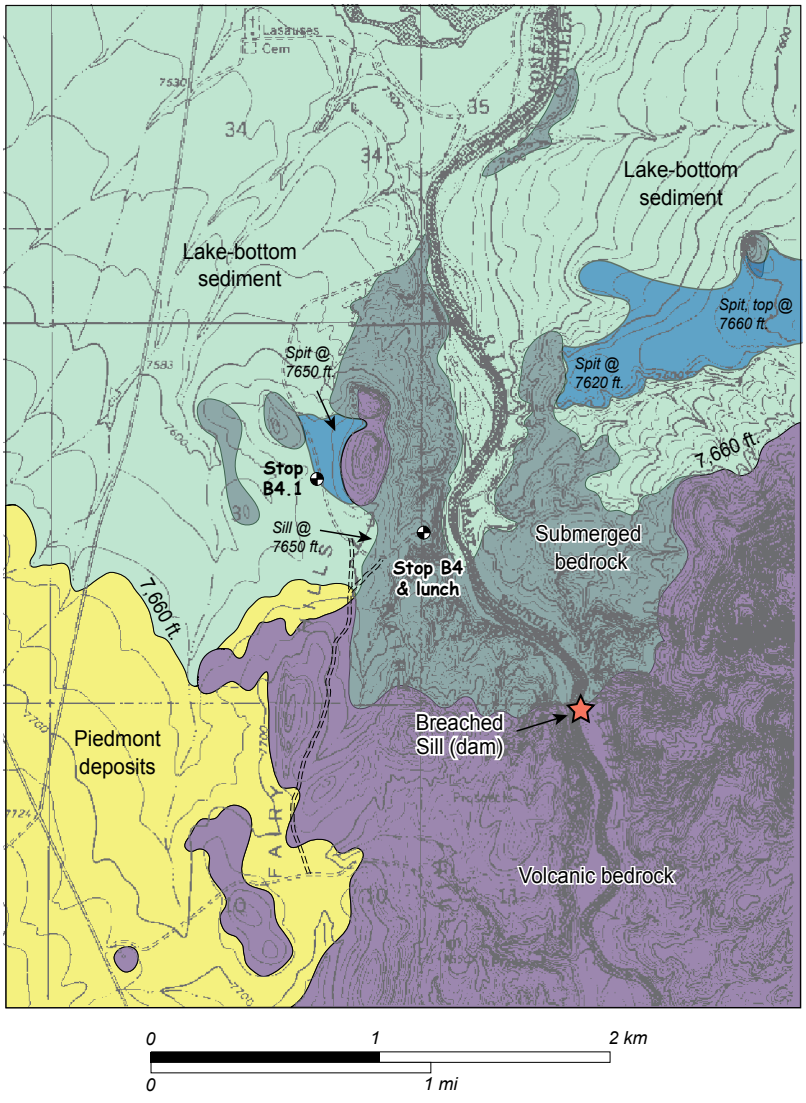

Figure B4–3. Schematic map showing extent of bedrock, surficial, and lacustrine deposits at highest (overflow) level of Lake Alamosa, about 7,660 ft, prior to overflow. Stop B4.1 is a drive by, past the site of a trench in sandy spit deposits. A threshold sill floored by bedrock is crossed before dropping into the canyon for stop B4. Base map scanned from Manassa NE and Mesito Reservoir quadrangles.

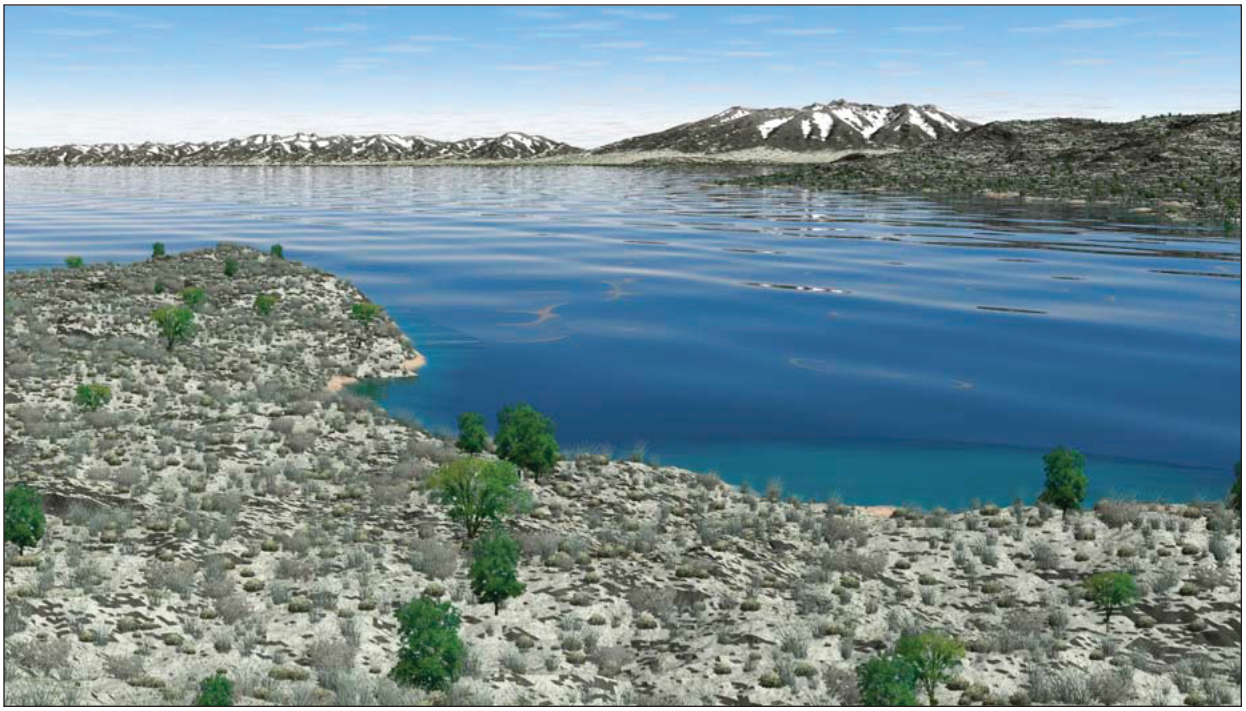

Figure B4–4. Re-creation of Lake Alamosa. View to the northeast from the area of stop B4. Highest peak in the background is Blanca Peak at 14,345 ft asl. Visualization created in Visual Nature Studio (v. 2.7, 3D Nature Co.) by Paco Van Sistine (USGS) using 30-m DEM and a lake elevation of 7,660 ft (2,335 m).

Figure B4–5. Long, west-sloping spit of Lake Alamosa. Top of spit descends from 7,660 ft at head to 7,620 ft at toe, above the "Indian Cave." View to the east with the eastern portion of the San Luis Hills in the middle ground and Blanca Peak in the background (upper left).

have been several pathways to the south, one of which is now abandoned but intact at the top of the hill to the west of us (fig. B4–3, sill at 7,650 ft or 2,332 m asl). This sill has no gravel on it, now, probably owing to scouring. The southward-flowing water must have found a softer avenue (along the river's present course) and cut a deep gorge through the Tertiary volcanic rock (fig. B4–6). We don't know how deeply or how quickly the gorge was cut, but there are several lines of evidence to suggest it was cut quickly and rather deeply.

First, in most cases the preserved barrier bars, lagoons (see stop B7), and spits (stops B3 and B4) are preserved at a very restricted range of elevations—typically 7,640–7,670 ft (2,329–2,337 m) asl. The highest ones are located in the southeastern part of the basin (south of stop B5), where storm surge coupled with wave action generated by the lake's long fetch may have formed higher than normal shorelines. Where multiple shoreline features are preserved (for example, the two spits at stop B3 or the two stacked bars and lagoons at stop B7), they are constructional features that are typically related to lake transgression rather than regression. Also, the Alamosa subbasin lacks the repetitious shorelines characteristic of slow drawdown, such as between the Provo and Gilbert shorelines of latest Pleistocene Lake Bonneville that Machette had previously mapped in Utah Valley (Utah).

Second, the isolated topographic ridges associated with intermediate-age (unit Qai) alluvial channels (stops B1 and B2) are graded to base levels that are relatively low

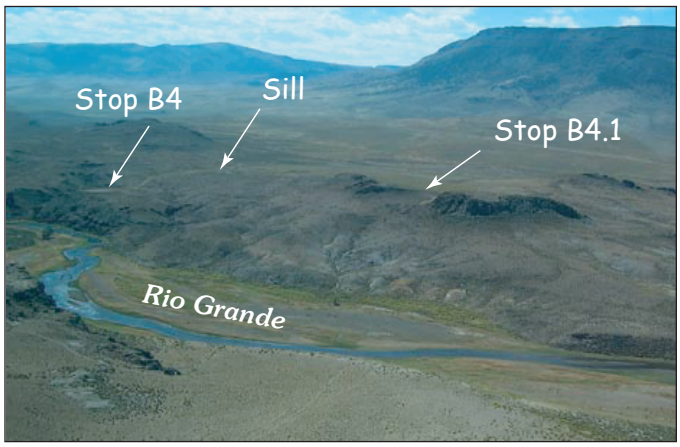

Figure B4–6. Canyon of the Rio Grande in the Fairy Hills, south of Lasauses. The sill, at 7,650 ft, is 185 ft (56 m) above the Rio Grande (elev. 7,465 ft here). View to the southwest; western portion of San Luis Hills in the background.

(7,530–7,540 ft or 2,295–2,298 m asl), perhaps only 30–40 ft (9–12 m) above the present channel of the Rio Grande. If these channels formed in response to lake lowering, then the canyon of the Rio Grande must have been cut deeply as a result of overtopping, perhaps excavating as much as 45 m of the 55 m of relief between the Lake Alamosa overflow and present river level.

Finally, although we suspect a catastrophic draining of the lake, we don't know if this was accomplished in a month, a year, a decade, or a hundred years. Nevertheless, it was probably accomplished in just a "moment of geologic time." O'Connor (1992) reports that the catastrophic overflow of Lake Bonneville and coincident downcutting through Red Rock Pass (about 108 m, Currey, 1990) might have been accomplished in as little as a month. Surely, the cutting associated with Lake Alamosa's overflow took longer since the entire gorge is in Tertiary bedrock, whereas much of the cutting at Red Rocks Pass was through surficial deposits and into bedrock. Although Lake Bonneville was several orders of magnitude larger than Lake Alamosa and thus had a much greater volume of water for cutting, we consider both events to be geologically instantaneous.

Interestingly, we have not found large-scale outbreak deposits along the Rio Grande to the south, which are characteristic of the Bonneville flood across the Snake River Plain. There is one feature that might be suggestive of catastrophic overflow from Lake Alamosa. Where the Rio Grande leaves the San Luis Hills and enters the Costilla Plain, the intermediate-age (post Lake Alamosa) terraces of the river (units Qam1 and Qam2 of Thomson and Machette, 1989) become extremely wide. In map pattern, these terraces suggest that the Rio Grande excavated widely and deeply into older alluvium (unit Qao) and the underlying Santa Fe Group sediment (unit QTsf) before flowing south across and cutting into Pliocene Servilleta Basalt of the Taos Plateau.

Path of the Rio Grande

Prior to overflow of Lake Alamosa, the Rio Grande probably had its headwaters in the present Red River basin (see Wells and others, 1987). Streams draining from the Sangre de Cristo Mountains north of Questa to San Luis probably drained out into Sunshine Valley and the Costilla Plain, both of which were largely closed or poorly drained basins (see field-trip discussions in chapter C and discussion of the Rio Grande in chapter G).

The modern Rio Grande north of Questa probably has been in the same channel since Lake Alamosa overflowed in middle Pleistocene time (440 ka) owing to progressive incision through the Servilleta Basalt. Upon exiting the Fairy Hills, the overflow entered the lower, southward-flowing part of Culebra Creek (where the bridge on Highway 142 crosses the present Rio Grande, fig. B–1 and B–3). From here, the overflow took a southerly route following the lowest ground between the southwest-sloping Costilla Plain and the southeast-sloping piedmonts of the San Luis Hills. Santa Fe Group basin-fill sediment containing abundant Precambrian clasts extends across the entire Costilla Plain and into Punche Valley, west of the present Rio Grande, indicating that the Santa Fe sediment and the unconformable cap of older gravel (unit Qao) that forms the Costilla Plain predates overflow of the lake. At the south end of the Costilla Plain (near the New Mexico–Colorado border), the overflowing lake water excavated basin-fill sediment and exhumed some previously buried Servilleta Basalt. The overflow continued to the south, generally taking a course along east margin of the east-dipping Servilleta Basalt (see stops C2 and C3). Finally, the overflow coursed between Cerro Chieflo and Guadalupe Mountain (near Cerro, N. Mex.) and entered the canyon of the Rio Grande (Red River) at La Junta Point (stop C1). At 440 ka, this river junction had the same geometry, but the Rio Grande above the junction may have looked much like the present day Niagara Falls. Since 440 ka, the falls have migrated headward about 10 km north as evidence by a 180-m-high steepened gradient (ancient knickpoint) in the Rio Grande (Wells and others, 1987). North of Cerro Chieflo, the modern Rio Grande has a shallower gorge that extends north into Colorado along a much shallower gradient.

Stop B4.1 (Optional) — Rounded Pebble Gravel of Lake Alamosa, Filled Soil Pit

Location: BLM Road 5003, west side of Rio Grande, about 1 mi (1.6 km) southeast of Lasauses Cemetery
Manassas NE 7.5' quadrangle (Station MNE–MM04–33a)
GPS: NAD27, Zone 13, 425136 m E., 4124048 m N.
Elevation: 7,650 ft (2,332 m) asl (just below maximum shoreline at 7,660 ft or 2,335 m asl)

Synopsis

This general area has well-rounded pebble gravels eroded from Tertiary volcanic rocks that form a sill for Lake Alamosa. The highest gravels are found along and slightly (5 m) above this part of BLM Road 5003. They record a maximum lake level of about 7,650–7,660 ft (2,332–2,335 m) asl, which is consistent with the elevations of barrier-bar lagoons to the northeast (optional stop B6). A soil pit was excavated about 20 m (65 ft) west of the road for cosmogenic nuclide dating, but the soil in the pit was extensively bioturbated and thus unsuitable for sampling. Nevertheless, the pit revealed very sandy pebble to small-cobble gravel that was deposited in a near-shore (shallow) beach environment.

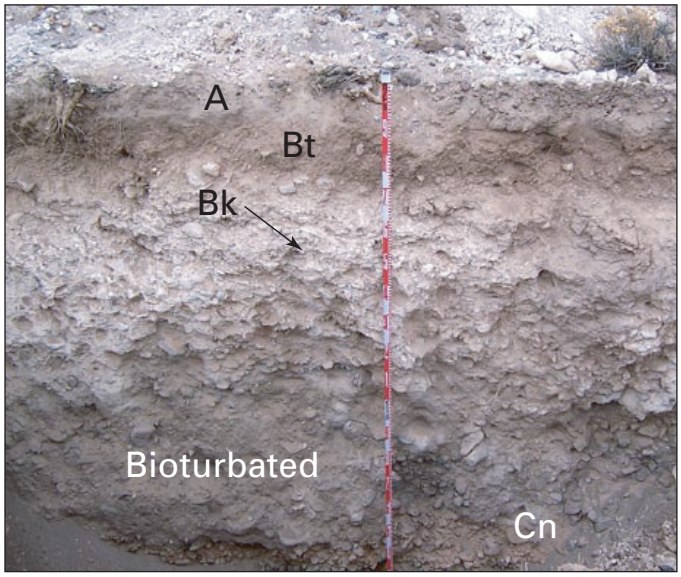

Figure B4.1–1. Strong calcic soil developed on sandy gravel at stop B4.1. This pit was not sampled for cosmogenic dating owing to extensive bioturbation of the lower part of the soil. Nevertheless, the Bk horizon is an indicator of middle Pleistocene age. Tape measure is extended 1.6 m in this view.

Discussion

On the route to the lunch stop (B4), we climbed uphill and crossed a bedrock-cored saddle just north of stop B4.1. This saddle is covered with small rounded pebbles (generally <2 cm in diameter) of locally reworked volcanic rocks. These gravels represent nearshore (shallow) beach deposits of Lake Alamosa at its highest stand (about 7,660 ft or 2,335 m asl).

A soil pit excavated along this gravel road exposed sandy pebble to small-cobble gravel (fig. B4.1–1) that was deposited just offshore (west of) the high shoreline. Further west and topographically lower, stream gullies expose fine-grained sand, silts and marls that represent deeper water deposits (Alamosa Formation) of Lake Alamosa.

The calcic soil in this pit (table B4.1–1) showed development comparable to that at stop B3 (the upper and lower spits). The calcic part of the soil (Bk horizon) extends from 41 cm to 194 cm (1.5 m thick), but it appears to have engulfed a former Bt horizon (see clay contents for 22–93 cm, table B4.1–1). Some of this clay is probably from loess (similar to the present A horizon) that was incorporated into the sandy gravel parent material, but some may be pedogenic since clay films were noted on ped faces and in pores. We described this soil but didn't sample it for physical analyses or cosmogenic dating owing to extensive bioturbation. The strength, thickness, and morphology of the Btk and Bk horizons are similar to the soils in similar age deposits at stop B3 (the upper and lower spits).

Table B4.1–1.Soil profile on sandy gravels at stop B4.1

Depth (cm)	Horizon	Soil texture	Estimated clay content (percent)	Ca CO_3 morphology	Color, <2 mm, dry	Geologic origin
0–22	A	Loam	13	Stage I	*10YR4/2*	Loess
22–41	Btk1	Gravelly loam	22	Stage II	*10YR5/3*	Lacustrine
41–93	Btk2	Gravelly sandy loam	20	Stage III	*10YR5/2*	Lacustrine
93–141	Bk3	Gravelly loamy sand	4	Stage III	*10YR6/2*	Lacustrine, horizon is bioturbated
141–194	Bk4	Gravelly loamy fine sand	4	Stage II–III	*10YR5/3*	Lacustrine, horizon is bioturbated
194+	2Cn	Fine sand to gravelly fine sand	2	Stage I or none	*10YR3/2*	Sand and sandy gravel beds (lacustrine)

Stop B5 (Optional) — Lagoons and Barrier Bars of Ancient Lake Alamosa

Author: Michael Machette

Location: Appleblossum Lane (north-south) and 24th Street N (east-west), Trinchera Creek Estates; about 8 mi (13 km) southwest of Blanca, Colo.
Blanca SE 7.5' quadrangle (BSE–MM05–67)
GPS: NAD27, Zone 13, 446639 m E., 4132967 m N.
Elevation: 7,650 ft (2,332 m) asl (at road intersection)

Synopsis

From this road intersection, you can see two sets of bay-mouth barrier bars that have blocked a north-trending shallow stream valley. The bars impounded the drainage and formed lagoons, which have been playas since Lake Alamosa was drained. The lower bar (to the north of us) has elevations of 7,645–7,655 ft (2,310–2,333 m) asl and declines in height from northeast to southwest, in the direction of its propagation. The upper bar (the Appleblossum bar) spans the stream valley and has a medial east-west elevation of about 7,662 ft (2,312 m) asl; it is attached to bedrock that borders the valley on both ends. A soil pit excavated on the crest of this bar penetrated sandy, well-rounded pebble to boulder gravel and laminated sands, all of which were deposited in shallow water. The soil on this barrier bar has a discontinuous 65-cm-thick Bk horizon, and it is not as well developed as the soils on the upper and lower spits of Saddle Mountain (stop B3) or in shoreline deposits in the Fairly Hills (stop B4.1). A second, exploratory pit on the margin of the playa south of the Appleblossum bar exposed unbedded silt and sand that is extensively bioturbated.

Discussion

This stop is located along the southeast margin of ancient Lake Alamosa, about 13 mi (20 km) northeast of the lake's outlet (stop B4). We were first attracted to this area by unusual topographic features that are near the highest shorelines of Lake Alamosa, specifically between about 7,640 ft (2,329 m) and 7,665 ft (2,336 m) asl (fig. B5–1). This area is covered by the northwestern part of the Blanca SE 7.5-minute topographic map, which has 10-ft contours. We first noted numerous closed depressions, typically 5–10 ft deep, but locally as much as 20 ft deep. Closed depressions can be formed by numerous processes, such as dissolution (sinkholes), eolian deflation (blowouts), or blockage (by volcanic flows, debris flows, sand dunes, or lacustrine spits and bars).

The first two processes—solution collapse and deflation—seemed unreasonable because the surficial deposits in this area are typically sand and gravel (alluvium) and underlain by a platform of volcanic rock (upper Oligocene Conejos Formation as mapped by Michael Machette and Ren Thompson, unpub. mapping, 2007). Thus, we conclude that these closed depressions were formed by blockage by lacustrine spits and bars related to high shorelines of Lake Alamosa. In addition, we are amazed that these easily eroded features could still be so well preserved since their creation in middle Pleistocene time (about 440 ka). In the western United States, geomorphic evidence of ancient lakes in this time range is rarely seen. For example, Reheis and others' (2002) Kirk Bryan Award–winning paper (for 2007) on ancient Pliocene to middle Pleistocene lakes in the western Great Basin documents sedimentary evidence for lakes that are 650 ka and older, but shoreline notches or constructional features (such as bars) were found at only three (of many) locations—Thorne Bar, Lone Mountain, and Lone Tree Hill—all in Nevada (fig. 1, Reheis and others, 2002).

Local Geology

The lacustrine spits, bars, and lagoons are formed along the margin of a series of unnamed bedrock hills composed primarily of andesite flows, breccias, and lahars of the Conejos Formation (about 29–30 Ma, upper Oligocene). Longshore drift along the southern shores of Lake Alamosa built a series of gravelly bars that blocked embayments and valleys that existed before Lake Alamosa rose above about 7,640 ft asl (fig. B5–1). On the north side of the hills (at this stop) the bars were built by west to southwest currents, whereas on the south side of these hills the currents were easterly.

Faint shorelines are preserved on the windward (west and north) side of the hills, but shoreline notches dating from the ancient lake's high stand are completely covered, presumably with eolian sand and bedrock-derived colluvium. At certain times of the day and from certain perspectives, these shorelines are apparent as horizontal breaks in slope and different types of vegetation grow on the sandy colluvium and bare bedrock. For example, on a previous field trip USGS Scientist Emeritus Jim Erdman noticed that spike dropseed *(Sporobolus contractus)*, a cool-season bunchgrass, is "aspect dominant" (the plant that dominates the landscape) on sandy deposits along the shorelines at Saddleback Mountain (Erdman, written commun., 2007). So these breaks in slope and vegetation changes are the most conspicuous signatures of the middle Pleistocene shorelines in the San Luis Valley.

Barrier Bars and Lagoons

In this area, we were interested in trenching one of the bar or lagoon features to characterize the texture and bedding of the deposits, the soils formed on a bar, and to sample underlying lake gravel for cosmogenic dating (^{36}Cl). As you will notice from the topographic map of the area (Blanca SE quadrangle; a portion is shown on fig. B5–1), the area was subdivided for land sales in the 1970s. This scheme is typical of many areas in southern Colorado and New Mexico—potential buyers are

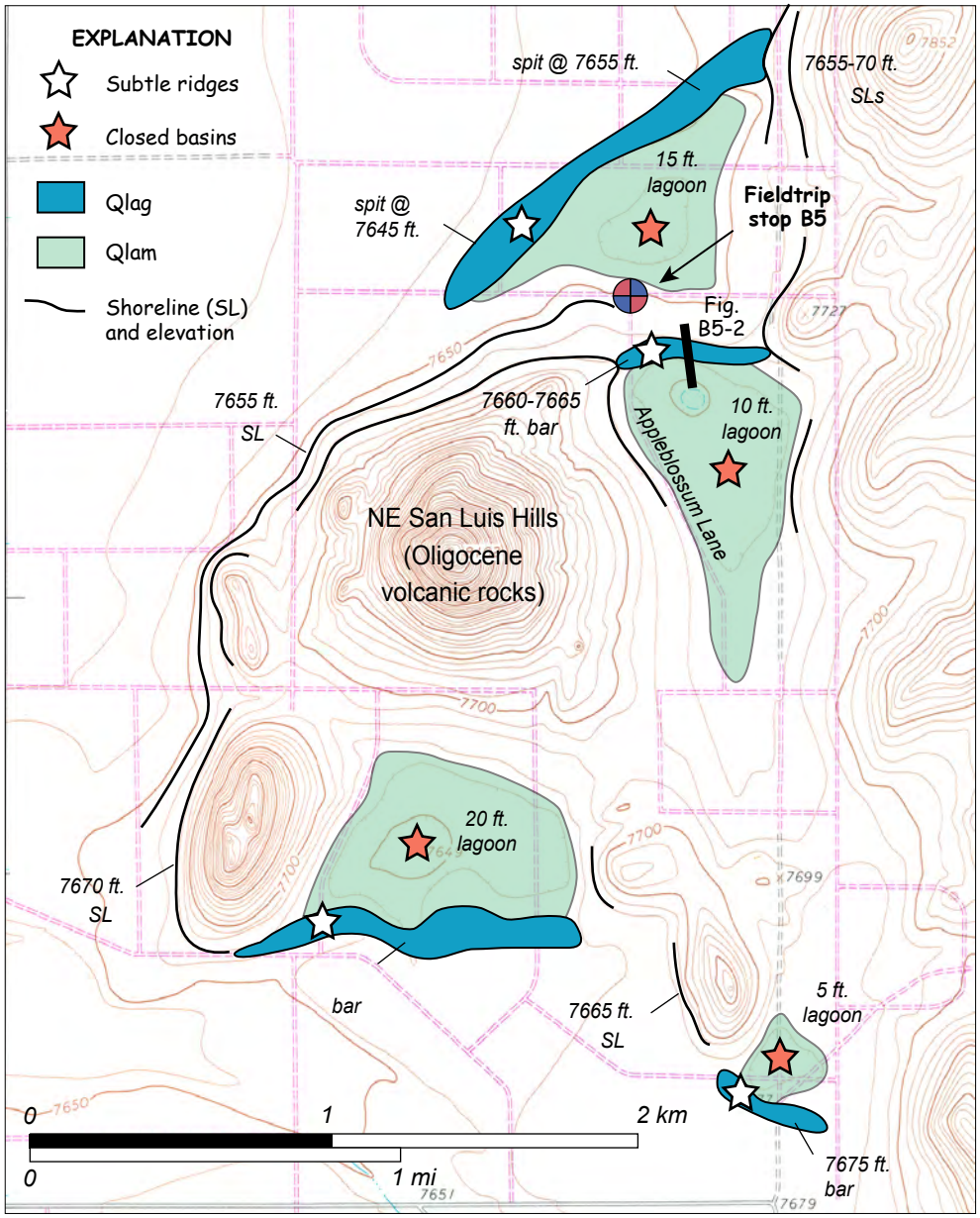

Figure B5–1. Lacustrine features of Lake Alamosa near stop B5. Map unit Qlag is coarse-grained (sandy gravel), whereas unit Qlam is finer grained (sand, silt and clay). Base map scanned from Blanca SE quadrangle.

shown stunning photographs of the mountains (Sangre de Cristo Mountains, 20 km to the east), trout fishing in streams (not here), and so forth, with the lure of inexpensive property for retirement or vacation homes. Look around—now, almost 40 years later and not a neighbor in sight!

In this subdivision tract, which is unit 6 (of 8) in Trinchera Creek Estates, there are no permanent residents or houses. The roads in this development were platted and graded in 1982, 25 years ago. There is no accompanying infrastructure such as water, sewer, power, or phone. In addition, landowners here do not have water rights, so drilling a well is not permitted. As a result, most of these lots (which are typically 5 acres) are not likely to be developed for residential use. Nevertheless, the developer and county officials recognized that closed depressions occasionally hold water that would be a flood hazard. Thus, the three larger and deeper lagoons shown in figure B5–1 were set aside as "Public Use Exempt" land in the development plan. "Public Use Exempt" land is typically used for parks or open areas and these are under county ownership. Even though taxes on these 5-acre parcels are about $30 per year, most of the parcels have been repurchased by local real estate companies or have reverted to county ownership because the owners have defaulted on their taxes. Here is your retirement opportunity and a chance to build a home on the shores of (ancient) Lake Alamosa.

We trenched the crest of the east-west-trending bar here, which is informally named for Appleblossum Lane, the graded dirt road on the west side of the lagoon (fig. B5–1). The pit was about 3 m deep and exposed a strong calcic soil in sandy gravel over laminated sand. The gravelly bar deposits (upper 2.7 m) coarsen downwards, partly as a result of accumulation and incorporation of sandy eolian deposits in the upper meter of the deposits. The lower part of the pit encountered well-laminated silty to sandy deposits that appear to be a backwater (lagoonal) facies. Figure B5–2 shows a schematic cross section through the bay-mouth bar and lagoon that is based on our topographic profile, the pit, and a second trench on the south side of the barrier bar. The second trench exposed massive, bioturbated sandy silts with lenses and stringers of lacustrine gravel. We have interpreted this bar as being deposited as the lake rose in elevation, such that individual gravel packages climb across and bury the southern, leeward slopes of previous bars and intertongue with finer-grained lagoonal deposits.

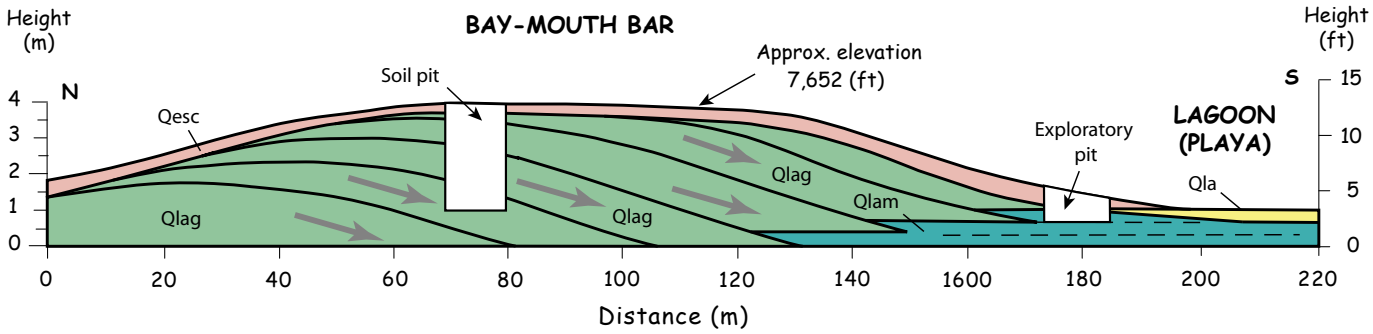

Figure B5–2. Topographic profile and schematic cross section through bay-mouth bar and lagoon at stop B5. Gray arrows show probable direction of transport across bar as it grew to the south. Map units: Qesc, eolian sand and colluvium; Qla, playa deposits; Qlag (coarse-grained) and Qlam (fine-grained), bar deposits of the Alamosa Formation. Topographic profile measured by Robert Schultz (Colorado Division of Water Resources, Mosca) and Harland Goldstein (USGS, Denver) along line shown in fig. B5–1. Vertical exaggeration is about 6x. Geology based on mapping of Michael Machette and Ren Thompson, unpub. mapping, 2007.

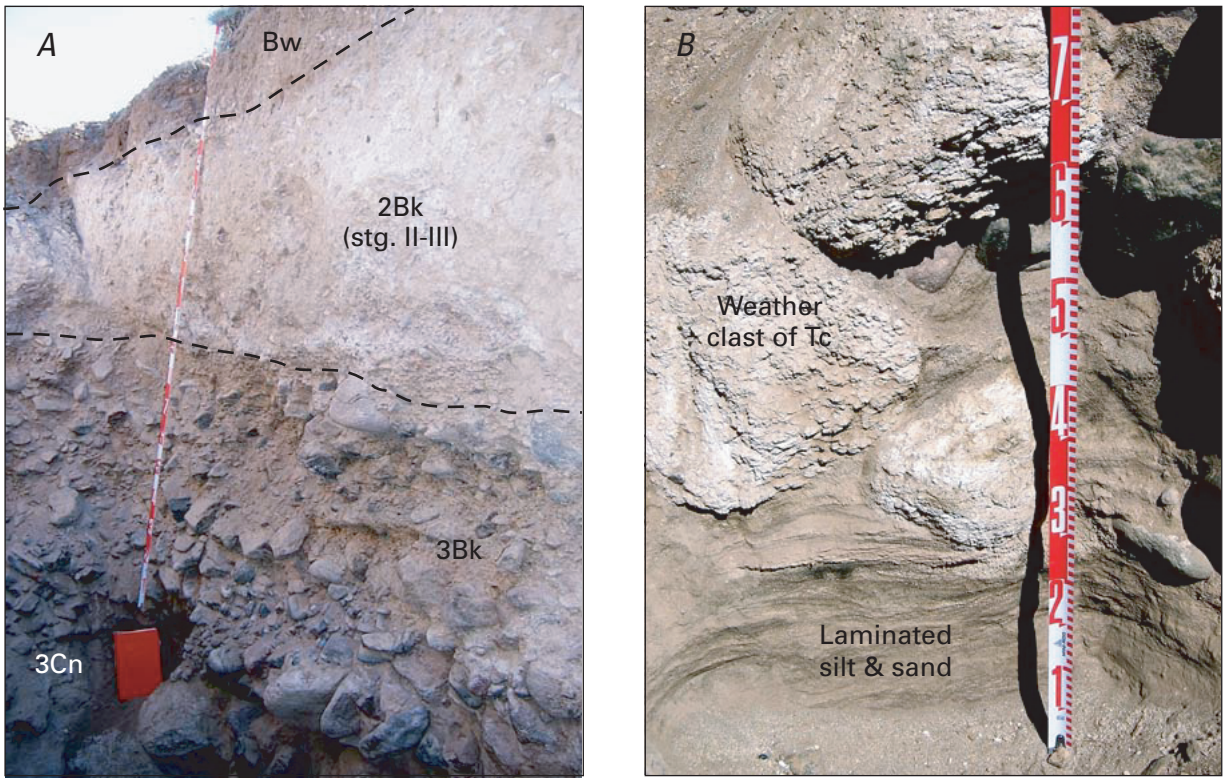

Figure B5–3. Soil pit on upper bay-mouth bar at stop B5. *A* , Calcic soil in upper part of bar deposits. Upper parent material is a gravelly sand; lower parent materials (2 and 3) are sandy, pebble to cobble gravels (subangular to well rounded). Tape measure (2 m long) and field notebook for scale. *B*, Coarse gravel (weathered clasts of unit Tc, Conejos Formation) within and over laminated silt and sand (unit 4) at base of pit.

Soil Pit in Bar

The soil on the Appleblossum Lane bar is not as well developed as soils on the spits at stop B3 or on the spit that formed on the south side of Sierra Del Ojito (see mapping of Machette and Thompson, 2005). The B horizon here is poorly formed (Bw with minor carbonate in lower half; see figs. B5–3A and B5–4). The upper 36 cm of the profile are formed in slightly gravelly sand (mainly eolian), whereas the next 66 cm (down to 100 cm) is formed in sandy pebble gravel (parent material 2). The 2 Bk (and subhorizons) are visibly whitened but have only about 5–7 percent $CaCO_3$ in the <2 mm fraction of the soil, which composes about 75–80 percent of the unit. The low gravel and high sand content of the 2Bk horizon (from 36 to 110 cm) probably reflects burial of the gravel spit and deposition of sand in the final stages of the lake filling. To the south of stop B5, the subtle 1-m-high bar at an elevation of 7,670 ft (2,337 m) asl (fig. B5–1) is the highest lacustrine feature that we have found in the San Luis Valley.

Although the Bk horizon is weakly developed in terms of carbonate and morphology (stage II–III), there is a weak clay bulge (3–4 percent clay, <2 mm fraction) and abundant silt, some of which might have been translocated from the surface or upper horizons (or both). The 2Bk3 horizon (at 78–100 cm) and 3Bk horizon (110 to 145 cm) contain almost 20 percent silt, which is quite a bit for a lacustrine pebbly sand (unit 2) and sandy gravel (unit 3).

Although it is undated, we consider the Appleblossum Lane bar (and similar features shown in fig. B5–1) to have formed at the same time as the spits at Saddleback Mountain (stop B3). They all fall in a restricted elevation range and were deposited as Lake Alamosa rose to its final and highest level (about 7,660 ft or 2,335 m asl) and overflowed its hydrologic sill in the Fairy Hills (stop B4).

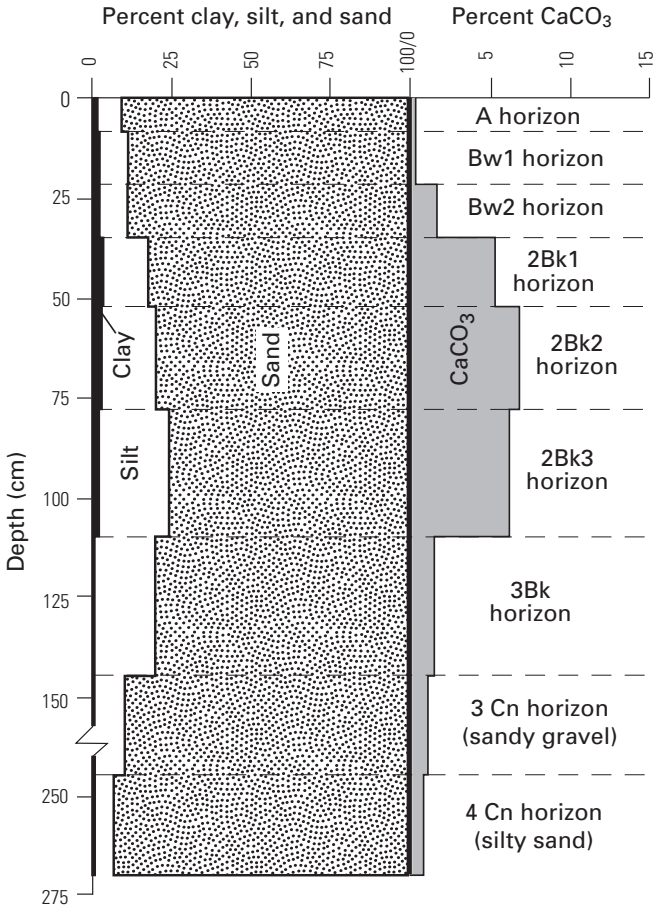

Figure B5–4. Profile data for soil on crest of barrier bar, stop B5. Note break in vertical axis from 160–240 cm (within 3Cn horizon).

Stop B6 (Optional) — And the Wind Blows—Fluted Ventifacts on the Ancient Shore of Lake Alamosa

Author: Michael Machette

Location: Thatcher Road (unmarked), S side of Trinchera Creek, about 8.2 mi (13.2 km) southwest of Blanca, Colo.
Lasauses 7.5' quadrangle (LaS–MM04–38)
GPS: NAD27, Zone 13, 4432787 m E., 4135480 m N.
Elevation: 7,655 ft (2,336 m) (at crest of road)

Synopsis

This ridge of resistant volcanic rocks of the Conejos Formation shows evidence of prolonged erosion from sand blasting (the presence of ventifacts). Finger-size troughs, cones, and broad mullions on the windward and leeward sides of intact bedrock blocks reflect hundreds of thousands of years of wind erosion at a location where sand is available and the wind is funneled into a valley. The base of this ridge was cut by the highest stand of Lake Alamosa (elevation 7,660 ft or 2,335 m asl) at this site, and there is a persistent gravel bench from here south along bedrock hills for at least 1 km on the southeast side of Trinchera Creek. The ridge may have been initially cut as part of the channel of Trinchera Creek, but this cutting would have predated the highest stand of Lake Alamosa, about 440 ka. Ventifacts are present hundreds of meters south and tens of meters above the ridge, thus eliminating water erosion as a significant factor in their formation.

Local Geology

This stop is located on southeast margin of ancient Lake Alamosa at an elevation of 7,660 ft (2,335 m) asl, which is commonly the highest elevation at which we find lacustrine spits (stops B3 and B4), barrier bars and lagoons (stop B5), and eroded shorelines (this stop). The bedrock in this area is upper Oligocene porphyritic andesite flows, breccias, and lahars of the Conejos Formation (unit Tc, fig. B6–1) (Thompson and Machette, 1989). Of these rock types, the flows are particularly resistant to erosion and thus form small hills, buttes, and ridges, such as the one at this stop.

The base of this ridge was cut by the highest stand of Lake Alamosa, and there is a persistent gravel bench from here south for at least 1 km (0.6 mi) on the west side of the hills. Further south, a prominent saddle between hills of volcanic rock is covered with locally derived beach gravel. Shallow road cuts through this gravel show strong calcic soil development (see also stops B3 and B4.1) that supports our inference of a middle Pleistocene age. South of the hills shown in figure B6–1, the lake deposited a long spit (unit Qlag) that extends southwest for at least 1 km on the west side of the hills and south of Trinchera Creek.

Trinchera Creek occupies the narrow valley to the north of this stop and is one of the few eastern tributaries to the Rio Grande that flows on a perennial basis. This stream originates in the Sangre de Cristo Mountains east of Blanca Peak and flows westward through the Garland mesas (southeast of Fort Garland), across the central Sangre de Cristo fault zone, and into the San Luis Basin. There are older (unit Qao), intermediate (unit Qai), and younger terraces (unit Qay) along the margins of Trinchera Creek from near Smith Reservoir (south of Blanca) west to the Rio Grande, a distance of about 13 mi (21 km) (fig. B6–1).

The older alluvium (unit Qao) generally predates the highest stand of Lake Alamosa as mapped by Machette and Thompson (2005) and Michael Machette and Ren Thompson (unpub. mapping, 2007), although some elements of unit Qao may be coeval with the lake. Conversely, the intermediate-age alluvium (unit Qai) is always mapped as younger than the lake deposits (unit QTla, Alamosa Formation), as demonstrated at stops B1 and B2. Intermediate alluvium was graded to lowering base levels as the Rio Grande became established as a through-going stream through the San Luis Hills. Likewise, the younger alluvium (unit Qay) and Holocene alluvium (units Qa, Qfp, and Qaa; fig. B6–1) form terraces and the modern floodplain and channels of Trinchera Creek. No significant eolian deposits have been mapped in the area around stop B6, but most of the piedmont to the north and west of here is mantled by latest Pleistocene to Holocene eolian sand (units Qed, Qes, and Qeso of Michael Machette and Ren Thompson, unpub. mapping, 2007; see also fig. B7–1 at Hansen Bluff). This area seems to be a corridor of sand transport, rather than a repository of eolian sand.

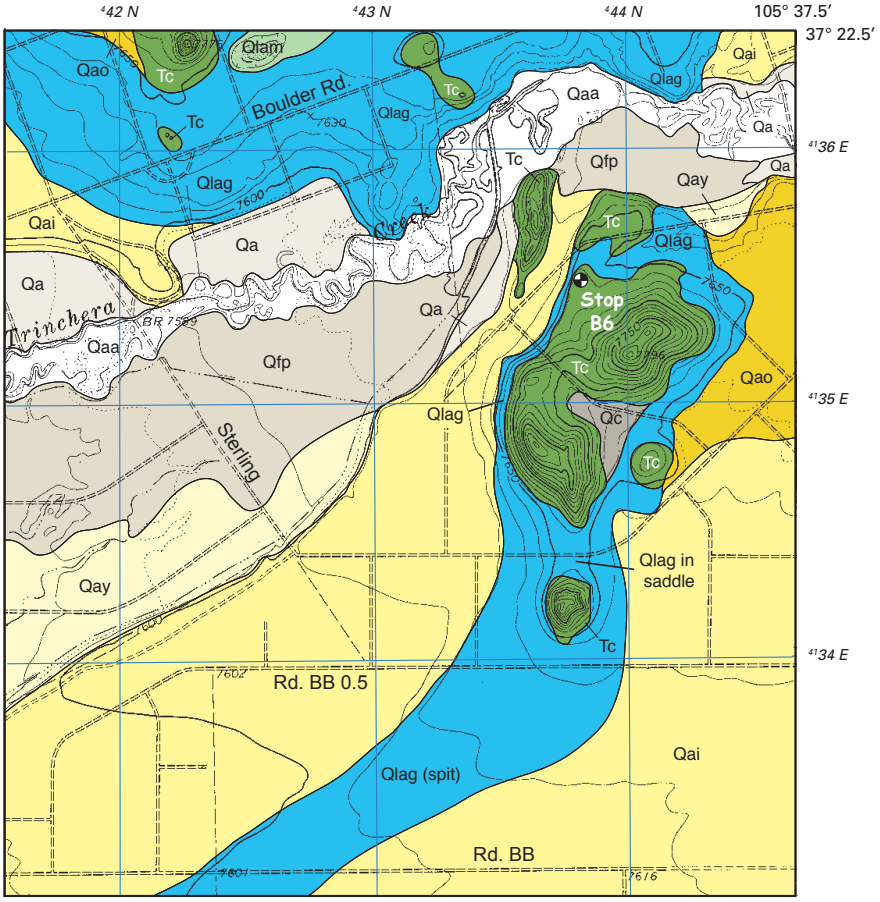

Figure B6–1. Bedrock, alluvial deposits, and lacustrine deposits of Lake Alamosa at stop B6, along Trinchera Creek. Map units: Qaa, active alluvium; Qa, Holocene alluvium; Qfp, floodplain alluvium; Qay, younger (latest Pleistocene) alluvium; Qai, intermediate alluvium (late to middle Pleistocene); Qao, older alluvium (middle Pleistocene); Qc, colluvium; Qlag (coarse-grained) and Qlam (fine-grained) near-shore coarse-grained deposits of Lake Alamosa (middle Pleistocene, uppermost part of unit QTla); and volcanic rocks of the Conejos Formation (29–30 Ma). Geology modified from Michael Machette and Ren Thompson, unpub. mapping, 2007.

Ventifacts (modified from Wikipedia (http://www.wikipedia.org/); see also selected references)

> *"Ventifacts are rocks that have been abraded, grooved, or polished by wind driven sand. These geomorphic features are most typically found in arid environments where there is little vegetation to interfere with eolian particle transport, where there are frequently strong winds, and where there is a steady but not overwhelming supply of sand. Ventifacts can be abraded to eye-catching natural sculptures [see fig. B6–2] . . . . Individual stones, such as those forming desert pavement, are often found with grooved, etched, surfaces where these same wind driven processes have slowly worn away the rock. When ancient ventifacts are preserved without being moved or disturbed, they may serve as ancient wind indicators. The wind direction at the time the ventifacts formed will be parallel to grooves or striations cut in the rock."*

Julie Laity (Geography Dept., California State University, Northridge), who is an authority on wind erosion in the southwestern United States, made the following observations on the basis of photographs of the ventifacts at stop B6:

1. On the basis of the scale, beveling of the form, and the degree of fluting, the area appears to have received sustained abrasion. The scale of the ventifact-form features (such as flutes) increases with the strength of the wind. Is there any sand in the area today? [No.] Sand is not always present in large quantities in fossil ventifact fields, as the area may have been largely a corridor of transportation.

2. Normally, ventifacts appear in topographic positions where water fluting is unlikely (for example, near hill crests). However, I have seen ventifacts within relict channels—some are found south of Ludlow, Calif., where the wind blew sand down the channel after streamflow ceased (assumed climatic change)—but this occurrence is rare. Are your ventifacts found in an area where the wind would accelerate (near a hill crest or in a topographic saddle)? [Yes.]

With reference to the Wikipedia discussion and Dr. Laity's observations, this site has the following attributes that are conducive to their formation:

1. Climate, present and past: Modern conditions are cold (41°F or 5°C, MAT) and relatively dry (about 7 in. or 180 mm, mean annual precipitation (MAP)) in Alamosa (see http://www.wrcc.dri.edu) about 20 mi (32 km) to the west. The elevation in this part of the basin ranges from about 7,550 ft to 8,000 ft (2,301 m to 2,438 m) asl. Glacial climates must have been considerably colder and probably drier than present.

2. Sand is and has been available from the floor of ancient Lake Alamosa and later from terraces and stream channels of Trinchera Creek.

3. Wind conditions. The monthly mean wind speed varies from 5 to 12 mph (2.2 to 5.4 m/s) and averages 8 mph (3.6 m/s). However, monthly peak gusts have been 48 to 67 mph (21.5 to 30.0 m/s) from the southwest>west>northwest in the past two decades in Alamosa (see http://www.wrcc.dri.edu).

4. Topography. This site is along a north-south ridge, perpendicular to the prevailing winds (southwest to northwest). In addition, there is higher topography in the form of bedrock-cored hills to the north and south of Trinchera Creek (fig. B6–1). These conditions are conducive to accelerating ambient winds by a venturi effect.

However, the presence of flutes on the leeward (east) side of the blocks is a bit troubling. Laity (written commun., 2007) says that "it is uncommon for these type of ventifacts to form on the leeward side: in having looked at thousands of ventifacts at dozens of sites . . , erosion is always on the windward side of the rock. . . . Furthermore, I stood for about three hours in a hellacious sand storm in the Mojave observing ventifact formation: no abrasion occurred on the leeward side—in most cases, it is mantled (and thus protected) by sand falling out of suspension or by a wind tail."

Thus, one must consider whether there have also been strong westerly winds at this site, or whether the flutes on the east side of the bedrock blocks might be of another (fluvial?) origin.

The ventifacts at stop B6 formed on wind-polished blocks of porphyritic andesite (unit Tc, fig. B6–1); they are characterized by finger-size troughs, percussion cones, and broad mullions on the front and back sides of intact bedrock (fig. B6–2). These features reflect hundreds of thousands of years of wind erosion at a location where sand is available and the wind is strong. Further east, near Smith Reservoir (south of Blanca), dreikanter-type (three-sided) ventifacts are well developed on blocks of Servilleta Basalt—Pliocene tholeiitic flood basalts that are common to the south of the San Luis Hills (see stops in chapter C). This basalt appears to have been at or near the surface since it was emplaced about 3.7 Ma.

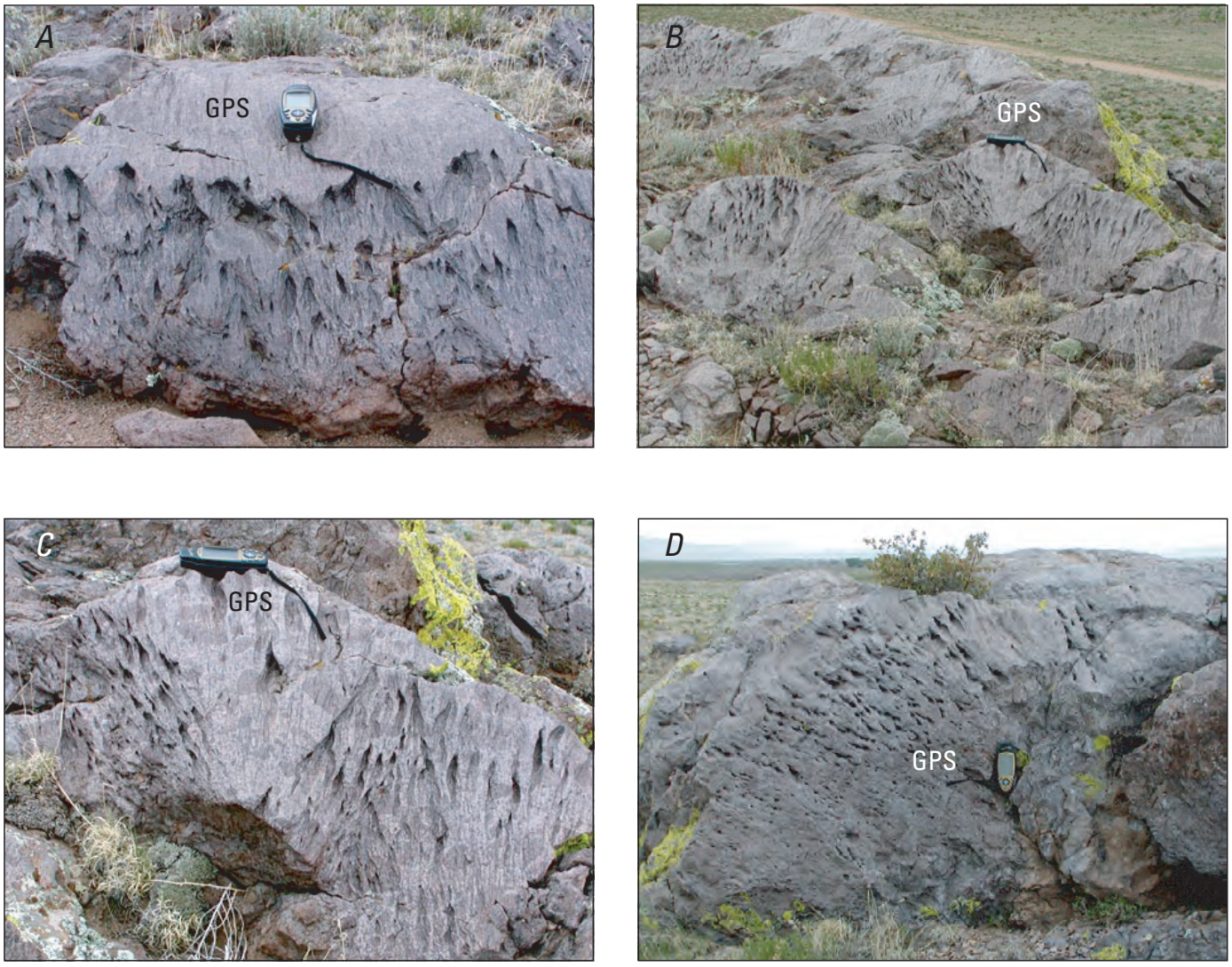

Figure B6–2. Ventifacts in upper Oligocene porphyritic andesite (Conejos Formation). GPS (15 cm long) for scale. *A*, Flutes in leeward (east) side of large wind-polished boulder. View to west (upwind). *B*, Broader view of flutes in leeward (east) side of large wind-polished boulders. Note variations in orientation. View to west (upwind). *C*, Closeup view of flutes shown in *B*. Note that the flutes cut across flow bands and clasts within the andesite. *D*, Radially oriented cones and flutes in windward (west) side of large wind-polished boulder. View to east (downwind).

Stop B7 (Optional) — Hansen Bluff—Alamosa Formation

Author: Michael Machette
Location: Hansen Bluff
Alamosa East 7.5' quadrangle (BSE–MM04–23)
GPS: NAD27, Zone 13, 433322 m E., 4136731 m N.
Elevation: About 7,525 ft (2,294 m) asl (Wildlife Refuge parking lot below measured section D of Rogers and others, 1985)

Synopsis

Although we don't have time to visit this site, Hansen Bluff (fig. B7–1) is one of the most important locations in terms of understanding the Alamosa Formation. Karel Rogers and her colleagues conducted integrated, multidisciplinary studies of these bluffs in the late 1970s and early 1980s and published a number of excellent papers describing the Quaternary geology, environments of deposition, faunal and floral remains, magnetostratigraphy, and age control for the section. They followed up by drilling a 127-m-long core to extend the sedimentary record into the Pliocene. The main contributions that we have made at Hansen Bluff are to map the local geology, to recognize a stratigraphic unconformity between the fine-grained Alamosa Formation and the overlying coarser sandy gravel beds (older alluvium, unit Qao), and to suggest how these deposits fit into the broader history of Lake Alamosa.

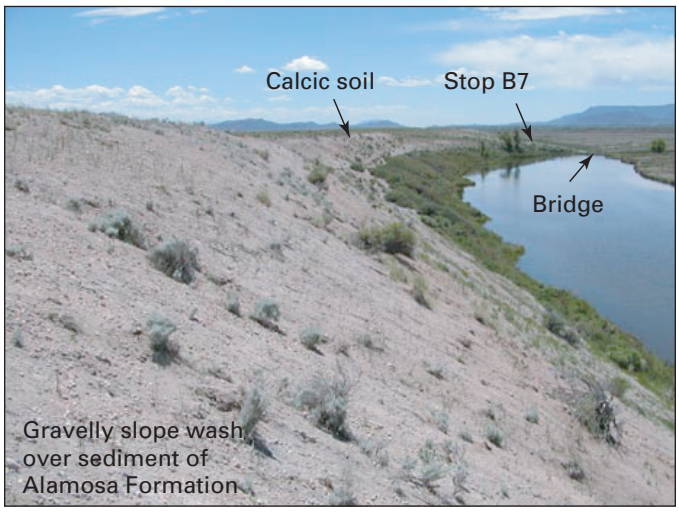

Figure B7–1. View of Hansen Bluff looking south from scenic drive near northernmost measured section (C) of Rogers (1984, fig. 1). Meander loop of the Rio Grande to right; San Luis Hills in the background. Location is 433378 mE, 4137274 mN (UTM Zone 13, NAD 83).

Discussion

Past Work

When vertebrate paleontologist Karel Rogers was at Adams State College (Alamosa, Colo.) in the 1970s and early 1980s, she assembled a team of paleontogists and geologists to study Hansen Bluff, a series of low stream-cut banks that lie just east of the Holocene channel of the Rio Grande, about 15 km east-southeast of Alamosa. Her colleagues included several USGS scientists who have retired (Rick Forrester) or passed away (Charles Reppening and J. Platt Bradbury) in the past few years. In the late 1970s, exposures of the bluffs were better and the area was not yet part of the Alamosa National Wildlife Refuge. Over a span of a decade they conducted detailed, multidisciplinary studies of these bluffs and published a number of excellent papers describing the geology, ecology, depositional environments, faunal and floral remains, magnetostratigraphy, and age control for the section. They followed up by drilling an additional 127 m to further extend the sedimentary record into the Pliocene. Among their many papers, those that are most important to the stratigraphy of the Alamosa Formation include an initial overview by Rogers (1984), a review paper by Rogers and others (1985) that is difficult to find (now), a specialized paper focusing on the Alamosa local fauna by Rogers (1987), a paper on the magnetostratigraphy, ages and sedimentation rates by Rogers and Larson (1992), and a final comprehensive review paper by Rogers and 11 others (1992).

Roughly sixty years earlier, USGS geologist Claude E. Siebenthal had described the sediments along Hansen Bluff, which he named for the bluff bank opposite the Hansen Ranch (Siebenthal, 1910, p. 11). Siebenthal conducted the first comprehensive survey of the geology and water resources of the San Luis Valley, completing his fieldwork in 1904 and the report in 1906. (He states that "untoward circumstances have intervened to prevent the publication of the report until the present" [1910]). Siebenthal's report focused on the groundwater potential of a prime and growing agricultural area in Colorado and provided the first stratigraphic evidence for a large and ancient lake, which he alluded to but did not name. Siebenthal's (1910, p. 40–41) measured section of the Alamosa Formation at Hansen Bluff is somewhat generalized, but it includes various colored sands, pebbly sandy, and drab clay totaling 61.5 ft (about 19 m), including several beds with laminae (lake beds). Siebenthal found a great number of freshwater shells in the bluff and reported that drill holes around the valley had brought up fossils (bird or fish bones) as well as wood, rootlets, leaves, seeds and peaty moss. He speculated that sediment of the Alamosa Formation was likely of late Pliocene or early Pleistocene age (not a bad guess for 110 years ago).

By the 1980s, Rogers and her team had a much larger and more sophisticated tool bag to investigate the bluff than

Siebenthal. In addition to excellent paleontological reference collections, they had tephrochronlogy and magnetostratigraphy to provide time lines. For the purposes of this field trip, we are most interested in the age control that Rogers and her team provided for the Alamosa Formation at Hansen Bluff.

There is no type locality for the Alamosa Formation, which is commonly 300–500 m thick in the subsurface (Siebenthal, 1910). Because so little of its sediment is exposed in the San Luis Basin, Hansen Bluff should be considered as the type section for the upper (Quaternary) part of the Alamosa Formation.

Local Geology

The main contributions that we have made at Hansen Bluff are to map the local geology, to recognize a stratigraphic unconformity between the fine-grained Alamosa Formation and the overlying coarser sandy gravel beds (older alluvium, unit Qao), and to suggest how these deposits fit into the broader history of Lake Alamosa.

Only the upper part of the Alamosa Formation is exposed at Hansen Bluff. This unit is mapped as QTla (Pliocene to middle Pleistocene), although Rogers (1984) established that the exposed section is early Pleistocene (late Irvingtonian). Overlying the Alamosa Formation is sandy pebble to small cobble gravel (3–6 cm diameter clasts), which has a 1-m-thick, stage III calcic soil (fig. B7–2). The alluvium is derived from the Sangre de Cristo Mountains (including Blanca Peak), but it may also be reworked from basin-fill sediment of the Santa Fe Group, which is exposed near Fort Garland. Precambrian rock (such as gneiss, quartzite, and granite) is exposed only in the Sangre de Cristo Mountains, whereas Tertiary volcanic rock dominates the San Juan Mountains and its foothills west of the valley. Thus, the type of rock clasts in alluvium (Precambrian basement versus Tertiary volcanic rock) is a reliable indicator of source area and transport direction in this part of the San Luis Basin sediments.

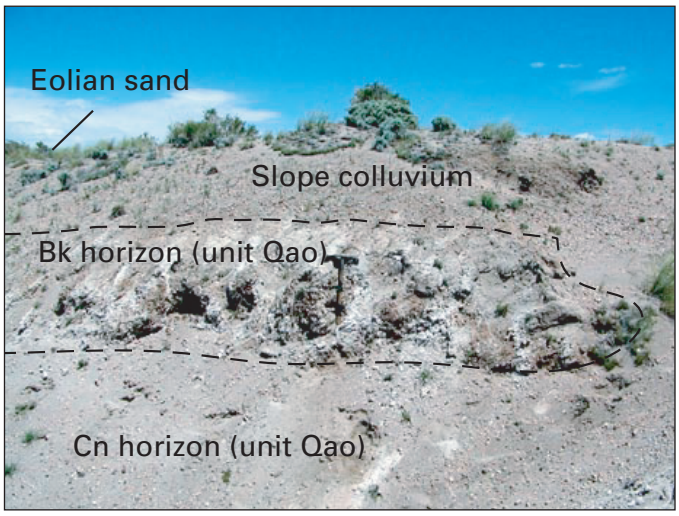

Figure B7–2. Strong but discontinuous calcic soil (Bk, stage III morphology) that caps Hansen Bluff. Soil pick (60 cm long) for scale. Location about 0.5 km north of stop B7, but this soil is representative of development in older alluvium (unit Qao) along bluff. View to the east.

To the east of Hansen Bluff, there are a series of sand-covered, piedmont-slope deposits at high, intermediate, and low levels: these are mapped as units Qao, Qai, and Qay, respectively (fig. B7–3). All of these deposits lie unconformably on the Alamosa Formation. The upper 8 ft (2.5 m) of Siebenthal's (1910) section is listed as "Recent" gravelly slope (slope colluvium) and indurated conglomerate (Bk horizon in sandy gravel), which we map as unit Qao. At this location, the surface of unit Qao is about 20 m (65–70 ft) above Holocene alluvium of the Rio Grande (units Qaa, Qfp, and Qa, fig. B7–3). The surface of Qai, which is inset into Qao as southwest-trending terrace deposits, projects about 15 m (50 ft) above the Holocene alluvium. Unit Qay is not widespread in this area, but it fills channels that project to only 3 m (10 ft) above the Holocene alluvium. All of the elevated alluvial surfaces were truncated along the bluff by lateral migration of the Rio Grande during the late Pleistocene and Holocene.

The cover of eolian sand east of the Hansen Bluff is quite impressive. Sand dunes (unit Qed) are concentrated along the bluff's western edge, but an extensive sheet of cover sands and coppice dunes extends several kilometers to the east. These sands are mapped (simply) as unit Qes, although older components (unit Qeso, Machette and Thompson, 2005; Michael Machette and Ren Thompson, unpub. mapping, 2007) are found in areas of blowouts in unit Qes cover. The older sands have Bw to weak Bt (argillic) horizons over stage I–II Bk horizons. We suspect that these older sands are of late or latest Pleistocene age.

Some authors have suggested that Hansen Bluff is an uplifted fault block (for example, Rogers, 1984), although there is little evidence or requirement for such a fault. Burroughs (1972) showed the bluff as a fault-line escarpment of the Lasauses fault, which extends north-south along the Rio Grande through the Fairy Hills (stop B4). However, there are no fault scarps on middle Quaternary or younger surficial deposits either to the north or south of Hansen Bluff, so there need not be a fault. We suspect that the Lasauses fault is a Neogene structure that has not been active in the Quaternary.

Hansen Bluff—Stratigraphy and Age

The age of the Alamosa Formation exposed in Hansen Bluff is based on a variety of data and assumptions (see discussion of Rogers and Larson, 1992). Two tephra beds (volcanic ashes) were exposed during the excavations: the upper tephra was identified as the Bishop ash, which was erupted from Long Valley caldera in eastern California at about 0.74 Ma. A second tephra was found about a meter lower in section, but it was not typed to a unique source and, thus, is of unknown age (and little use to us). A third tephra, the 2.02 Ma Huckleberry Ridge ash from the Yellowstone area

of northwestern Wyoming, was found in an adjacent drill hole, 78 m below the surface.

The two identified ashes are now considered to be slightly older (0.76 Ma Bishop Ash, Sarna-Wojcicki and others, 2000; 2.06 Ma Huckleberry Ridge ash, Lanphere and others, 2002; respectively) as a result of better radiometric dating ($^{40}Ar/^{39}Ar$) and laboratory calibrations. The Bishop Ash lies about 11 m above the base of the 17-m-high exposure at Hansen Bluff. The total sediment package between the 0.76 Ma and 2.06 Ma tephras is about 84 m thick. Thus, 84 m of sediment deposited in 1.30 m.y. yields a long-term (average) sedimentation rate of 6.5 cm per 1,000 yr. A more important assumption here is that of constant sedimentation, which is a first-order approximation that Rogers had to make. Because Lake Alamosa was a climatically driven lake, the sedimentation rates should have fluctuated greatly depending on the position of lake level, environment of deposition, and climate (all factors recognized by Rogers and her colleagues). On the basis of sedimentation rate, Rogers and Larson (1992) estimated that the Hansen Bluff section ranges from about 0.67 Ma and 0.9 Ma, with the Alamosa Formation extending back to at least 2.6 Ma at the bottom of the drill hole (at 127 m depth).

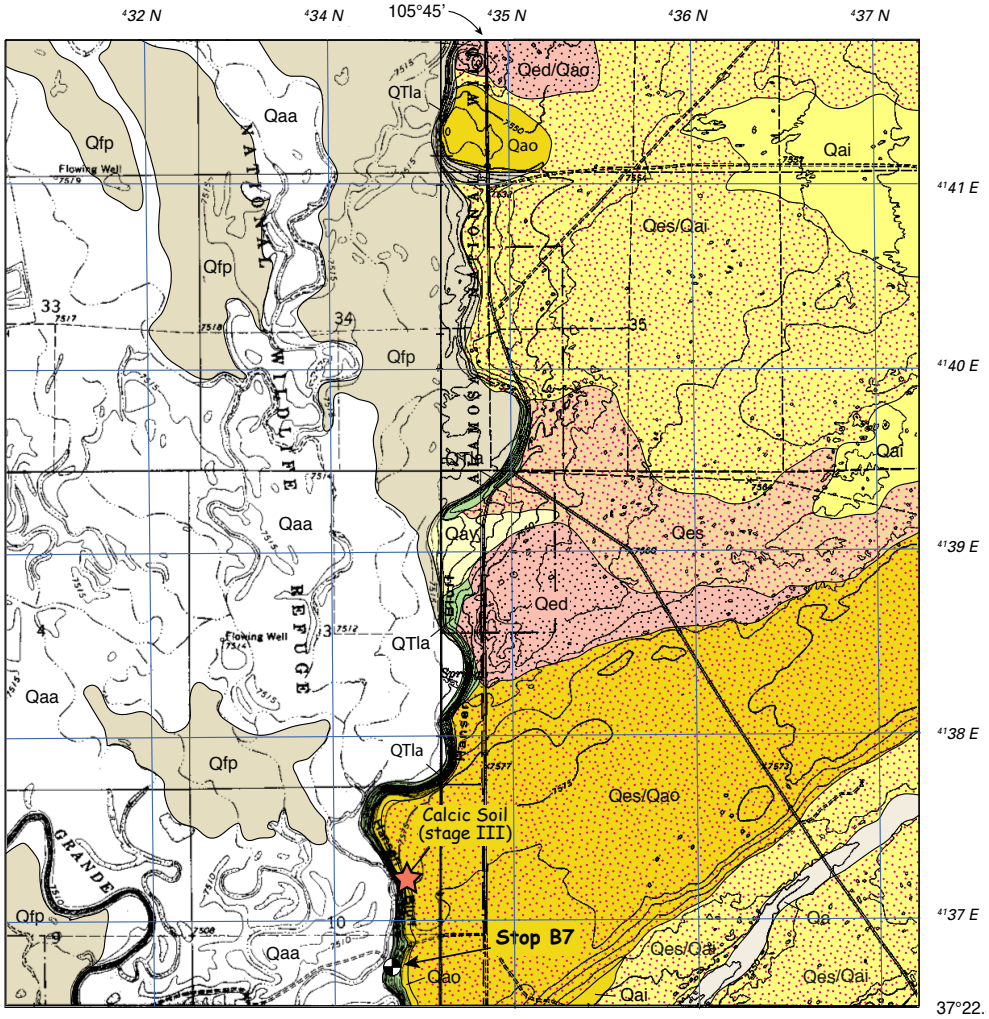

UTM coordinates in km, Zone 13, NAD 27. Base scanned from southeast corner of Alamosa East quadrangle (1966 ed.) and southwest corner of Baldy quadrangle (1965 ed.)

Figure B7–3. Hansen Bluff, suggested type section for the Alamosa Formation. Map units: Qes, eolian sand; Qed, dune sand; Qaa, active alluvium; Qfp, floodplain alluvium; Qa, undivided Holocene alluvium; Qay, younger alluvium (late Pleistocene); Qai, intermediate alluvium (late to middle Pleistocene); Qao, old alluvium (middle Pleistocene); and QTla, Alamosa Formation. Photographs shown in figures B7–1 and B7–2 were taken at location marked by red star (calcic soil). Geology modified from Machette and Thompson (2005) and Michael Machette and Ren Thompson, unpub. mapping, 2007).

Rogers and Larson (1992, fig. 2) assembled a magnetostraphic record for the Alamosa Formation surface exposures (Hansen Bluff) and cored section, using the two dated ash beds to anchor the magnetic polarity zonation (fig. B7–4). The Bishop Ash is normally magnetized and lies at the base of the Bruhnes Normal Chron (0–0.78 Ma). Conversely, the Huckleberry Ridge Ash (at 2.06 Ma) lies within one of the Reunion normal events within the Matuyama Reversed Chron in the late Pliocene (Rogers and Larson, 1992, fig. 2). On the basis of depth and sedimentation rate, the base of the drill hole appears to be in the Gauss Normal Chron, and thus is >2.48 Ma.

For comparison, we have used a recent composite benthic oxygen-isotope record (Lisiecki and Raymo, 2005) to infer possible correlations with major glacial and interglacial stages for the exposed section at Hansen Bluff (fig. B7–4). If the upper part of the section were about 0.67 Ma, this would correlate with OIS 17 (a major interglacial interval), whereas the basal part of the section (0.9 Ma) would correlate with a time just before OIS 22 (a major glacial interval). Within the exposed section, there should be a sedimentary record of climatically oscillating Lake Alamosa (and an adjacent piedmont) that contains three major glacial cycles (OIS 22, 20,

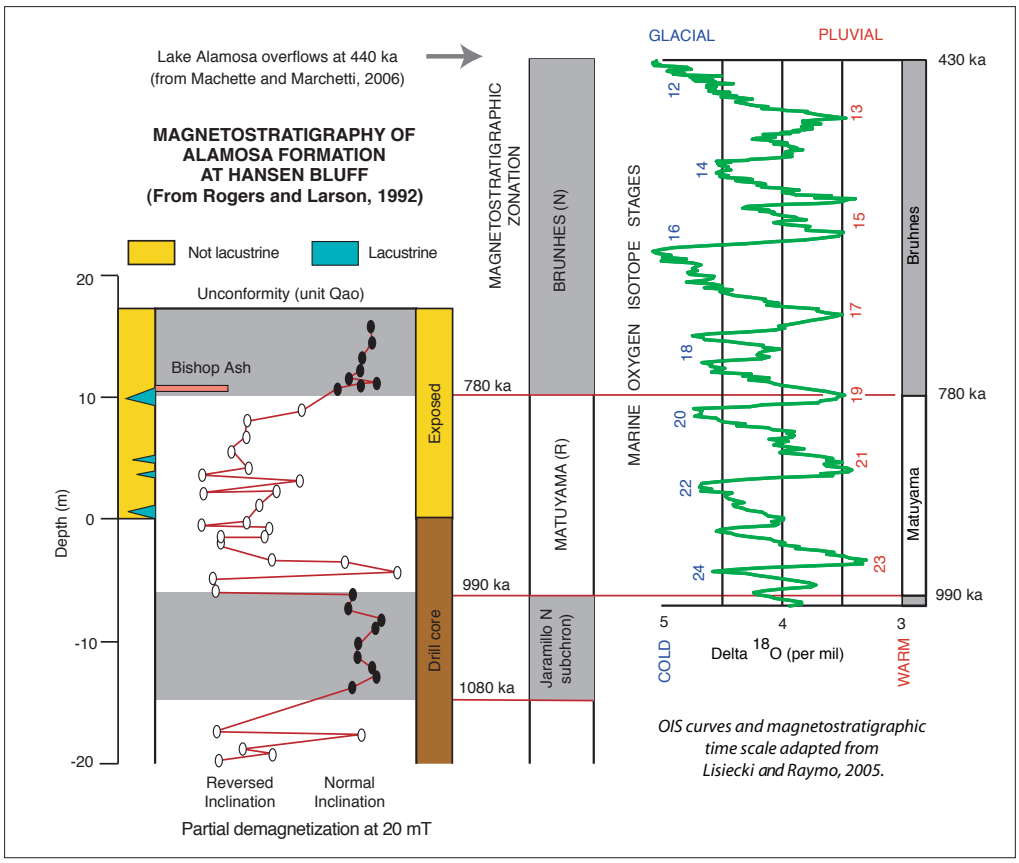

Figure B7–4. Magnetostratigraphic record at Hansen Bluff (modified from Rogers and Larsen, 1992, fig. 2). Upper 17 m of sediment are exposed; lower sediment is from drill core. Record is modified to fit magnetostratigraphic zonation and ages of Lisiecki and Raymo (2005). Interpretation of lacustrine versus nonlacustrine environments of deposition are from Rogers (1984, fig 3). By our interpretation, the upper part (ca. 670–440 ka) of the Alamosa Formation is not preserved at Hansen Bluff.

and 18) and all or parts of four interglacial cycles (OIS 23, 21, 19, and 17).

If our model of a climatically driven Lake Alamosa is correct (see chapter G), then the glacial cycles should relate to deep, large lakes (such as the records show for Lake Bonneville and Lake Lahontan, see Reheis and others, 2002), and the interglacial cycles should relate to shallow, restricted lakes (or playas). The sedimentologic and fossil records at Hansen Bluff (Rogers, 1984; Rogers and others, 1985) show only four intervals of lacustrine sedimentation (Rogers, 1984, fig. 3). We plotted these lacustrine versus nonlacustrine intervals on the left side of figure B7–4, strictly for comparison with the glacial records from marine oxygen isotope stages (Lisiecki and Raymo, 2005). These correlations suggest that Lake Alamosa rose to the level of Hansen Bluff (about 7,520–7,560 ft or 2,292–2,304 m asl) four times from 0.9 to 0.67 Ma, but not for long each time (because most lake beds are thin). The portions of lacustrine beds in the section do not appear to map simply into the chronology of glacial events inferred from the marine oxygen-isotope data (assuming linear sedimentation rates), but they do support our inference of recurrent, high stands in Lake Alamosa during the early to middle Quaternary.

Stop B8 — Mesita Hill: An Early Pleistocene Volcano Adrift in a Sea of Dirt

Speakers: Michael Machette, Ren Thompson, and Bob Kirkham

Location: Entrance to Jake and Hank Mine (cinder quarry) at Mesita Hill, about 2 mi (3.2 km) west-northwest of Mesita, Colo.
Sky Valley Ranch 7.5' quadrangle
GPS: NAD27, Zone 13, 443580 m E., 4106700 m N.
Elevation: 7,800 ft (2,377 m) asl (at entrance gate)

Synopsis

Mesita Hill is an early Pleistocene basaltic shield volcano in the Costilla Plain between San Pedro Mesa and the Rio Grande. With an $^{40}Ar/^{39}Ar$ age of 1.03±0.01 Ma (Appelt, 1998), the volcano is the youngest eruptive center within the San Luis Basin and in the Rio Grande rift north of Albuquerque, N. Mex. Younger volcanoes, generally considered to be associated with crustal extension, exist further north in west-central Colorado, including Dotsero "crater" (4,150±30 ^{14}C yrs B.P., Giegengack, 1962) and Willow Peak volcano (0.28±0.04 Ma, Kunk and others, 2002), but they are well outside of the present physiographic boundary of the rift. The Mesita volcano is cut by an intrarift fault, informally known as the Mesita fault (figs. B8–1 and B8–2). The fault shows recurrent post-4 Ma movement including offset of the western flank of Mesita volcano, offset of middle Pleistocene alluvium of the Costilla Plain, and offset of late-middle and late Pleistocene alluvium of the Costilla drainage south of Mesita.

Stop B8 includes a walking traverse from the parking area on the south side of the reclaimed quarry pit, skirting the east side of the remaining pit to the north end of the cinder quarry, followed by a short excursion (about 0.5 km) to the northern flank of the volcano and subsequent return to the starting point by a route along the footwall of the Mesita fault. There are three principal topics of discussion planned for stop B8 that correspond with stops along the walking traverse delineated on figure B8.1. The first stop (stop B8.1) provides an opportunity to discuss the volcanic history of this beautifully exposed basaltic cone and flows and to examine sedimentary deposits and structures preserved on the north rim of the excavation pit. The origin of these sedimentary deposits has been the subject of some debate that centers on the posteruption geologic history of Mesita Hill, whether Mesita Hill is a primary feature or an exhumed feature, and the associated geologic histories involved these vastly different interpretations. This debate will be examined in light of the observed deposits and models for basin evolution and the origin of the Costilla Plain. The second topic (stop B8.2) involves a discussion of the results of cosmogenic dating of lava flows and its application to surface-exposure dating at Mesita volcano. The final stop (stop B8.3) on our volcano tour provides an overview of the Mesita fault, a down-to-west intrabasin fault with recurrent Quaternary movement that cuts the 1.0 Ma basalt flows on the west side of the volcano.

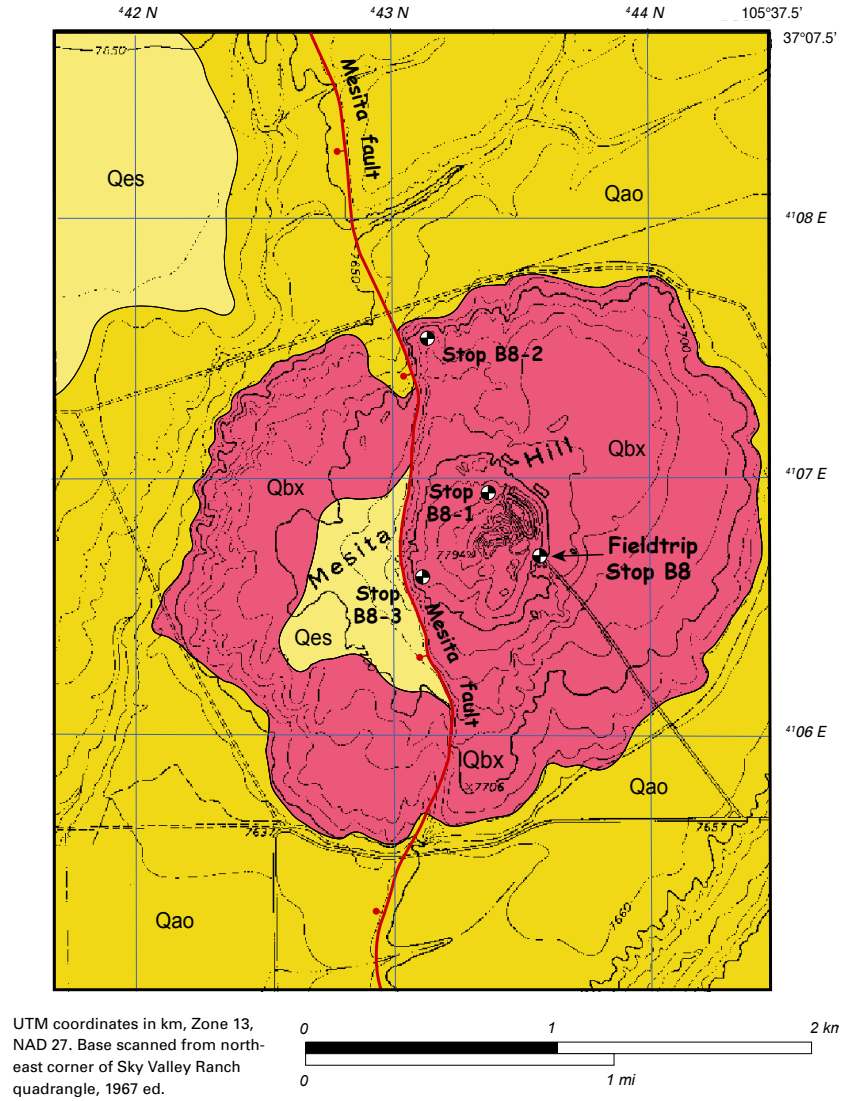

Figure B8–1. Geologic map showing Mesita Cone, a 1.0 Ma volcano. Map units: Qes, eolian sand; Qao, old alluvium (Costilla Plain); Qbx, basalt of Mesita Cone. Geology modified from Thompson and Machette (1989).

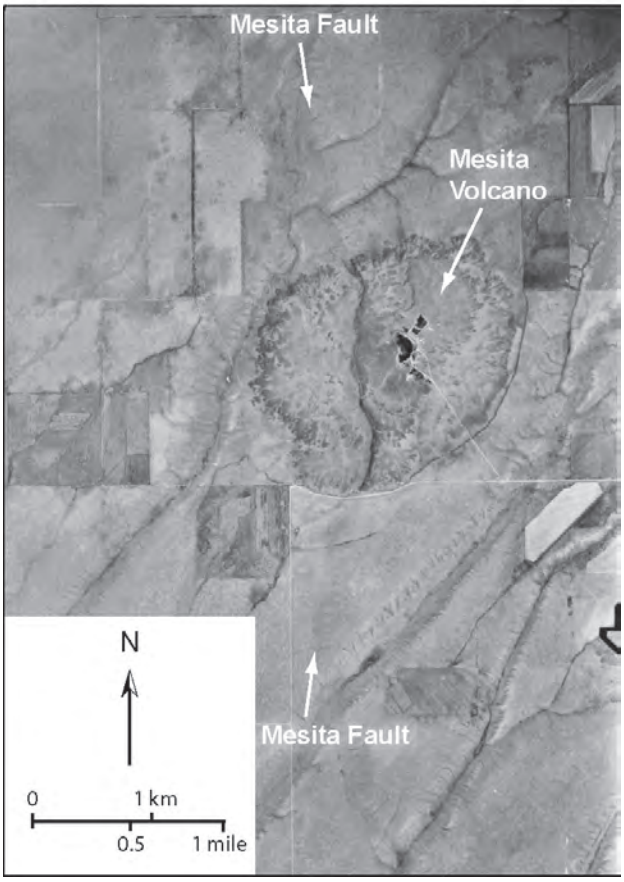

Figure B8–2. Aerial photograph taken in 1953 showing Mesita fault (white arrows) cutting 1.0 Ma Mesita volcano and middle Pleistocene alluvium (unit Qao of Thompson and Machette, 1989). Also visible are early excavations associated with the Hank and Jake Mine (quarry in Mesita cone).

Stop B8.1 — Cinder Pit (Reclaimed), Mesita Volcano

Location: Main cinder pit
Sky Valley Ranch 7.5' quadrangle
GPS: NAD27, Zone 13, 443406 m E., 4106841 m N.
Elevation: 7,750–7,780 ft (2,362–2,371 m) asl

Discussion

Johnson (1969) originally mapped Mesita volcano at a scale of 1:250,000 on the geologic map of the Trinidad 1° x 2° quadrangle. Colton (1976) also mapped the volcano at a scale of 1:250,000 and was the first to map the Mesita fault that cuts the volcano (fig. B8–1). Epis (1977) conducted a detailed study of the volcano as part of an unpublished ground-water availability study by Zorich-Erker Engineering, Inc. (1980) that included a 1:24,000-scale map and cross section of Mesita volcano and adjacent Costilla Plain (figs. B8.1–1 and B8.1–2). Thompson and Machette (1989) show the volcano on their 1:50,000-scale map of the San Luis Hills area, but they incorrectly assumed it was Pliocene in age, prior to the 1.0 Ma $^{40}Ar/^{39}Ar$ age determination of Appelt (1998). These documents and the results of new interpretations presented in Thompson and others (chapter H, this volume) are the basis for discussion at this stop.

Epis (1977) and Thompson and Machette (this volume) map the central part of the volcano as predominantly consisting of near-vent pyroclastic deposits associated with the eruption of Mesita volcano. Epis described the vent area as being composed predominantly of cinders—a resource that was developed by the Mickelsen family in 1950 or 1951. George Oringdulph, Sr., and Henry Quiller acquired the property in the mid-1950s and mined there until 1981 when they sold the operation. The property changed ownership a few times since then, but Hecla Mining Company (Coeur d'Alene, Idaho) ended up with the property in the mid-1980s when they bought out Ranchers Exploration (mining history from Rob Oringdulph, oral commun., 2006). The mine operated until the late 1990s but is now scheduled for reclamation by the owner. Although mining had disturbed some, but not all, of the important stratigraphic relationships that were preserved near the edifice of the volcano, the reclamation activities scheduled for

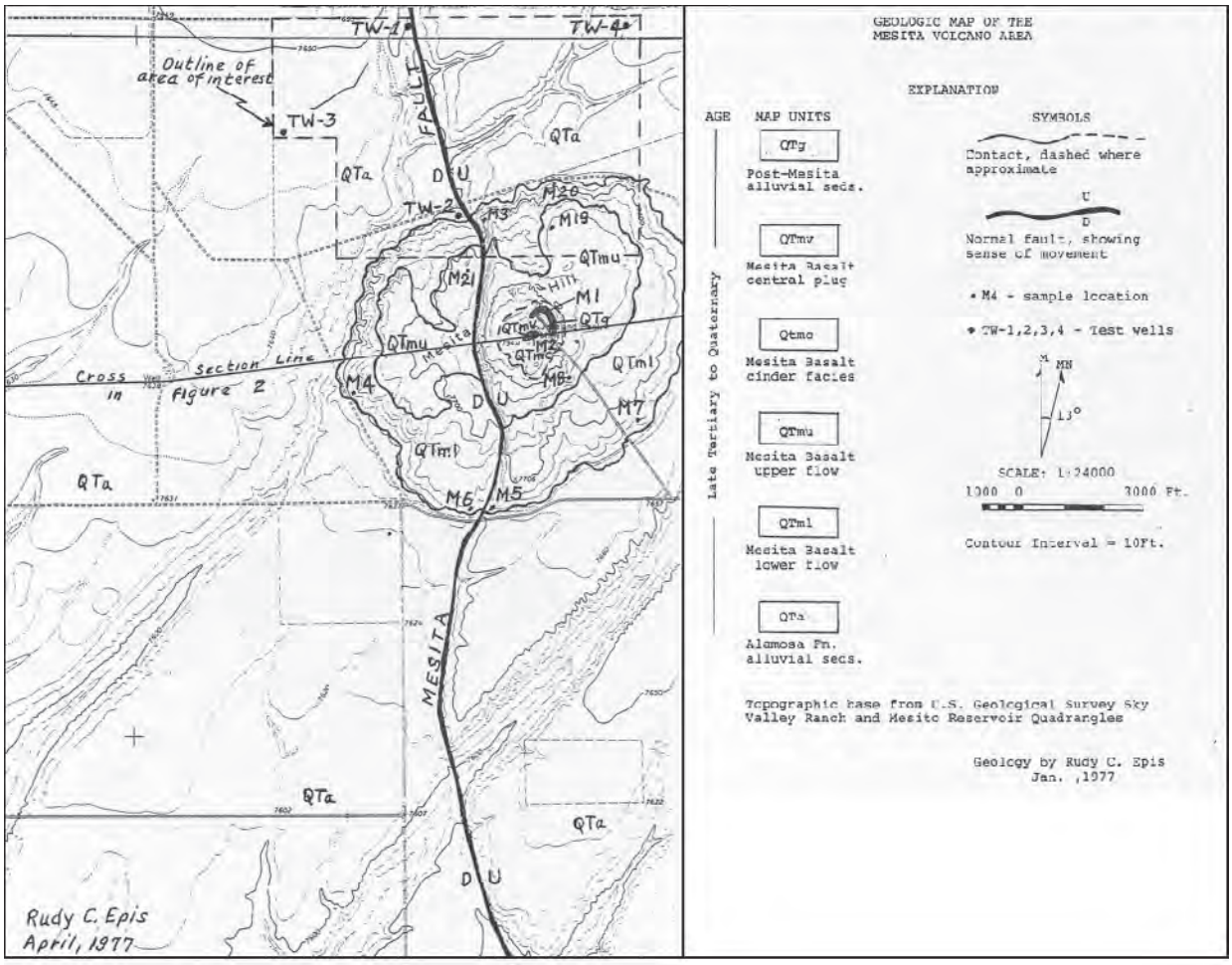

Figure B8.1–1. Geologic map of Mesita Hill reproduced from Epis (1977). USGS topographic base of 1967 compiled from photography flown in 1965.

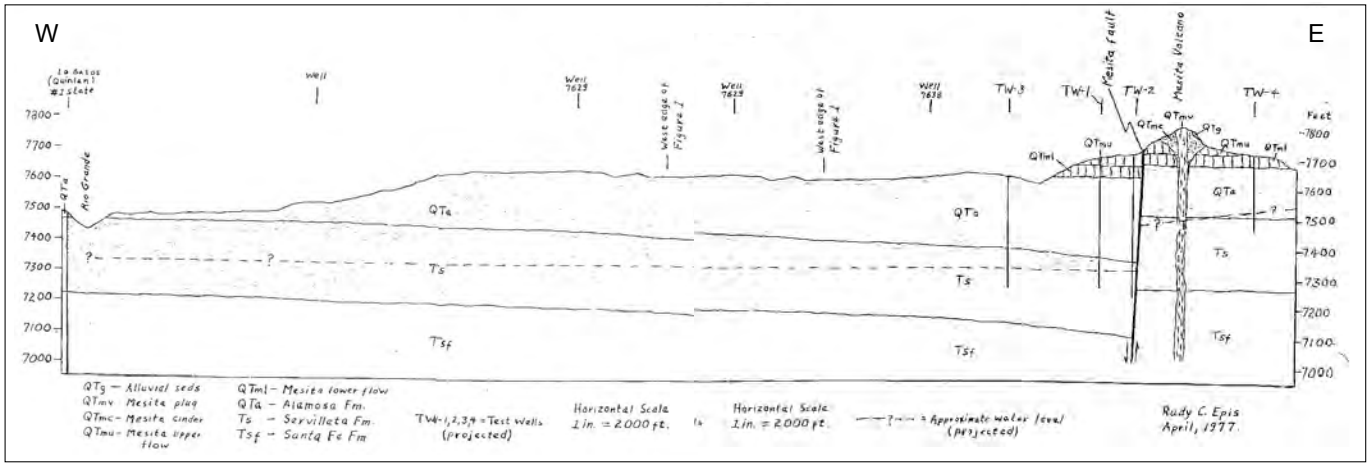

Figure B8.1–2. Geologic cross section through Mesita Hill, reproduced from Epis (fig. 2, 1977).

this summer (2007) will destroy what remains of the quarry and primary stratigraphic relations preserved therein.

Mesita volcano is a low-relief shield consisting of a symmetric summit cone built on a platform of lava flows. The existing USGS Sky Valley Ranch quadrangle, compiled photogrammetrically in 1967 from aerial photographs taken in 1965, demonstrates that the preexcavation summit cone of Mesita volcano rose to an elevation of approximately 7,810 ft, approximately 60 ft (18 m) above the top of the plateau-forming lava flows underlying the cone. In 1965, quarry operations were restricted to a small pit on the northeast shoulder of the summit cone (fig. B8.1–1) and the original summit was undisturbed. The lava-flow plateau underlying the cinder cone comprises two eruptive phases of compositionally similar lava denoted in figures B8.1–1 and B8.1–2 as map units QTml and QTmu respectively. The lower unit (QTml) was incorrectly described by Epis (1977) as a single lava flow, but in fact it contains multiple lava flows, the boundaries of which are distinct on aerial photographs (Thompson and others, chapter H, this volume) and preserved flow contacts in the footwall of the Mesita fault. The upper unit (QTmu) represents late stage eruption of lava prior to cessation of volcanic activity. This final phase of eruption was likely Strombolian in character and was responsible for the formation of the cinder cone and the thin lava flows extending both northeast and west from the current summit cone.

On the basis of limited geochemical data, all of the Mesita volcano lava flows and near-vent deposits are basaltic andesite, similar in composition to other small-volume eruptions of the Taos Plateau volcanic field. Petrographically, the rocks are weakly porphyritic to microporphyritic with pilotaxitic texture. Phenocrysts, where present, are predominantly plagioclase with lesser amounts of olivine. The rock's microcrystalline groundmass consists of plagioclase, pyroxene, olivine, and iron-titanium oxides. Ubiquitous but scarce xenocrysts of plagioclase and lesser quartz can be as large as 1 cm and are characteristic of other small-volume eruptive centers in the region, resulting in the informal usage of the term XBA (xenocrystic basaltic andesite) to describe such rocks (Lipman and Mehnert, 1979; Thompson and Lipman, 1994a,b). In spite of the propensity of these rocks to have excess "old" argon resulting from disaggregation and possible magmatic recycling of xenocrysts of Precambrian age, Appelt's (1998) $^{40}Ar/^{39}Ar$ age of 1.03±0.01 Ma from groundmass yielded a reasonable plateau age. Unfortunately, since we only have Appelt's reported sample locality to go on, we don't know if the sample was collected from "in place" rock (unit Qtmu) or a block of material stockpiled from quarry. If the sample were collected from a natural outcrop, it would date the younger of the two lava-flow sequences.

Beautiful examples of cinder, spatter, spatter agglutinate, incipient lava flows, and bombs are exposed within the remaining quarry pit. The bombs are primarily of the spindle variety, characteristic of Strombolian eruptions of basaltic andesite. Notably absent are dikes of similar composition that are commonly found in cinder quarries. This absence likely reflects the short-lived nature of the eruptive activity at Mesita volcano. Preexcavation aerial photography taken in 1936 shows two northwest-trending dikes that cut the northern end of the cinder cone and may have served as vent areas for at least part of the eruption cycle. Epis (1977) maps a central vent "plug" (figs. B8.1–1 and B8.1–2), but no evidence for this plug is visible in the earlier photographs or in the remaining pit quarry. Regardless of the exact location or geometry of the vent area, the eruption could have occurred over a period as short as a few days to weeks.

A small remnant of sedimentary deposits locally overlies volcanic rocks on the northeast flank of the Mesita volcano. Epis (1977) provided the first record of these deposits, but Robert Kirkham and Eric Harmon (2006, oral commun. to Kirkham) also observed the sediments in the mid-1970s. Epis mapped the deposit as a crescent-shaped remnant of sediment on the north and northeast rim of the volcano (fig. B8.1–1). His report is an appendix to an unpublished document by Zorich-Erker Engineering, Inc. (1980). Because this document is difficult to obtain, Epis' 1977 map is reproduced herein as figure B8.1–1. The remnant of sediment is the dark-shaded area labeled "QTg" on his map. Epis refers to these deposits as "Post-Mesita alluvial sediments" and described them as "alluvial muds, sands, and gravels." This evidence led Epis to conclude, "the region was formerly buried by alluvial sediments and is now being exhumed and dissected by the entrenchment of the Rio Grande and its tributary drainages." Kirkham (2006) also pointed out the remnant of sediment and stated that its presence suggested the volcano could be an exhumed feature.

Unfortunately, some outcrops of the sediment have been removed or disturbed by mining activities. Figure B8.1–3 shows these sediments in the north wall of the mine pit, as they appeared in 2006. As part of planned reclamation activities by the Hecla Mining Company for the summer of 2007, the pit may be reclaimed. These sediments and features may be disturbed, buried, or completely removed prior to the FOP field trip.

The sediment in the remnant consists of beds of very poorly sorted to moderately well sorted, weakly bedded to nonstratified, silty medium-grained to very fine grained sand, sandy silt, and gravelly sand. The matrix is arkosic, not volcaniclastic. Most pebble- and cobble-size clasts are composed of angular to subangular basalt (cinders, scoria, and flow rock) that is locally derived from Mesita volcano, although rare subrounded pebbles of quartz and gneiss are present. Although the volcanic clasts are reworked as colluvium, the enclosing matrix sediment is arkosic. Machette and Thompson believe that that the matrix might be eolian sediment derived from arkosic sands (upper part of Santa Fe Group) that underlie the adjacent Costilla Plains, whereas the volcanic clasts are certainly locally derived (colluvium) (see discussion in chapter H, this volume). Conversely, Kirkham believes that the arkosic sediment is water laid and part of a once more extensive (and thicker) basin-fill sequence. The main question about the perched sedimentary package of Epis (1977) comes down to (1) whether wind was capable of transporting the rare,

Figure B8.1–3. Photographs of sediments preserved on the north rim of existing quarry (stop B8.1). *A*, Unconformity between primary pyroclastic deposits (a), volcanic colluvium (b), and overlying sedimentary deposits (c). *B*, Pebble- to cobble-size volcanic and Precambrian(?) clasts in sediments overlying volcanic deposits. *C*, Closeup view of sedimentary structures and clasts near basal contact with volcanic deposits. Photographs by R.M. Kirkham, 2006.

small (1–2 cm) pebbles of quartz and gneiss found within the sedimentary deposit or (2) whether this is a remnant of fluvial sediment deposited on the volcanic cone and now preserved ≥30 m (100 ft) above the Costilla Plains. If the volcano was buried or nearly buried by sediment and subsequently exhumed, its evolution could be characterized by the cross sections shown in figure B8.1–4. Exhumation must have occurred prior to deposition of the middle Pleistocene older alluvium of Thompson and Machette (1989; unit Qao), which is estimated to be 500±100 ka.

However, the exhumation model proposed by Epis (1977) and supported by Kirkham (2006) introduces local and regional complexities not consistent with other geomorphic and geologic observations. For example, if one raises the unit Qao surface of Thompson and Machette (1989) to an elevation of 7,777 ft (the elevation of the sediments observed at stop B8.1), it dramatically increases the amount of basin-fill sediment that would have covered the Costilla Plain and encroached upon the San Luis Hills, and it should have left a geologic signature on the early Pleistocene landscape well beyond Mesita Hill—in fact, around the entire margin of the Costilla Plain, according to Machette and Thompson.

Locally, these fluvial deposits would have completely covered the lower flanks of Mesita volcano and much of the summit cone. Although the summit cone has all but been removed by mining operations, the lower flanks of the volcano, including pressure ridges and ramp structures associated with primary emplacement, are well preserved (Thompson and others, chapter H this volume). Fresh-appearing aa surfaces appear little modified by alluvial processes, such as bed-load scouring or local channel cut and fill. Exotic clasts of gneiss and quartz are seldom observed as lag deposits over much of the volcano, particularly in filled depressions on the aa surfaces. Results from an ongoing effort to cosmogenically date the flows using ^{3}He techniques (stop B8.2) may help to resolve the burial history of the volcano. A surface-exposure age near 1 Ma (the time of the eruption) would support an interpretation that the basalt flows were never buried, whereas an exposure age much less than 1 Ma would support burial and exhumation of the flows (and by inference the cone).

If sedimentation of the Santa Fe Group was 30 m (100 ft) higher, then one could predict its extent throughout the Costilla Plain (and west to the San Luis Hills). Using a depositional surface pinned at 7,777 ft at Mesita volcano and parallel to that mapped for the unit Qao alluvium by Thompson and Machette (1989) would lead to burial of the 5.3 Ma Culebra volcano (just south of the intersection of State Highway 142 and the Rio Grande, fig. B–3). It would extend part way up

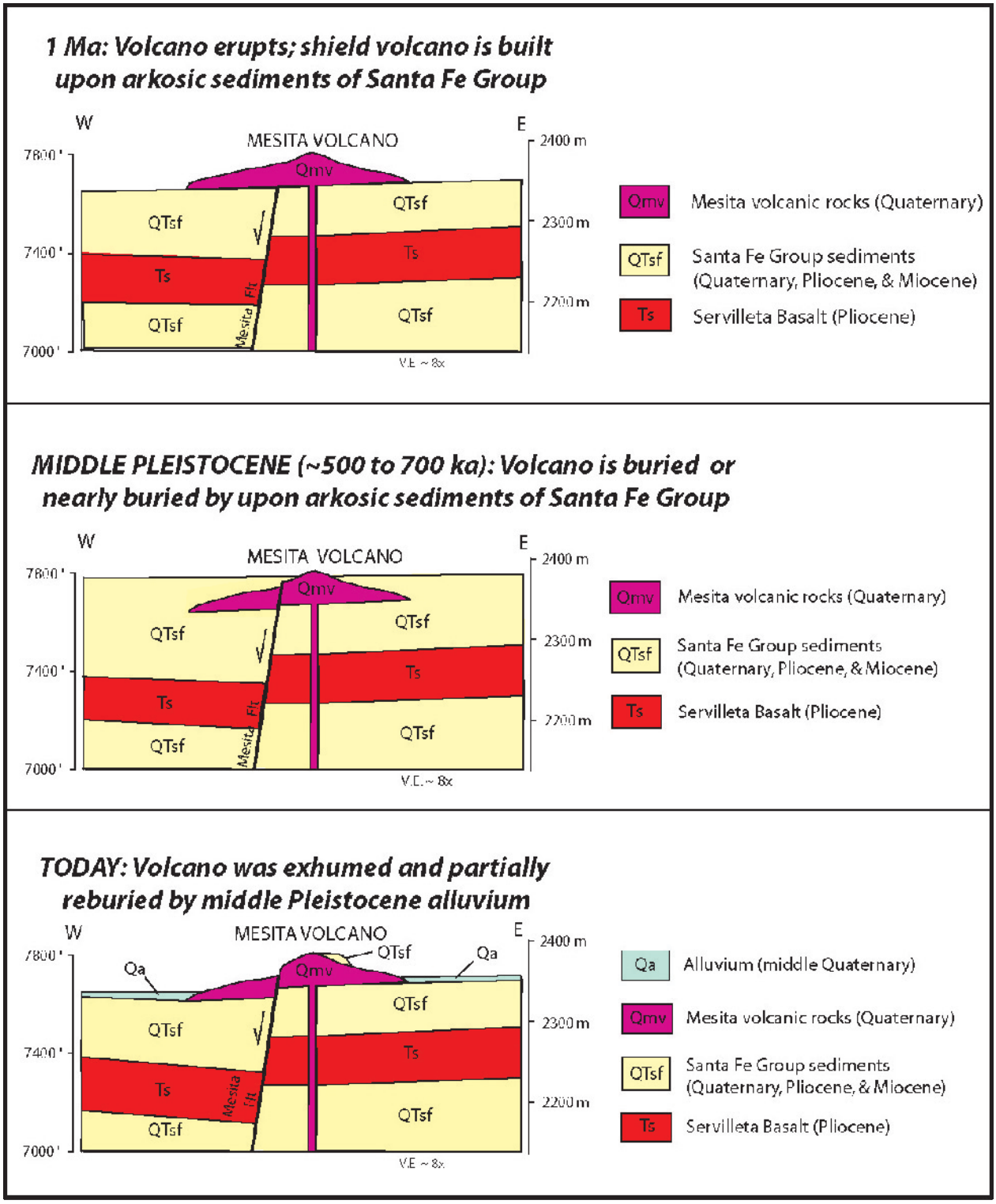

Figure B8.1–4. Schematic geologic cross sections showing geomorphic evolution of Mesita Hill proposed by Kirkham (2006), based on map relations depicted in Epis (1977).

the higher mesas of the San Luis and Fairy Hills (underlain by Conejos Formation volcanic deposits) and could have buried the eventual spillway area of Lake Alamosa (stop B4). Although the lower flanks of Culebra volcano contain clasts of Precambrian rock related to a paleochannel of the Rio Culebra, no exotic clasts are found near the summit region, suggesting the unit Qao surface never exceeded an elevation of about 7,635 ft at the position of the Rio Grande. Additionally, mapping in the Fairy Hills region of the San Luis Hills has revealed no remnants of Precambrian-rich alluvial sediments that would correlate with the perched sediment on Mesita volcano. Perhaps most intriguing about the hypothesis of 30 m higher deposition on the Costilla Plain is the implication that alluvial sediments of the Rio Culebra drainage could have extended northwest into the Fairy Hills, above the hydrologic threshold for Lake Alamosa at stop B4. No sedimentologic evidence exists for a higher level of basin filling—with the exception of the "fluvial sediment" on Mesita cone.

Mapping of sediment of the Santa Fe Group in the San Luis area (Machette and others, 2007) suggests that Santa Fe deposition continued into the middle Quaternary. About 4.5 km (2.8 mi) northeast of San Luis, Colo., Machette found volcanic ash interbedded in the uppermost part of the Santa Fe Group. This ash (sample SL–MM06–9) consists of nicely preserved, angular, predominantly solid, ribbed, and platy glass shards that match well with bimodal Lava Creek B (639±2 ka) volcanic glass samples from the Yellowstone caldera of northwestern Wyoming (Elmira Wan, USGS, written commun., 2006). The ash bed is overlain by several meters of slightly deformed sediment (unit QTsf) that is unconformably truncated by older alluvium (unit Qao). Thus, in the San Luis area (about 10 km north-northeast of stop B8), the upper part of the Santa Fe Group may be as young as 600 ka.

The overflow of Lake Alamosa occurred at about 440 ka (see Machette and others, chapter G, this volume), which led to downcutting of the Rio Grande and its tributary streams (such as Rio Culebra and Rio Costilla) on the Costilla Plain. If one presumes an approximate age of 500 ka for the pre-overflow unit Qao deposits, including the perched deposits at Mesita Hill, then there may have been only a very short period of time (60 k.y.) for basin-wide exhumation after the end of Santa Fe Group sedimentation. The tectonic or climatic driver for such rapid and complete denudation of the basin is unclear and the geologic impact of such a widespread erosion event has not been identified elsewhere in the basin.

Stop B8.2 (Optional) — ^{3}He Dating of Basalt Flows, North Flank of Mesita Volcano

Location: North flank of Mesita Volcano
Sky Valley Ranch 7.5' quadrangle (SVR–MM06–124)
GPS: NAD27, Zone 13, 443130 m E., 41067505 m N.
Elevation: 7,740 ft (2,359 m) asl

Synopsis

The second topic for discussion at the Mesita volcano (stop B8.2) involves cosmogenic ^{3}He surface-exposure dating of lava flows as a technique for resolving the burial history of the volcano, as discussed at stop B8.1. If the cosmogenic dating yields an exposure age near 1 Ma, then the volcano probably is a relict feature that was never buried. If the exposure age is much less than 1 Ma, then the volcano probably is an exhumed feature. Samples were being processed in the spring of 2007, with anticipation of having results by the time of the field trip (September 2007).

Discussion

In the fall of 2006, we collected three samples of flows from the Mesita Volcano for cosmogenic ^{3}He surface-exposure age. The samples were taken from slightly weathered flow surfaces located on the north flank of the volcano (fig. B8.2–1). At the time this field-trip guidebook was written (spring 2007), we are in the process of separating and concentrating the minerals olivine and pyroxene from the basalt. Once mineral separates are obtained, we will crush the separates under vacuum and determine the ^{3}He/^{4}He inventory in mantle-derived fluid inclusions. The samples will then be degassed at about 1400°C and the total concentrations of ^{3}He and ^{4}He will be measured by mass spectrometry. Cosmogenic ^{3}He concentrations will be determined using the mantle correction, and exposure ages will be determined using the latest ^{3}He production rate and cosmogenic scaling factors. Since ^{3}He is a stable isotope, the temporal limit

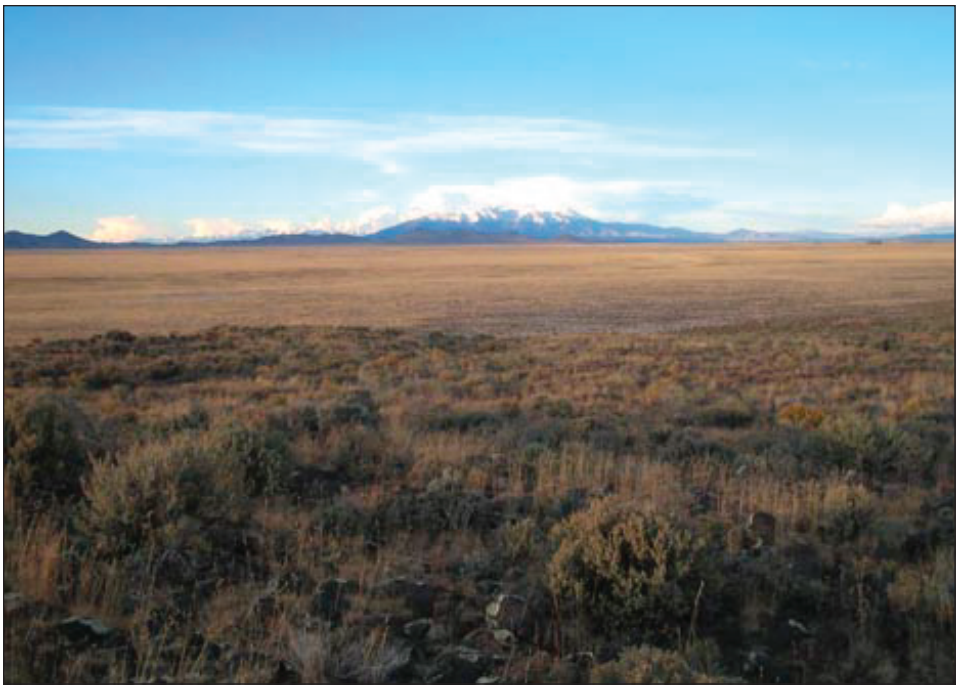

Figure B8.2–1. Surface morphology of basalts on the north flank of Mesita Volcano in foreground. View to the north shows northeast part of the San Luis Hills in the middle distance on the left and Blanca Peak is in the background. Photograph taken in October, 2006.

Figure B8.2–2. Locality on north flank of Mesita volcano that we sampled for ^{3}He surface-exposure dating. Machette, Thompson, and Shroba are shown from left to right, respectively.

of the dating method is constrained only by the erosion rate of the surface that is being sampled. Cosmogenic ^{3}He exposure ages in excess of several million years have been obtained in slowly eroding landscapes around the world (for example, Chile's Atacama Desert, Dry Valleys of Antarctica). See stop B3.3 for a discussion of the ^{3}He surface-exposure dating of basalts on spits of Lake Alamosa.

Strategy for Age Dating

The goal of sampling at B8.2 is simply to determine the exposure duration of the Mesita Volcano flow surfaces (fig. B8.2–2). We will use these data to test the plausibility of the burial or nonburial hypotheses discussed at stop B8.1. If the Mesita Cone and nearby Costilla Plain were not buried by some unknown thickness of alluvium (the burial hypothesis), then the exposure ages of the surfaces we sampled should be close to 1.0 Ma—which is the crystallization age of the Mesita Cone—and the ages should approach 1.0 Ma when a reasonable erosion rate is added into the age determination. If, however, the cone and Costilla Plain were buried by alluvium for a significant amount of time (such as 500 k.y.), then the exposure ages should be considerably younger than 1.0 Ma and not approach 1.0 Ma even when corrected for potential erosion rates.

Stop B8.3 — The Mesita Fault

Location: West flank of Mesita Volcano
Sky Valley Ranch 7.5' quadrangle
GPS: NAD27, Zone 13, 443100 m E., 4106660 m N.
Elevation: 7,820 ft (2,383 m) asl (upthrown block of fault)

Synopsis

Basalt flows dated at 1.0 Ma (stop B8.1) on the western margin of the Mesita volcano are displaced as much as 13 m by the Mesita fault, a down-to-the-west intrabasin fault that shows a well-documented history of progressive growth since Pliocene time. Quaternary alluvial deposits (mainly to the south of the volcano) are offset progressively less with decreasing age, whereas middle Pliocene flows of Servilleta Basalt (about 4.0±0.3 Ma) are offset substantially more than the 1.0 Ma basalt flows of the Mesita volcano. The offset of five geologic datums of Pliocene to late Quaternary age allows us to calculate long-term and interval slip rates through time, which on this fault are relatively constant at about 0.012 mm/yr. For comparison, the southern Sangre de Cristo fault zone shows an order of magnitude higher slip rates (see chapters C and J, this volume).

Discussion

The Mesita fault has been mapped from about 5 km (3 mi) north of Mesita Hill, south across the Costilla Plain 7 km (4.3 mi) into northern New Mexico. The southernmost mappable trace is on the northeast flank of Ute Mountain (recent mapping of the Sunshine and Ute Mountain areas by C.A. Ruleman, unpub. mapping, 2007). The fault's 22-km-long scarp (fig. B8.3–1) was first mapped by Colton (1976) as part of a reconnaissance study of landslides. The Mesita fault (#108 in Kirkham and Rogers, 1981, p. 25) forms a conspicuous west-facing scarp along the eastern side of the Sky Valley Ranch and Mesito Reservoir quadrangles, where it downdrops the west side of the Mesita cone by about 13 m (Kirkham and Rogers, 1981). Machette and Personius (1984) reported various amounts of offset of Quaternary alluvium along the fault, and Personius and Machette (1984) summarized the

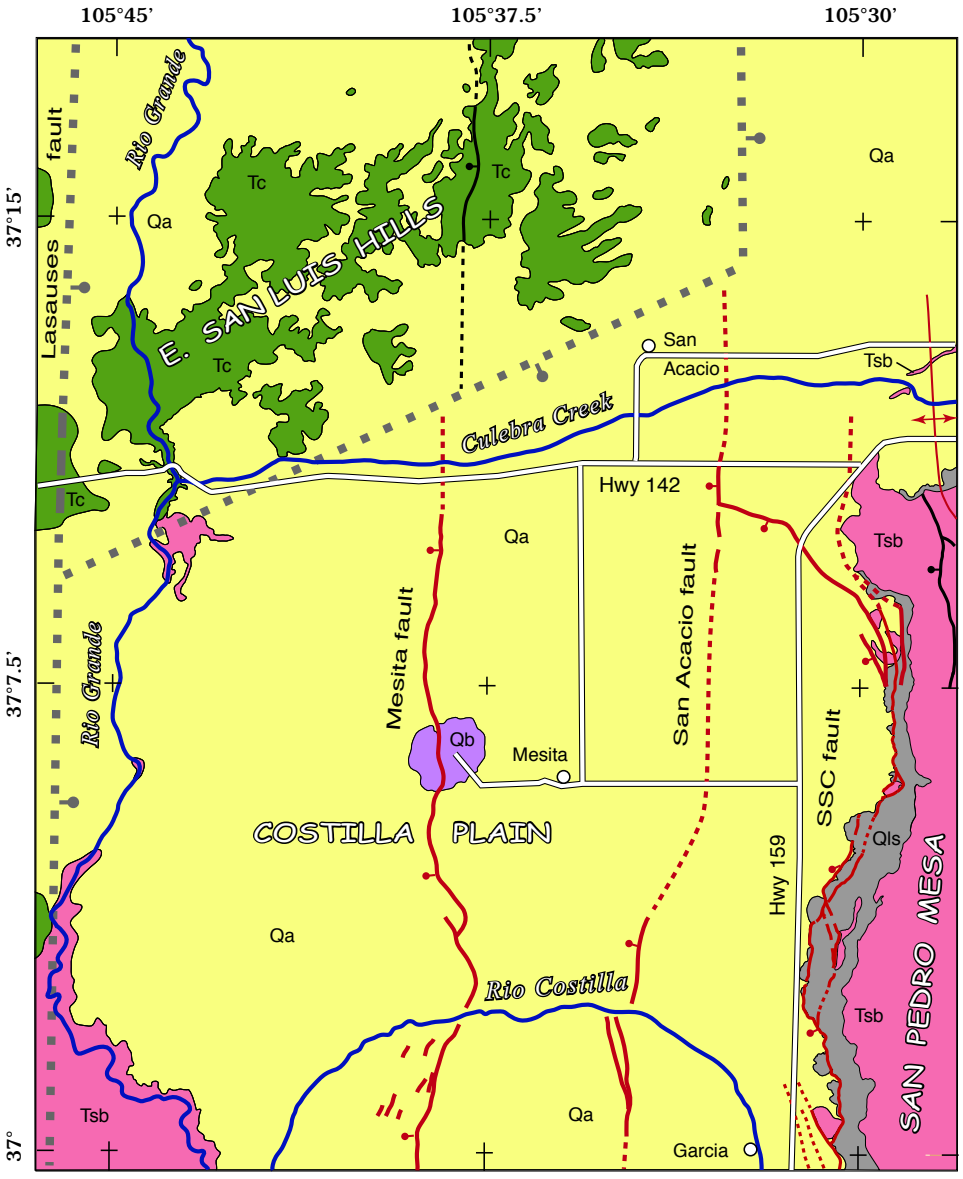

Figure B8.3–1. Costilla Plain (in Colorado) showing Quaternary faults (red lines) and older structures (black lines). Major Neogene faults that block out the San Luis Hills are shown by thicker gray dashed or dotted lines. Bedrock units lumped into the following: Qb, Mesita basalt (1.0 Ma); Tsb, Servilleta and age-equivalent basalts; Tc, Oligocene volcanic rocks. Quaternary units shown as Qa, with exception of landslide deposits (Qls) along San Pedro Mesa. SSC fault: southern Sangre de Cristo fault zone. Geology modified from Thompson and Machette (1989) and Thompson and others (2007).

fault in a regional overview of Quaternary faulting in northern New Mexico and southern Colorado. The Mesita fault is shown as structure 2015 in the U.S. Geological Survey Quaternary fault and fold database (see http://earthquake.usgs.gov/regional/qfaults/).

Quaternary Faulting

The intrabasin Mesita fault is positioned midway between the Sangre de Cristo fault zone on the east and the San Luis Hills on the west (fig. B8.3–1). To the south, the Mesita fault ends northeast of Ute Mountain where extension is transferred in an opposite sense to the intrabasin, down-to-the-east Sunshine Valley fault (see discussion in chapter C, this volume). The southern Sangre de Cristo fault zone, which is the main east-bounding structure for the Rio Grande rift in this region, is rather complex here. This 250-km-long fault system has three discrete fault zones, herein described from north to south. (See chapter J, this volume, for a more complete discussion of the Sangre de Cristo fault system and new designations of its individual fault zones.)

1. Northern fault zone: Extends about 104 km from Poncha Pass across the northern part of the San Luis Valley, along the west margin of Sangre de Cristo Mountains, east of the Great Sand Dunes and to the south flank of the Blanca Peak massif;

2. Central fault zone: Extends about 60 km from the south flank of the Blanca Peak massif through Fort Garland, along the west margin of Culebra Range and east side of the Culebra graben to the border with New Mexico; and

3. Southern fault zone: Extends about 96 km from southeast of San Acacio along the west side of San Pedro Mesa (stop B9) and the Sangre de Cristo Mountains of New Mexico to southeast of Taos at Talpa (see Personius and Machette, 1984), where it merges with the northeast-trending Embudo fault.

As part of their mapping of the San Luis Hills, Thompson and Machette (1989) measured the surface offset of Pleistocene alluvial deposits along the Mesita fault. The Mesita cone is surrounded by an apron of flows that spread outward from the eruptive center; a flow near our parking site (see location under B8) was dated at 1.01±0.03 Ma by Appelt (1998). Scarps formed on flows on the west side of the cone show consistent down-to-the-west offset of 8–10 m, less than the 13 m reported by Kirkham and Rogers (1981) probably owing to a blanket of eolian sand that covers parts of hanging-wall (western) block. The scarps extend about 2 km (1.3 mi) across the basalt of Mesita Hill; from there north and south, the scarps are formed on older alluvium (unit Qao of Thompson and Machette, 1989) of probable early(?) middle Pleistocene age. North of the volcano for about 6 km (4 mi), the scarps are about 2–3 m high on unit Qao. They are not present on the Holocene floodplain of Culebra Creek, nor to the north across late to middle Pleistocene alluvium and piedmont slope deposits. However, there is a coincident, down-to-the-west fault in upper Oligocene rocks (Conejos Formation) in the eastern part of the San Luis Hills (see Thompson and Machette, 1989) about 8 km (5 mi) northwest of San Acacio (fig. B8.3–1), which may reflect the northern part of a pre-Quaternary Mesita fault.

To the south of Mesita Hill, the fault traverses several ages of alluvial deposits: from young to old, they were mapped as unit Qay (latest Pleistocene, about 12–20 ka), unit Qam (now mapped as unit Qai; about 50–200 ka, late to middle Pleistocene), and unit Qao (about 500±100 ka, middle to early(?) middle Pleistocene). The scarps on these alluvial units are progressively higher and show progressively more surface offset with age. For example, scarps on unit Qao are 7–8 m high between Mesita Hill and Rio Costilla; scarps on unit Qai are commonly 2–3 m high south of Rio Costilla; and the single scarp mapped on unit Qay is 1.4 m high. The ages used for this slip-rate analysis are broad geologic estimates based on soil development, geomorphic expression, and regional mapping. Although Personius and Machette (1984) reported that the youngest movement on the fault was late Pleistocene (10–130 ka), we suspect that there also has been movement in the latest Pleistocene (10–35 ka) on the basis of the offset of unit Qay.

On the basis of the differential offset of the Quaternary geologic units Qay, Qai, Qao, and Qbx, there are three time intervals that record offset along the Mesita fault. However, subsurface data from ground-water investigations in the late 1970s provide additional information about an older offset (fourth interval) of the Servilleta Basalt by the fault. Water-well data are quite abundant in the San Luis Basin, but most are from the Alamosa subbasin where there are logs for thousands of wells that penetrate as much as 500 m (1,640 ft) of the Alamosa Formation. South of the San Luis Hills, there are far fewer holes drilled for water, and few go deeper than 150 m (492 ft). Nevertheless, this is a valuable data set for tracking the depth and configuration of the Servilleta Basalt, which is a regionally extensive set of Pliocene basalt flows that form an important marker bed in basin-fill sediment of the Santa Fe Group.

In addition to the domestic and limited agricultural water-well data for the Costilla Plain, a drilling program was conducted as part of a provocative water play in the late 1970s. At that time, the San Marcos Pipeline Company (later to be acquired by Enron) proposed to mine 15,000-acre-ft of ground water from the Costilla Plain and pipe it over La Veta Pass to its proposed San Marco coal-slurry plant in Walsenberg (see Zorich-Erker Engineering, Inc., 1980, v. 1, p. 2). There it would be used to pipe coal slurry to Texas for use in power-generation plants. This is just one of the many water plays that the San Luis Basin has and will continue to suffer through as water and energy demands grow in the western United States. In order to develop its well field, the San Marcos Pipeline Company drilled 33 test and production wells on and around the north side of Mesita Hill.

Zorich-Erker Engineering, Inc. (1980) used its drill-hole data and previously drilled water-well data to structure contour the top of the Servilleta Basalt and make several cross

sections. Cross section A-A' extends west to east across the Costilla Plain and crosses the Mesita fault about 2 km (1.3 mi) north of Mesita Hill. The map interpretation is based on the assumption that the uppermost Servilleta Basalt flow in each well is coeval. However, recent mapping by Thompson and others (2007) shows there are multiple flows intercalated with sediment of the Santa Fe Group, and it suggests that down-to-the-west faults (such as the Mesita and Sangre de Cristo) may limit the lateral extent of the flows coming from the west. For example, cross section A-A' in Zorich-Erker Engineering, Inc. (1980, pl. 3) shows about 42 m of offset on the Mesita fault, assuming that the upper Servilleta Basalt (unit Tsb) is the same on both sides. Conversely, if the upper flow were restricted to the west (downthrown) side of the fault, then the second (lower) flow to the west might correlate to the upper flow to the east. In that case, the offset on unit Tsb would be about 53 m. These subsurface offsets of the Servilleta Basalt are substantially more than reported by Epis (15 m, 1977) or Burroughs (15–30 m, 1978), which were based on less robust data. For the purposes of this discussion, we use an offset of 42–53 m for the Servilleta Basalt as measured from our interpretations of cross section A-A'.

Fault Slip Rates

The Mesita fault is one of the few extensional faults in the Rio Grande rift that has multiple offset and age data. It is relatively common to have paleoseismic slip data for multiple late Pleistocene or Holocene faulting events, and occasionally a comparison with an older dated unit; however, in this case we have four estimates of fault offset for Quaternary units and an additional estimate for offset of the 4.0±0.3 Ma Servilleta basalt.

We have plotted the offset versus age data in figure B8.3–2. The long-term slip rate for the Mesita fault is about 0.012 mm/yr (or m/k.y.) and is based on 12 m of differential offset between unit Qay (1.4 m) and unit Qbx (about 13 m). The younger units generally fall on this long-term rate line, mainly owing to large age error limits used. In addition, the 42–53 m of estimated offset on the 4.0±0.3 Ma Servilleta Basalt (unit Tsb) falls right on line. The Pliocene offset rate for the Mesita fault is 0.012 mm/yr (using 48 m of offset in 4 m.y.), virtually the same as the 1.0 m.y. rate. Admittedly, the slip rate on the Mesita fault is slow, but it is typical of intrabasin faults that are secondary to faster-moving range-bounding faults, such as the Sangre de Cristo and Wasatch fault zones (see chapters C and H, this volume)

For comparison, we also plotted the 50-k.y. slip rate that Crone and Machette (2005) determined for the central Sangre de Cristo fault zone as a result of trenching at Rito Seco Creek (Crone and others, 2006), located about 5 km (3 mi) northeast of San Luis, Colo. This rate is about 0.17 mm/yr—more than an order of magnitude faster than the Mesita fault. The late Pleistocene rate of the central Sangre de Cristo fault zone is comparable to the long-term rates that Kirkham (2005) calculated using the Servilleta Basalt (about 0.13 mm/yr) and middle Miocene volcanic rocks (about 0.145 mm/yr).

The Mesita fault is only 22 km long (in middle Quaternary deposits), and thus it is probably not capable of generating extremely large earthquakes (**M**>7) or large surface offsets (that is, >2 m). If one uses 1.5 m as a characteristic offset for earthquakes in the **M** 6.5–6.9 range, then the offset recorded in unit Qay (1.4 m) might reflect a single faulting event of this

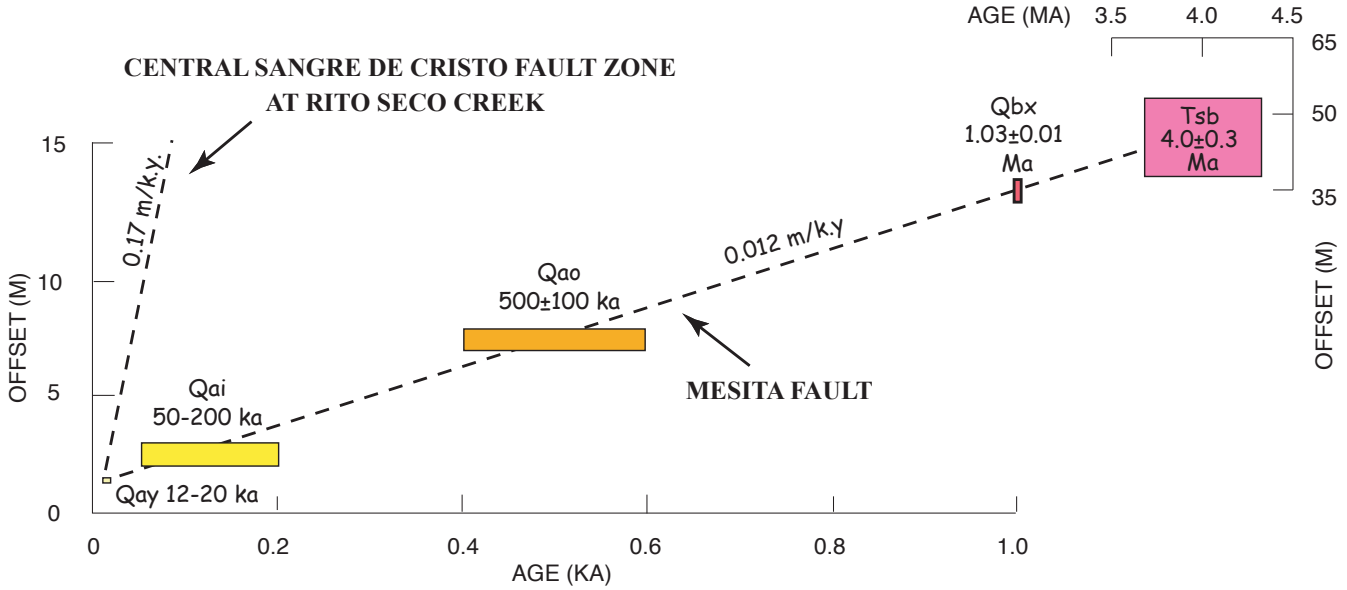

Figure B8.3–2. Amounts of offset of geologic units and slip rates for the Mesita fault. Age of Mesita basalt flow (unit Qbx) is precise, whereas age of Servilleta Basalt (unit Tsb) is range for dated flows in area. Dashed lines indicate average slip rate of Mesita fault for past 1.0 m.y., versus central Sangre de Cristo fault zone (past 50 k.y.) near San Luis, Colo. (see Crone and others, 2005, 2006). Unit Tsb is offset 42–53 m (138–173 ft) as measured from cross-section A-A′ in Zorich-Erker Engineering, Inc. (1980, plate 3).

magnitude. Similarly, the 3-m offset in unit Qai could be the result of 2 events and the 7–8 m offset in unit Qao could be the result of 5 events. Using 500 ka for unit Qao, yields a "back of the envelope" recurrence interval of >100 to 125 k.y. for the Mesita fault (that is, 4 events in a maximum of 500 k.y.). Similar low slip rates have been documented for relatively inactive intrabasin faults in the Rio Grande rift of New Mexico (Machette, 1998) and the Basin and Range province of Utah and Nevada (Machette, 2005).

The Sunshine Valley fault to the south in northern New Mexico (see chapter C), which may be an en echelon, opposite-sense extension of the Mesita fault, shows offset amounts and patterns in late to middle Pleistocene alluvium that are similar to offsets in the Mesita fault, and thus it probably also has extremely low slip rates.

Stop B9 — Landslides and the Sangre de Cristo fault Zone Along San Pedro Mesa

Speaker: Michael Machette

Location: Entrance to Melby Ranch (Wild Horse Mesa) on Colo. Highway 159, about 3.2 km south of Colo. Highway 248 to Mesita, Colo.
Garcia 7.5' quadrangle
GPS: NAD27, Zone 13, 453790 m E., 4102500 m N.
Elevation: 7,666 ft (2,337 m) asl (at entrance to Melby Ranch)

Synopsis

This stop provides a convenient place to view and discuss landslides and the southern Sangre de Cristo fault zone, which bounds the western margin of San Pedro Mesa—the high (8,500–8,900 ft or 2,590–2,713 m asl) basalt-covered surface to the east. The nearly 1,000-ft- (300-m-)high western escarpment of San Pedro Mesa is riddled with landslides, some quite massive (that is, many square kilometers in area). Faulting and landsliding have left large blocks of the Pliocene Servilleta Basalt at various altitudes and orientations. Landslides, rockfalls, colluvium, and ramps of eolian sand obscure the underlying problem unit—poorly consolidated sediment of the Santa Fe Group. To the west of us is the Costilla Plain, an extremely large, coalesced alluvial fan-piedmont slope complex that was deposited by Culebra Creek in middle Pleistocene time. Drillhole logs show that downdropped flows of Servilleta Basalt (4.0±0.3 Ma) are 30–50 m beneath the Costilla Plain, having been displaced about 300–400 m by the Sangre de Cristo fault zone and buried by Santa Fe Group sediment in the past 4 m.y.

Introduction

Stop B9 is just east of Highway 159 (Fort Garland to Questa) and near the western base of San Pedro Mesa, at the parking area for Melby Ranch Estates (formerly Wild Horse Mesa Estates). This a real-estate company that has developed several thousand 5- to 35-acre parcels on San Pedro Mesa. Most of the lots have been sold, and many continue to be resold either through this real-estate company, by others in the area, or by individual owners. Power is available on limited parts of the mesa, mainly along a western power line and along the eastern margin of the mesa. There are no County-supplied utilities (such as sewer, water, phone, or electric), so many of the homes are "off the net" (self-supporting). There have been no successful domestic water wells drilled on the mesa, and numerous 600 ft (183 m) deep wells have proven dry. However, the developer allows homeowners to haul water from his wells east of the mesa. There are fewer than 30 year-round households on the mesa and perhaps an equal number of summer-only residents.

Local Geology

The western margin of San Pedro Mesa, the high (8,500–8,900 ft or 2,590–2,713 m asl) basalt-covered plateau to the east of this stop, is structurally controlled by uplift along the northern part of the southern Sangre de Cristo fault zone, whereas the eastern margin is controlled by down-to-the east movement on the San Luis fault zone (on the east side of the mesa). For the most part, these fault zones underlie extensive landslide deposits all along the mesa's margins, but where the southern Sangre de Cristo fault zone crosses into New Mexico it is largely is coincident with the bedrock-alluvial contact along the east margin of Sunshine Valley (see stop C7 and chapter I, this volume).

Faulting has downdropped large blocks of Pliocene Servilleta Basalt, and landsliding has broken and jostled these blocks into various orientations. The combination of landslides, rock falls, colluvium, and ramps of eolian sand have obscured the poorly consolidated basin-fill sediment (unit Tsf, lower part of the Santa Fe Group, Pliocene to upper Oligocene) that typically underlies the basalt. Although it is poorly exposed, sparse road cuts indicate that most of the basin-fill sediment beneath San Pedro Mesa consists of moderately oxidized siltstone, sandstone, and lesser amounts of sandy pebble conglomerate.

To the west of this stop is the Costilla Plain, which was named by Upson (1939, 1971) for the small community of Costilla, N. Mex. (fig. C–1, chapter C, this volume). The Costilla Plain is an extremely large coalesced alluvial fan-piedmont slope that extends from Culebra Creek south to the subtle drainage divide between Costilla and Ute Mountain, in northernmost New Mexico (see discussion of this area in chapter C). The plain is underlain by old alluvium (unit Qao) deposited by the Rio Culebra in middle Pleistocene time. This alluvium consists of sandy pebble to small-cobble gravel at the north end of San Pedro Mesa, but becomes finer downstream (west and southwest) to pebbly sand near the Colorado–New Mexico border. The alluvium is unconformable on the upper part of the Santa Fe Group (unit QTsf), which is Pliocene to middle Pleistocene in this region (see mapping of Machette and others, 2007, and Thompson and others, 2007). In general, Quaternary alluvium (units Qay, Qai, and Qao; fig. B9–1) is coarser grained than the underlying basin-fill sediment as a result of having been deposited by higher energy, glacially fed streams. Conversely, the basin-fill sediment is relatively fine grained (primarily sandstone, siltstone, and claystone) having been deposited in quieter water, distal alluvial fan, fluvial, or playa environments. These same relations are apparent in the Sunshine Valley of northern New Mexico (see also stop C4).

Landslide Deposits

Three general types of landslides were mapped around the margins of San Pedro Mesa (fig. B9–2) by Thompson and others (2007). They include (1) younger landslide deposits (unit Qlsy) that show hummocky terrain, closed depressions, angular blocks of basalt, and localized accumulations of eolian sand and other cover deposits; (2) older landslide deposits (unit Qlso) that show subdued terrain, integrated drainage, fewer and more subangular blocks of basalt, and discontinuous mantles of eolian sand, colluvium, and alluvium; and (3) massive (as much as 2 km long) relatively intact rotated blocks of basalt than have either slid into place (unit Tsb[lb]) or have been faulted into place (unit Tsb) along strands of the southern Sangre de Cristo fault (see following discussion).

The most recent movement of these landslide deposits is considered to be middle to late Pleistocene (Thompson and others, 2007), although they have probably been mobile throughout much of the past 4 m.y. Figure B9–3 shows and aerial view of these landslide deposits. Their morphology, which is a guide for mapping, is quite apparent and disparate. In general, the younger landslide deposits extend further onto the Costilla Plain and generally cover strands of the fault zone that displace the older landslide deposits. This is not to

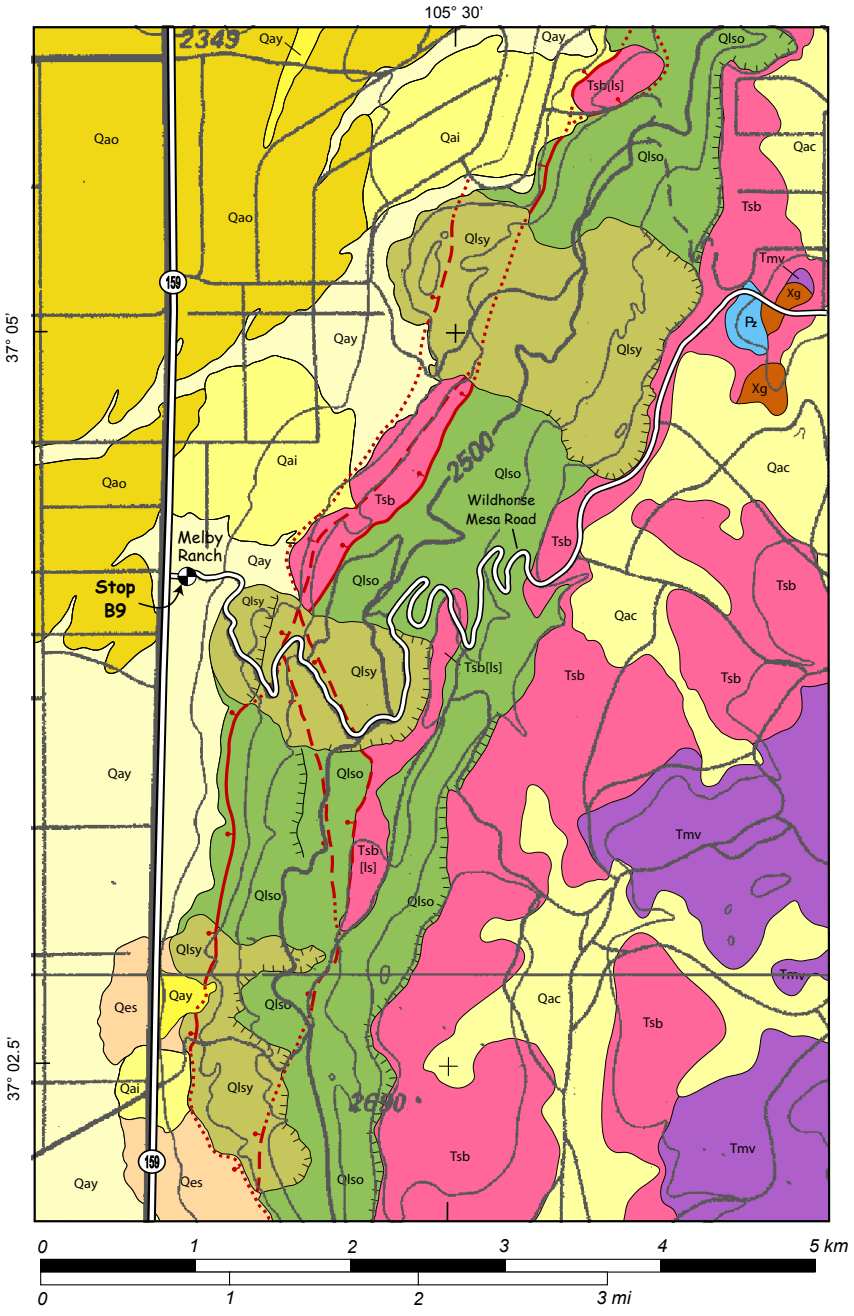

Figure B9–1. Western part of San Pedro Mesa. Quaternary traces of the Sangre de Cristo fault zone are shown in red. Map units: Xg, Early Proterozoic granite; Pz, Paleozoic rocks; Tmv, Miocene(?) volcanic rocks; Tsb, Pliocene Servilleta Basalt ([ls], landslide blocks); Qlso, older landslides; Qlsy, younger landslides; Qao, old alluvium; Qay, young alluvium; Qac, alluvium and colluvium; Qes, eolian sand. Geology simplified from Thompson and others, 2007. Base scanned from 1:100,000-scale Alamosa 30 x 60-minute sheet with metric contours.

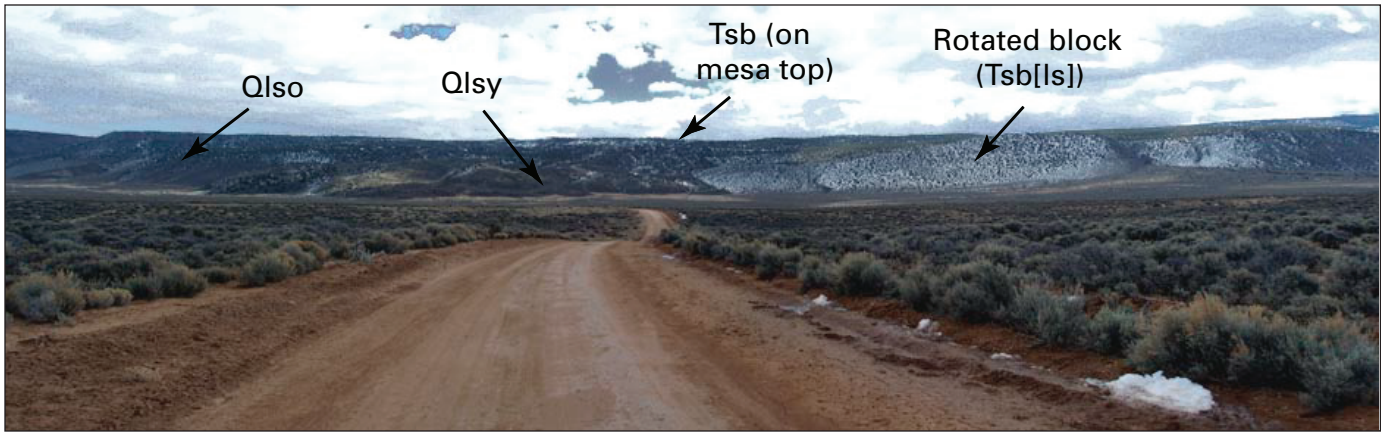

Figure B9–2. Panoramic view of west side of San Pedro Mesa. View to the east, taken from Highway 159 about 1 mi (1.6 km) north of stop B9 (see fig. B9–3). Labels: Qlso, older landslides; Qlsy, younger landslides; Tsb, Servilleta Basalt (about 4 Ma); Tsb[ls], landslide block of Servilleta Basalt.

say that the younger landslides are not faulted, but rather that discrete fault scarps are rarely preserved within the relatively weak, unconsolidated landslide debris. For example, Machette and others (2006) have documented very young movement (about 300 years old) along the Nephi segment of the Wasatch fault zone in central Utah. Massive landslide deposits about 1 km north of their Willow Creek trench site and due east of Mona, Utah, show no definitive traces, yet the fault is mapped up to the margins of the landslide. The Mona landslide is late Pleistocene in age (see Hardy and others, 1997) as shown by Lake Bonneville shorelines (>14.5 ka) on the distal (western) end of the landslide.

Conversely, most of the older landslide deposits (unit Qlso) marginal to San Pedro Mesa along the southern Sangre de Cristo fault zone have linear fronts (fig. B9–3), suggesting that they are faulted. No prominent fault scarps were noted during their mapping by Thompson and others (2007) owing to colluvial and eolian deposits that have accumulated at the base of steep landslide toes. In many instances, photograph lineaments that mark the fault zone are related to vegetation and soil-texture changes. However, because nontranslational landslides commonly have lobate forms when deposited, the linearity of their toes strongly suggests structural control.

Southern Sangre de Cristo Fault Zone

San Pedro Mesa is bounded by the northern part of the southern Sangre de Cristo fault zone, which is one of three fault zones that make up the larger Sangre de Cristo fault system (see chapter I). At the northern end of the mesa, the Servilleta Basalt is offset by numerous strands of the fault as it splays out (like a horse's tail) and changes trend from north-south to more north-northwesterly (see fig. B8.3–1 and mapping of Thompson and others, 2007). The westernmost strand of the fault zone abuts the San Acacio fault, which is one of two intrabasin faults in this part of the Costilla Plain. South of San Pedro Mesa (near Costilla, N. Mex.; see stop C7), the southern Sangre de Cristo fault zone emerges from landslide deposits and forms the bedrock-alluvial contact in the Sunshine Valley. Although this portion of the fault zone has more typical Basin and Range morphology, when mapped in detail it shows multiple surface traces with a complex rupture pattern (C.A. Ruleman, unpub. mapping, 2007).

San Pedro Mesa represents a Pliocene land surface that is now uplifted as a prominent horst block. It is bordered by the southern Sangre de Cristo fault zone on the west and by the San Luis fault zone on the east. The Sanchez graben lies just to the east of the horst—it is bordered by the central Sangre de Cristo fault zone on the east and the San Luis fault zone on the west (see new mapping by Thompson and others, 2007). The Sanchez graben is filled by Neogene sediment and Miocene to upper(?) Oligocene volcanic rocks that lie on Precambrian rock encountered at about 6,230 ft (1,900 m) depth in the Energy Operating Co. Williamson No. 1 well (R.M. Kirkham, written commun., 2005; see Thompson and others, 2007, for location of well, depths, and source of data). This well indicates that there is a minimum of 2,134 m (7,000 ft) of structural relief on the Precambrian rock across the San Luis fault zone. Conversely, Precambrian rock is exposed high in the Culebra Range to the east of the Sanchez graben and somewhere at depth beneath the Costilla Plain, west of the southern Sangre de Cristo fault zone.

The western escarpment of San Pedro Mesa rises southward 13 mi (21 km) to the State line, with the southernmost remnant of basalt preserved on an unnamed mesa about 5 mi (8 km) south of Costilla, N. Mex. (see discussion at stop C7). At the northern end of the mesa (near the north-south to east-west bend in Highway 159; fig. B8.3–1), the Servilleta Basalt is at basin level. It rises gently to the south, so that at the radio tower (about 10 mi to the north of stop B9) it is about 70 m (230 ft) above the Costilla Plain. At stop B9, the top of the mesa is at about 8,600 ft (2,621 m) asl, roughly 900 ft (275 m) above us. From here south to the State line, the top

the mesa climbs gently about 340 ft (104 m) to an elevation of about 8,940 ft (2,725 m) asl, or roughly 1,220 ft (372 m) above the Costilla Plain. Thus, San Pedro Mesa appears to be a northward-tilted ramp that transfers motion from the southern Sangre de Cristo fault zone in New Mexico to the central Sangre de Cristo fault zone in Colorado (see discussion in chapter H, this volume).

South of Costilla, N. Mex., San Pedro Mesa continues as an unnamed surface to the north side of Cedro Canyon (see fig. C–1, chapter C, this volume). This mesa is covered by the southernmost remnant of the Servilleta Basalt on the uplifted (footwall) block of the southern Sangre de Cristo fault zone. The basalt (unit Tsb) was dated at 4.3 Ma by Lipman and Reed (1989) by whole-rock K-Ar methodology. The basalt rests on an ancient land surface that Menges (1988) traced south into a prominent bench on the range front and used as a paleodatum to estimate uplift along the southern Sangre de Cristo fault zone (see further discussion in chapter H).

Little is known about the rupture history of the southern Sangre de Cristo fault zone. Kelson and others (2004) have conducted the only paleoseismic investigation of this fault zone at a site near Taos, N. Mex. (see also chapter I). Dating of the most recent event was poorly constrained, but they concluded that the fault had latest Pleistocene movement. Conversely, scarp morphology studies along the New Mexico portion of the fault zone indicated Holocene rupture to Menges (1988) and Personius and Machette (1984), and recent mapping by C.A. Ruleman (unpub. mapping, 2007) (see stop C6) documents Holocene ruptures. As previously mentioned, we didn't find any fault scarps formed on alluvial deposits along San Pedro Mesa; thus, we are unable to estimate the time of the most recent faulting event. However, on the basis of the fault's expression in landslide deposits, we suspect that the New Mexico portion of the fault zone may have latest Pleistocene movement.

For comparison, the central Sangre de Cristo fault zone offsets latest Pleistocene alluvium at the mouth of Rito Seco Creek, which is located about 3 mi (4.8 km) northeast of San Luis, Colo., and about 14 mi (22 km) north-northeast of this stop. A paleoseismic investigation by Crone and others (2006) dates the most recent movement at Rito Seco Creek at about 9 ka and documents four discrete surface faulting events in the past 50 k.y. The paleoseismic record at that site suggests slip rates of about 0.17 mm/yr and average recurrence intervals of roughly 12 k.y. (Crone and Machette, 2005). As such, the Sangre de Cristo fault system is the most active and longest Quaternary fault in the Rio Grande rift, which extends from central Colorado to northern Mexico.

Subsurface Geology

Drill-hole logs (Zorich-Erker Engineering, Inc., 1980) show that the uppermost flows of Servilleta Basalt are 30–50

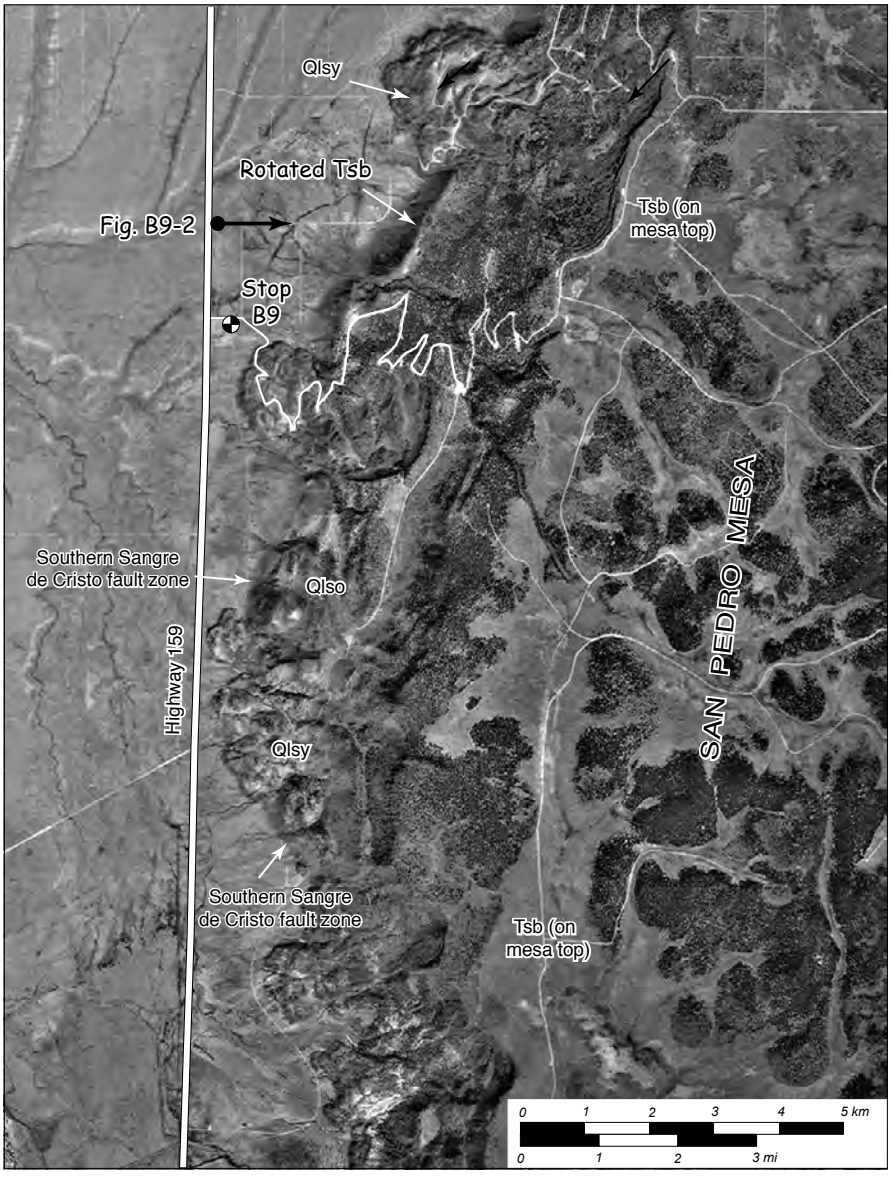

Figure B9–3. Landslides along west side of San Pedro Mesa. Compare with geologic map shown in figure B9–1. Map units: Qlsy, younger landslides; Qlso, older landslides; Tsb, Servilleta Basalt (about 4 Ma). Scanned image is from USGS HAP aerial photograph 428–112, 9–16–83, 1:80,000 scale.

m (100–165 ft) beneath the Costilla Plain and they increase in depth to the east towards the southern Sangre de Cristo fault zone. These relations are shown diagrammatically in figure B9–4, which is a west-northwest–east-southeast section that crosses the Costilla Plain about 2 km north of stop B9. The cross section suggests that there has been about 300–400 m (1,000–1,300 m) of offset along the fault zone in the past 4 m.y. (We use 4.0±0.3 Ma for the probable age range of Servilleta Basalt in this area.) The relations shown in this cross section are quite similar to those of the Sunshine Valley (fig. C7–5), with the exception that Pliocene Lake Sunshine occupied an east-tilted block that abuts southern Sangre de Cristo fault zone. Lake Sunshine is analogous to Lake Alamosa but was not as long lived. As mentioned previously, there is little net offset of the Servilleta Basalt at the northwest end of the San Pedro Mesa, but the 300–400 m of offset along the Colorado portion suggests long-term slip rates of 0.075–0.10 mm/yr of the southern Sangre de Cristo fault zone (compare with New Mexico rates, stop C7 and chapter J, this volume).

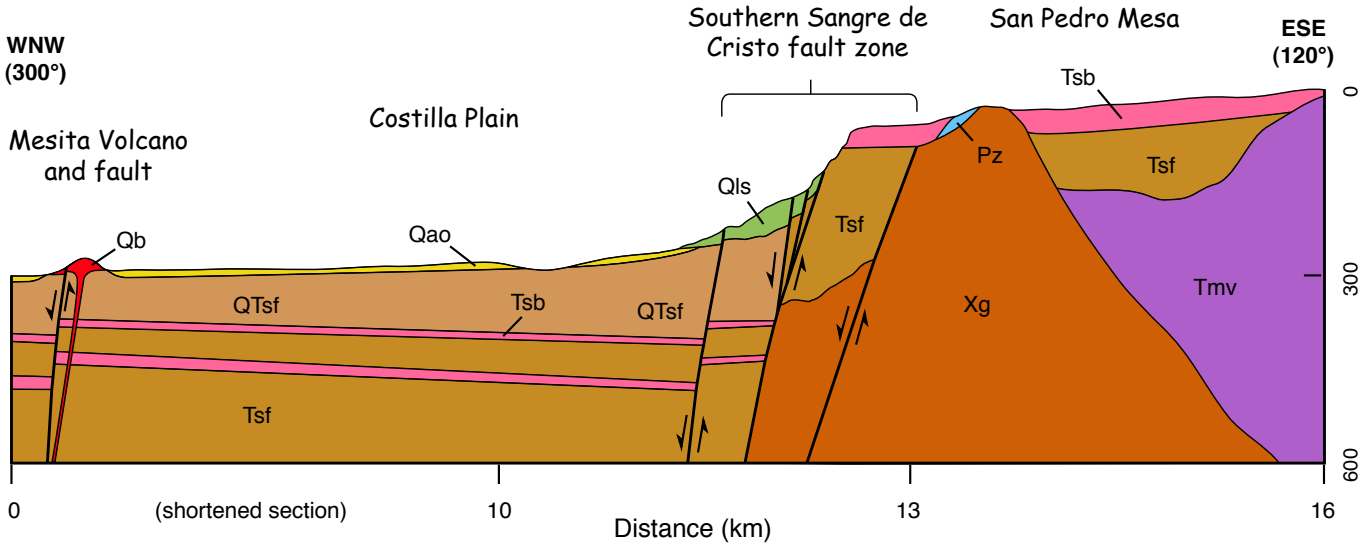

Figure B9–4. Diagrammatic cross section of the Costilla Plain and San Pedro Mesa. Map units: Qls, landslides (Quaternary); Qao, older alluvium (middle Pleistocene); Qb, Mesita basalt (1.0 Ma); QTsf, Santa Fe Group, upper part (middle Pleistocene to Pliocene); Tsb, Servilleta Basalt (about 4 Ma); Tsf, Santa Fe Group, lower part (Pliocene to upper Oligocene); Tmv, middle(?) Miocene volcanic rocks; Pz, Paleozoic sandstone; Xg, Early Proterozoic granitic rock. Based on unpublished geologic mapping of Michael Machette and Ren Thompson (2007) and drill-hole data of Zorich-Erker Engineering, Inc. (1980). Depths (in meters) are exaggerated about 3x and Costilla Plain part of section (0–11 km) is shortened to fit on cross section.

References Cited

Appelt, R.M., 1998, $^{40}Ar/^{39}Ar$ geochronology and volcanic evolution of the Taos Plateau volcanic field, northern New Mexico and southern Colorado: Socorro, New Mexico Institute of Mining and Technology, M.S. thesis, 58 p.

Birkeland, P.W., 1999, Soils and Geomorphology, 3d ed.: New York, Oxford University Press, 430 p.

Burroughs, R.L., 1972, Geology of the San Luis Hills, south-central Colorado: Albuquerque, University of New Mexico, Ph.D. dissertation, 139 p.

Burroughs, R.L., 1978, Alamosa to Antonito, Colorado (p. 33–36, in Northern rift guide 2, Alamosa, Colorado—Santa Fe, New Mexico), *in* Hawley, J.W., ed., Guidebook to Rio Grande rift in New Mexico and Colorado: New Mexico Bureau of Mines and Mineral Resources Circular 103, 241 p.

Colton, R.B., 1976, Map showing landslide deposits and late Tertiary and Quaternary faulting in the Fort Garland–San Luis area, Colorado: U.S. Geological Survey Open-File Report 76–185, scale 1:250,000.

Crone, A.J., and Machette, M.N., 2005, Paleoseismic activity on the Sangre de Cristo fault near San Luis, Colorado: Geological Society of America Abstracts with Programs, v. 37, no. 7, p. 558 (Paper 256–2).

Crone, A.J., Machette, M.N., and Mahan, S.A., 2006, Paleoseismic investigation of Rito Seco site, central section of the Sangre de Cristo fault zone, Colorado—Data related to late Quaternary surface faulting on the Sangre de Cristo fault, Rito Seco site, Costilla County, Colorado: U.S. Geological Survey Scientific Investigations Map SI–2955, 1 oversize pl. (http://pubs.usgs.gov/sim/2006/2955).

Currey, D.R., 1990, Quaternary palaeolakes in the evolution of semidesert basins, with special emphasis on Lake Bonneville and the Great Basin, U.S.A., *in* Davis, O.K., ed., Paleoenvironments of arid lands: Palaeogeography, Palaeoclimatology, Palaeoecology, v.76, no. 3–4, p.189–214.

Endlich, F.M., 1877, Part I—Geology, Chap. II—San Luis Valley, *in* F.V. Hayden's Ninth Annual Report of the United States Geological and Geographical Survey of the Territories . . . for the year 1875: Washington, D.C., Government Printing Office, p. 140–149, and plate XVII.

Epis, R.C., 1977, Surface and subsurface geology of the Mesita volcano area, Costilla County, Colorado, *in* Zorich-Erker Engineering, Inc., Ground water availability of the San Marco property near Mesita in Costilla County, Colorado: Report submitted to San Marco Pipeline Company, Denver, Colorado, dated September, 30, 1980, v. III, Appendix A, 20 p., plus map and cross section.

Giegengack, R.F., 1962, Recent volcanism near Dotsero, Eagle County, Colorado: Boulder, University of Colorado, M.S. thesis, 54 p.

Gosse, J.C., and Phillips, F.M., 2001, Terrestrial in situ cosmogenic nuclides—Theory and application: Quaternary Science Reviews, v. 20, no. 14, p. 1475–1560.

Hardy, K.M., Mulvey, W.E., and Machette, M.N., 1997, Surficial geologic map of the Nephi segment of the Wasatch fault zone, eastern Juab County, Utah: Utah Geological Survey Map 170, 14 p. pamphlet, 1 plate, 1:50,000 scale.

Johnson, R.B., 1969, Geologic map of the Trinidad 1 x 2 degree quadrangle, south-central Colorado: U.S. Geological Survey Miscellaneous Investigations Map I–558, scale 1:250,000.

Kelson, K., Bauer, P.W, Love, D., Connell, S.D., Mansell, M., and Rawling, G., 2004, Initial paleoseismic and hydrologic assessment of the southern Sangre de Cristo fault at the Taos Pueblo site, Taos, New Mexico: New Mexico Bureau of Geology and Mineral Resources Open-File Report 476, 46 p.

Kirkham, R.M., 2006, Surprises in the Culebra graben, a major sub-basin within the San Luis basin of the Rio Grande rift: Geological Society of America Abstracts with Programs, v. 38, no. 6, p. 14.

Kirkham, R.M., Brister, B.S., Grauch, V.J.S., and Budahn, J.R., 2005, Culebra graben—A major intrarift structure in the San Luis Basin, Rio Grande rift: Geological Society of America Abstracts with Programs, v. 137, no. 6, p. 14 (Paper 8–4).

Kirkham, R.M., and Rogers, W.P., 1981, Earthquake potential in Colorado: Colorado Geological Survey Bulletin 43, 171 p., 3 pls.

Kunk, M.J., Budahn, J.R., Unruh, D.M., Stanley, J.O., Kirkham, R.M., Bryant, Bruce, Scott, R.B., Lidke, D.J., and Streufert, R.K., 2002, $^{40}Ar/^{39}Ar$ ages of late Cenozoic volcanic rocks within and around the Carbondale and Eagle collapse centers, Colorado—Constraints on the timing of evaporite related collapse and incision of the Colorado River, *in* Kirkham, R.M., Scott, R.B., and Judkins, T.W., eds., Late Cenozoic evaporite tectonism and volcanism in west-central Colorado: Geological Society of America Special Paper 366, p. 213–234.

Lal, D., 1991, Cosmic ray labeling of erosion surfaces—In-situ nuclide production rates and erosion models: Earth and Planetary Science Letters, v. 104, p. 424–439.

Lanphere, M.A., Champion, D.E., Christiansen, R.L., Izett, G.A., Obradovich, J.D., 2002. Revised ages for tuffs of the Yellowstone Plateau volcanic field—Assignment of the Huckleberry Ridge Tuff to a new geomagnetic polarity event: Geological Society of America Bulletin 114, p. 559–568.

Licciardi, J.M., Kurz, M.D., Clark, P.U., and Brook, E.J., 1999, Calibration of cosmogenic ^{3}He production rates from Holocene lava flows in Oregon, USA, and effects of the Earth's magnetic field: Earth and Planetary Science Letters, v. 172, p. 261–271.

Lipman, P.W., and Mehnert, H.H., 1979, The Taos Plateau volcanic field, northern Rio Grande rift, New Mexico, *in* Reicker, R.C., ed., Rio Grande rift—Tectonics and magmatism: American Geophysical Union, Washington D.C., p. 289–311.

Lipman, P.W., and Reed, J.C., Jr., 1989, Geologic map of the Latir volcanic field and adjacent areas, northern New Mexico: U.S. Geological Survey Miscellaneous Investigations Series Report I–1907, 2 sheets, 1:48,000 scale.

Lisiecki, L.E., and Raymo, M.E., 2005, A Pliocene-Pleistocene stack of 57 globally distributed benthic δ^{18}O records: Paleooceanography, v. 20, no. 1, 17 p., doi:10.1029/2004PA001071.

Machette, M.N., 1978, Dating Quaternary faults in the southwestern United States using buried calcic paleosols: U.S. Geological Survey Journal of Research, v. 6, no. 3, p. 369–381.

Machette, M.N., 1985, Calcic soils of the southwestern United States, *in* Weide, D.L., ed., Soils and Quaternary geology of the southwestern United States: Geological Society of America Special Paper 203, p. 1–21.

Machette, M.N., 1998, Contrasts between short- and long-term records of seismicity in the Rio Grande rift—Important implications for seismic-hazards analysis in areas of slow extension, *in* Lund, W.R., ed., Western States Seismic Policy Council (WSSPC) Basin and Range Province Seismic-Hazards Summit, Proceedings: Utah Geological Survey Miscellaneous Publication 98–2, p. 84–95.

Machette, M.N, 2005, Summary of the late Quaternary tectonics of the Basin and Range province in Nevada, eastern California, and Utah, *in* Lund, W.R., ed., Basin and Range Province Seismic Hazards Summit II, Western States Seismic Policy Council, Reno, Nevada, May 16–91, 2004, Proceedings: Utah Geological Survey Miscellaneous Publication 05–2 (CD-ROM), 18 p., 12 full-color figures, 2 tables.

Machette, M.N., Crone, A.J., Personius, S.F., Dart, R.L., Lidke, D.J., Mahan, S.A., and Olig, S.S., 2006, Paleoseismology of the Nephi segment of the Wasatch fault zone, Juab County, Utah—Preliminary results from two large exploratory trenches at Willow Creek: U.S. Geological Survey Scientific Investigations Map 2966, 2 oversize plates (http://pubs.usgs.gov/sim/2006/2966).

Machette, M.N., Long, T., Bachman, G.O., and Timbel, N.R., 1997, Laboratory data for calcic soils in central New Mexico—Background information for mapping Quaternary deposits in the Albuquerque Basin: U.S. Geological Survey Open-File Report 96–772, 60 p.

Machette, M.N., and Marchetti, D.W., 2006, Pliocene to middle Pleistocene evolution of the Rio Grande, northern New Mexico and southern Colorado: Geological Society of America Abstracts with Programs, v. 38, no. 6, p. 36 (Paper 18–2).

Machette, M.N., and Personius, S.F., 1984, Map showing Quaternary and Pliocene faults in the east part of the Aztec 1° x 2° quadrangle and west part of the Raton 1° x 2° quadrangle, northern New Mexico: U.S. Geological Survey Miscellaneous Field Studies Map MF–1465–B, scale 1:250,000 with 14-page pamphlet.

Machette, M.N., and Thompson, R.A., 2005, Preliminary geologic map of the northwestern part of the Alamosa ½° x 1° quadrangle, Alamosa and Conejos Counties, Colorado: U.S. Geological Survey Open-File Report 2005–1392, 1 sheet, 1:50,000 scale.

Machette, M.N., Thompson, R.A., and Drenth, B.J., 2007, Geologic map of the San Luis quadrangle, Costilla County, Colorado: U.S. Geological Survey Scientific Investigations Map 2963, 1 sheet, 1:24,000 scale (http://pubs.usgs.gov/sim/2007/2963).

Marchetti, D.W., and Cerling, T.E., 2005, Cosmogenic ^{3}He exposure ages of Pleistocene debris flows and desert pavements in Capitol Reef National Park, Utah: Geomorphology, v. 67, no. 3–4, p. 423–435.

Marchetti, D.W., Cerling, T.E., and Lips, E.W., 2005. A glacial chronology for the Fish Creek drainage of Boulder Mountain, Utah, USA: Quaternary Research, v. 64, p. 264–271.

Menges, C.M., 1988, The tectonic geomorphology of mountain-front landforms in the northern Rio Grande rift near Taos, New Mexico: Albuquerque, University of New Mexico, unpublished Ph.D. dissertation, 339 p.

O'Connor, J.E., 1992, Hydrology, hydraulics, and geomorphology of the Bonneville flood: Geological Society of America Special Paper 274, 83 p.

Personius, S.F., and Machette, M.N., 1984, Quaternary and Pliocene faulting in the Taos Plateau, northern New Mexico, *in* Baldridge, S.W., Dickerson, P.W., Riecker, R.E., and Zidek, Jiri, eds., Rio Grande rift—Northern New Mexico: New Mexico Geological Society 35th Annual Field Conference Guidebook, p. 83–90.

Reheis, M.C., Sarna-Wojcicki, A.M, Reynolds, R.L., Repenning, C.A., and Mifflin, M.D., 2002, Pliocene to middle Pleistocene lakes in the western Great Basin—Ages and connections, *in* Hersheler, R., Madsen, D.B., and Currey, D.R., eds., Great Basin aquatic systems history: Washington, D.C., Smithsonian Institution Press, Smithsonian Contributions to the Earth Sciences, v. 33, p. 53–108.

Rogers, K.L., 1984, A paleontologic analysis of the Alamosa Formation (south-central Colorado; Pleistocene, Irvingtonian), *in* Baldridge, W.S., Dickerson, P.W., Riecher, E., and Zidek, J., eds., Rio Grande Rift—Northern New Mexico: New Mexico Geological Society 35th Annual Field Conference Guidebook, v. 35, p. 151–155.

Rogers, K.L., 1987, Pleistocene high altitude amphibians and reptiles from Colorado (Alamosa local fauna: Pleistocene, Irvingtonian): Journal of Vertebrate Paleontology, v. 7, no. 1, p. 82–95.

Rogers, K.L., and Larson, E.E., 1992, Pliocene and Pleistocene sedimentation in south-central Colorado—Opportunity for climate studies: Quaternary International, v. 13/14, p. 15–18.

Rogers, K.L., Larson, E.E., Smith, G.A., Katzman, D., Smith, G.R., Cerling, T.E., Wang, Y., Baker, R.G., Lohmann, K.C., Repenning, C.A., Patterson, P.E., Mackie, G., 1992, Pliocene and Pleistocene geologic and climatic evolution in the San Luis Valley of south-central Colorado: Palaeogeography, Palaeoclimatology, Palaeoecology, v. 94, no. 1–4, p. 55–86.

Rogers, K.L., Repenning, C.A., Forester, R.M., Larson, E.E., Hall, S.A., Smith, G.A., Anderson, Elaine, and Browen, T.J., 1985, Middle Pleistocene (Late Irvingtonian: Nebraskan) climatic changes in south-central Colorado: National Geographic Research, v. 1, no. 4, p. 535–563.

Sarna-Wojcicki, Andrei M., Pringle, M.S., and Wijbrans, J., 2000, New $^{40}Ar/^{39}Ar$ age of the Bishop Tuff from multiple sites and sediment rate calibration for the Matuyama-Brunhes boundary: Journal of Geophysical Research, v. 105, no. B9, p. 21,431–21,444.

Sharp, W.D., Ludwig, K.R., and Hellstrom, J., 2005, U-series dating targets in arid and semi-arid environments: Geological Society of America Abstracts with Programs, v. 37, no. 7, p. 479, Paper 216–5.

Siebenthal, C.E., 1910, Geology and water resources of the San Luis Valley, Colorado: U.S. Geological Survey Water-Supply Report 240, 128 p.

Thompson, R.A., and Lipman, P.W., 1994a, Geologic map of the Los Pinos quadrangle, Rio Arriba and Taos Counties, New Mexico and Conejos County, Colorado: U.S. Geological Survey Map GQ–1749, scale 1:24,000.

Thompson, R.A., and Lipman, P.W., 1994b, Geologic map of the San Antonio Mountain quadrangle, Rio Arriba County, New Mexico: U.S. Geological Survey Map GQ–1750, scale 1:24,000.

Thompson, R.A., and Machette, M.N., 1989, Geologic map of the San Luis Hills, Conejos and Costilla Counties, Colorado: U.S. Geological Survey Miscellaneous Investigations Series Map I–1906, scale 1:50,000.

Thompson, R.A., Machette, M.N., and Drenth, B.J., 2007, Geologic map of San Pedro Mesa and surrounding area, Costilla County, Colorado: U.S. Geological Survey Open-File Report 2007–1074, 1 sheet, 1:24,000 scale (http://pubs.usgs.gov/ofr/2007/1074).

Upson, J.E., 1939, Physiographic subdivisions of the San Luis Valley, southern Colorado: Journal of Geology, v. 47, no. 7, p. 721–736.

Upson, J.E., 1971, Physiographic subdivisions of the San Luis Valley, southern Colorado, *in* James, H.L., ed., Guidebook of the San Luis Basin, Colorado: New Mexico Geological Society, p. 113–122 (Reprinted from Upson, 1939, with recent notes and bibliography by the author).

Wells, S.G., Kelson, K.I., and Menges, C.M., 1987, Quaternary evolution of fluvial systems in the northern Rio Grande rift, New Mexico and Colorado—Implications for entrenchment and integration of drainage systems, *in* Menges, C., ed., Quaternary tectonics, landform evolution, soil chronologies and glacial deposits—Northern Rio Grande rift of New Mexico: Friends of the Pleistocene—Rocky Mountain Cell Field Trip Guidebook, Oct. 8–11, 1987, p. 55–69.

Zorich-Erker Engineering, Inc., 1980, Ground water availability on the San Marco property near Mesita in Costilla County, Colorado: Denver, Colorado, Report prepared for San Marco Pipeline Company, 3 volumes with plates.

Selected Bibliography on Ventifacts

Breed, C.S., McCauley, J.F., Whitney, M.I., Tchakarian, V.P., and Laity, J.E., 1997, Wind erosion in drylands, *in* Thomas, D.S.G., ed., Arid zone geomorphology, 2d ed.: Chichester, England, Wiley, p. 437–464.

Bridges, N.T., Laity, J.E., Greeley, R., Phoreman, J., and Eddlemon, E.E., 2004, Insights on rock abrasion and ventifact formation from laboratory and field analog studies with applications to Mars: Planetary and Space Science, v. 52, p. 199–213.

Bryan, K., 1931, Windworn stones or ventifacts with a discussion and a bibliography: Washington, D.C., National Research Council Report, Commission on Sediments, 1929–30, p. 29–50.

Greeley, R., Bridges, N.T., Kuzmin, R.O., and Laity, J.E., 2002, Terrestrial analogs to wind-related features at the Viking and Pathfinder landing sites on Mars: Journal of Geophysical Research (Planets), v. 107, no. E1, p. 5–1 to 5–21.

Laity, J.E., 1992, Ventifact evidence for Holocene wind patterns in the east-central Mojave Desert: Zeitschrift für Geomorphologie, Suppl.-Bd., v. 84, p. 73–88.

Laity, J.E., 1994 Landforms of aeolian erosion, *in* Abrahams, A., and Parsons, A., eds., Geomorphology of desert environments: London, Chapman and Hall, p. 506–535.

Laity, J.E., 1995, Wind abrasion and ventifact formation in California, *in* Tchakerian, V.P., ed., Desert aeolian processes: London, Chapman and Hall, p. 295–321.

McCauley, J.F., Breed, C.S., Grolier, M.J. and El-Baz, F., 1980, Pitted rocks and other ventifacts in the western desert: Geographical Journal, v. 146, no. 1, p. 84–85.

Needham, C.E., 1937, Ventifacts in New Mexico: Journal of Sedimentary Petrology, v. 7, no. 1, p. 31–33.

Sharp, R.P., 1949, Pleistocene ventifacts east of the Bighorn Mountains, Wyoming: Journal of Geology, v. 57, no. 2, p. 175–195.

Sugden, W., 1968, Ventifacts, *in* Fairbridge, R.W., ed., Encyclopedia of geomorphology: New York, Reinhold Publishing Co., p. 1192–1193.

Wentworth, C.K., and Dickey, R.I., 1935, Ventifact localities in the United States: Journal of Geology, v. 43, no. 1, p. 97–104.